Université de Montréal

# Caractérisation morphologique, biochimique et physiologique des protéines de jonction lacunaire, les connexines 46 et 50, dans les cellules folliculo-stellaires TtT/GF de l'hypophyse antérieure

Par: Christopher Juan Garcia
Département de pathologie et biologie cellulaire,
Faculté de médicine

Mémoire présenté à la Faculté de médicine en vue de l'obtention du grade de maîtrise ès sciences (MSc) en pathologie et biologie cellulaire, option biologie cellulaire.

Avril 2014

*Université de Montréal*

# Morphological, biochemical and physiological characterization of the gap junction proteins, connexins 46 and 50, in the folliculo-stellate TtT/GF cells of the anterior pituitary gland

By: Christopher Juan Garcia
Department of Pathology and Cell Biology
Faculty of Medicine

Thesis presented to the Faculty of Medicine as a requirement for the granting of the degree of Master of Science (MSc) in Pathology and Cell Biology, option: Cellular Biology

April 2014

*Université de Montréal*

Faculty of Medicine

Department of Pathology and Cell Biology

**Thesis evaluation committee:**

Professor Lucien Ghitescu – Committee president

Professor Victor Gavino – Committee member

Professor María Leiza Vitale – Research supervisor

Professor R.-Marc Pelletier – Research co-supervisor

April 2014

# Résumé

Les cellules folliculo-stéllaires (FS) de l'hypophyse antérieure possèdent une forme étoilée et étendent de longues projections cytoplasmiques qui forment des pseudo-follicules entourant les cellules endocrines. Les cellules FS sont connectées entre elles par des jonctions lacunaires (des fois aussi connu sous le nom de jonction communicante) formant ainsi un réseau tridimensionnel continu. Un des rôles principaux des cellules FS est le maintien du microenvironnement de l'hypophyse antérieure, une activité qui est en partie réalisée par la sécrétion de divers facteurs de croissance et de cytokines. Ces messagers chimiques, y compris le bFGF, le VEGF, l'IL-6 et l'IL-1 contrôlent de nombreux processus cellulaires tels que l'expression des gènes d'hormones. Notre intérêt est de déterminer si la communication entre les cellules FS contribue à leur activité régulatrice. Dans notre étude, nous avons utilisé la lignée cellulaire TtT/GF qui partage de nombreuses caractéristiques morphologiques, physiologiques et biochimiques avec les cellules FS.

Les jonctions lacunaires/communicantes sont formées par l'association de deux connexons de cellules adjacentes qui unissent le cytoplasme des cellules connectées et permet la diffusion de petites molécules. Chaque connexon est formé par l'oligomérisation de six protéines connexine (Cx) de la famille $\alpha$, $\beta$ ou $\gamma$. Les connexons, intégrés dans la membrane d'une vésicule du cytoplasme, se migrent vers la membrane cellulaire où ils s'incorporent dans la couche bilipidique.

L'expression de la Cx43 ($\alpha$) par les cellules FS est régulée en réponse à des facteurs de croissance et des cytokines. Des changements dans le microenvironnement de l'hypophyse

antérieure causés par des molécules de signalisation sont susceptibles de modifier la Cx43, en particulier l'état de phosphorylation de la protéine. Ces modifications de la Cx43 peuvent ensuite déclencher des changements du comportement de jonctions lacunaires/communicantes formées par la Cx43, comme leur perméabilité et le renouvellement de la protéine Cx43.

Les tissus expriment généralement plus d'un type de connexine. Jusqu'aujourd'hui, la Cx43 est la seule connexine à avoir été identifiée dans les cellules FS. Le cristallin exprime les connexines α: Cx43, Cx46 et Cx50. Leur expression est modulée par des facteurs de croissance. Notre hypothèse de travail a été de vérifier si la Cx46 et la Cx50 étaient exprimées par les cellules FS et si celles-ci contribuaient au rôle modulateur des cellules FS hypophysaires.

Dans cette étude, nous avons identifié et caractérisé la Cx46 et la Cx50 dans la lignée cellulaire TtT/GF. Nous avons identifié les produits de transcription de Cx46 et de Cx50 par la technique d'analyse northern blot (*PCR*). Par la suite, les protéines Cx46 et Cx50 ont été identifiées en utilisant des anticorps dans des analyses western blot. Par microscopie confocale, nous avons déterminé la co-localisation de la Cx46 avec certaines marqueurs d'organites : réseau *trans*-Golgien, endosomes précoces et lysosomes. La Cx50 co-localise avec des marqueurs du réticulum endoplasmique, du réseau *cis*-Golgien et des endosomes précoces. Un protocole d'isolation des membranes résistantes aux détergents non-ionique a révélé que la Cx46 et la Cx50 n'étaient pas associées à des radeaux lipidiques ni aux cavéoles. Cependant, la microscopie confocale a montré une co-localisation cytoplasmique de la Cx50 et de la flotilline-1.

Nous avons poursuivi l'étude sur la localisation de la Cx46 dans le noyau en utilisant une technique d'isolation des fractions enrichies en noyau. Nous avons établi que plusieurs isoformes de la Cx46 sont exclusivement associées au noyau. De plus, avec la microscopie confocale nous avons démontrée une co-localisation de la Cx46 avec un marqueur du nucléole/corps de Cajal.

Nous avons démontré un effet du bFGF sur l'expression temporelle de la Cx46 et de la Cx50. L'expression de la Cx46 diminue au cours de longues expositions au bFGF tandis que les niveaux de Cx50 augmentent de façon transitoire au cours du traitement. Dans une autre étude nous avons démontré des changements importants dans les niveaux de la Cx46 et de la Cx50 dans l'hypophyse antérieure des visons durant le cycle de reproduction annuel.

Notre étude démontre que les cellules FS expriment la Cx46 et la Cx50. Nous avons aussi établi que la Cx46 et la Cx50 sont localisées dans différentes structures sous-cellulaires, ce qui suggère des rôles différents dans les cellules FS pour ces protéines de jonction lacunaire/communicante. Il est possible que la Cx46 et la Cx50 ne jouent pas un rôle majeur dans la communication intercellulaire dans les cellules FS quiescentes. Nos résultats suggèrent que la Cx46 et la Cx50 peuvent avoir d'autres fonctions : des isoformes de la Cx46 peuvent contribuer à la biogenèse des ribosomes tandis que la Cx50 pourrait avoir un rôle dans la communication dans les cellules stimulées au bFGF. Nos études établissent une base pour des recherches futures.

Mots clés: Cx, Connexines, jonction lacunaire, jonction communicante, cellules folliculo-stellaires, TtT/GF, hypophyse antérieure, bFGF, vison.

# Summary

The folliculo-stellate (FS) cells of the anterior pituitary are star-shaped and extend long cytoplasmic processes forming pseudo-follicles encircling hormone-secreting cells. Dispersed throughout the anterior pituitary gland, FS cells are joined to form a continuous three dimensional network through communicating gap junctions. One of the primary roles of FS cells is the maintenance of the anterior pituitary microenvironment, accomplished through the expression and secretion of various growth factors and cytokines. These chemical messengers, including bFGF, VEGF, IL-6 and IL-1 mediate a range of cellular processes such as hormone gene expression. Our aim is to study whether intercellular communication among FS cells contributes to the modulatory activity of the FS cells within the anterior pituitary gland. To pursue this, we use the TtT/GF cell line that shares many morphological, physiological and biochemical characteristics with FS cells.

Gap junctions are formed by the joining of two connexons/hemichanels from adjacent cells that link their cytoplasms allowing for the passive diffusion of small molecules. Connexons/hemichannels are themselves formed by the oligomerization of six connexin (Cx) proteins from the family α, β or γ, which then migrate into the lipid bilayer of the cell membrane.

FS cells express Cx43 (α-connexin), which is regulated in response to growth factors and cytokines. Changes in the anterior pituitary microenvironment due to signaling molecules results in modifications to Cx43, particularly in the phosphorylation status of the protein. Such

alterations yield alterations in the physiological behaviour of Cx43 gap junctions such as permeability and turnover.

Tissues generally express more than one connexin type and to date, Cx43 has been the sole connexin to be identified in FS cells. The ocular lens expresses the α-connexins: Cx43, Cx46 and Cx50, which are modulated by growth factors that are also present in the anterior pituitary. Based on these facts, we hypothesize that Cx46 and Cx50 are also expressed by the FS cells and contribute to the FS modulatory role in the anterior pituitary gland.

In the present study, we have identified and characterized Cx46 and Cx50 in the TtT/GF cell line. We identified Cx46 and Cx50 transcripts through northern blots and identified the corresponding protein products using antibodies and western blot analyses. Through confocal microscopy, we determined that Cx46 co-localized with the organelle markers: *trans*-Golgi, early endosomes and lysosomes. Cx50 co-localized with markers for the ER, *cis*-Golgi and early endosomes. An isolation procedure using a non-ionic detergent we showed that neither Cx46 nor Cx50 were associated to lipid rafts or caveolae. However, confocal microscopy showed a cytoplasmic co-localization between Cx50 and flotillin-1.

We pursued a finding that localized Cx46 to the nucleus and using a nuclear isolation technique, demonstrated that several isoforms of Cx46 are exclusively located in the nuclear compartment. Furthermore, with confocal microscopy we found a co-localization of Cx46 with a nucleolus/coiled body marker.

We demonstrated an effect of bFGF on the temporal expression patterns of Cx46 and Cx50 and showed that Cx46 levels decreased over longer exposures to the growth factor while Cx50 levels transiently increased. Lastly, drastic changes were noted in an *in situ* study of Cx46 and Cx50 in the male and female mink anterior pituitary during the annual reproductive cycle.

Our study indicates that addition to Cx43, FS cells also express Cx46 and Cx50. We also demonstrated that Cx46 and Cx50 localize to different sub-cellular structures, suggesting different roles in the FS cells. While they may not play a major role in intercellular communication in quiescent FS cells, our results suggest that Cx46 and Cx50 may serve other functions: Cx46 isoforms may contribute to ribosome biogenesis and Cx50 may have communication-related responsibilities in stimulated cells. Importantly, our identification and characterization studies provide a foundation on which future studies can be built.

Key words: Cx, Connexin, gap junction, folliculo-stellate cells, TtT/GF, anterior pituitary, endocrinology, bFGF, mink.

# List of tables

# List of figures

# List of abbreviations

3-D – 3-Dimensional

ACTH – Adrenocorticotropic hormone

ATP – Adenosine triphosphate

bFGF – Basic fibroblast growth factor

C-terminal – Carboxyl-terminal

$Ca^{2+}$ – Calcium ion

cAMP – Cyclic adenosine monophosphate

cDNA – Complementary DNA

CRH – Corticotropin-releasing hormone

Cx – Connexin

DAG – 1,2-diacylglycerol

DIG – Detergent-insoluble glycolipid

ER – Endoplasmic reticulum

FGF – Fibroblast growth factor

$FGF_R$ – Fibroblast growth factor receptor

FITC – Fluorescein-5-isothiocyanate

FS Cells – Folliculo-stellate cells

FSH – Follicle-stimulating hormone

GAPDH – Glyceraldehyde-3-phosphate dehydrogenase

GFAP – Glial fibrillary acidic protein

GH – Growth hormone

GHRH – Growth hormone-releasing hormone

GnRH – Gonadotropin-releasing hormone

HPRT-1 – Hypoxanthine phosphoribosyl transferase-1

IL – Interleukin

$IP_3$ – Inositol 1,4,5-triphosphate

kDa – kilo-Daltons

LH – Lutenizing hormone

MEF – Mouse embryonic fibroblast

MHCB – Myosin heavy chain IIB

mRNA – Messenger RNA

NO – Nitric oxide

No-RT – No reverse transcriptase

NPC – Neural progenitor cells

N-terminal – Amino terminal

PACAP – Pituitary adenylate cyclase-activating peptide

PBS – Phosphate buffered solution

PKA – Protein kinase A

PKB – Protein kinase B

PKC – Protein kinase C

PLC – Phospholipase C

PRL – Prolactin

PI3 – Phosphatidylinositol-3

$PIP_3$ – Phosphatidylinositol-3,4,5-triphosphate

POD – Peroxidase

RER – Rough endoplasmic reticulum

SDS-PAGE – Sodium dodecyl sulfate polyacrylamide gel electrophoresis

siRNA – Small interfering RNA

SUMO – Small-ubiquitin like modifier

T4 – Thyroxine

T3 – Triiodothyronine

TGF-β – Transforming growth factor β

TRH – Thyrotropin-releasing hormone

TRITC – Tetramethylrhodamineisothiocyanate

TSH – Thyroid-stimulating hormone

WGA – Wheat germ agglutinin

VEGF – Vascular endothelial growth factor

# Dedication

The work contained within this manuscript is dedicated

to my mother, Norma Garcia-Pastor

and to my father, Arnaldo Garcia.

# Words of gratitude

I am deeply grateful to my research supervisors Dr Maria Leiza Vitale and Dr R.-Marc Pelletier, who have given me the opportunity to conduct research under their supervision and who have also provided me with the training and skills that will serve me in all aspects of life. Working for them was an enriching, stimulating and rewarding experience.

Thank you to my colleagues Ahmed Barry and Dr Casimir Akpovi who, throughout the years, have helped me enormously with my research through insight and support. Being in the lab with both of you is something I looked forward to everyday. I am also thankful for the technical assistance that was provided to me by Dr Li Chen. Her willingness to share her expertise and knowledge helped me tremendously in completing my research project.

I am grateful for the financial assistance/scholarship that was awarded to me by the Faculty of Medicine allowing me to further pursue this research project. Furthermore, I acknowledge funding of the project by the NSERC (Natural Sciences and Engineering Research Council).

# Table of contents

# 1. INTRODUCTION

## 1.1. The pituitary gland

Located at the base of the skull embedded within the sphenoid bone, the pituitary gland is a critical relay station for endocrine functions in vertebrates. The gland is in intimate physical and functional association with the hypothalamus, from which it receives and relays chemical messages. This close relationship of both the neural and endocrine systems is demonstrated not only anatomically, by the presence of neural tissue in this endocrine gland but also by the physiological influence of hypothalamic secreting factors on the function of the pituitary gland.

### 1.1.1. Pituitary gland embryonic development

The adult pituitary gland results from the fusion of two separate tissues during embryogenesis, the adenohypophysis develops in the embryo starting from oral ectodermal tissue. The hypophyseal placode is the first primitive structure to develop from the oral ectoderm. As it grows, it folds upon itself dorsally to form Rathke's pouch, the succeeding structure in this developmental process. Rathke's pouch grows towards the evaginating infundibulum (forming the neurohypophysis), eventually becoming a distinct structure as it separates from the oral ectoderm (Rizzoti and Lovell-Badge 2005). Adenohypophyseal progenitor cells will differentiate into hormone secreting cells. As its name implies, the neurohypophysis, develops from the neural ectoderm during a time frame concurrent with that of the adenohypophysis. The developmental events begin with an evagination from the floor of the diencephalon eventually forming a funnel-shaped process known as the infundibulum that will extend towards Rathke's pouch (Figure 1).

The sphenoid bone will develop around the gland creating the *sella turcica* in the process (Drouin 2011).

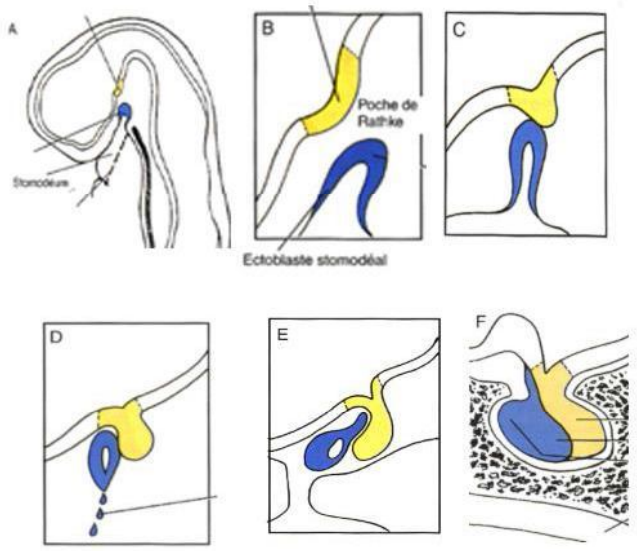


**Figure 1.** Embryological development of the pituitary gland (Larsen 2003).

Cell signalling pathways and transcription factors play critical roles in pituitary organogenesis and mediate the anatomical events that occur throughout this process. The early formation of Rathke's pouch, for example, is highly dependent on the pituitary homeobox factors, Pitx-1 and -2 (Rizzoti and Lovell-Badge 2005). The combined disruption of both transcription factors results in the cessation of adenohypophyseal development at a very early stage (Drouin 2011). Similarly, the differentiation of progenitor cells into hormone-secreting cells is also reliant on signalling pathways and transcription factors. For instance, the Notch signalling pathway regulates the expression of transcription factors that retain the multipotency of pituitary progenitor cells and must therefore be silenced to induce their terminal differentiation. In the

eventuality that the activity of Notch pathway proteins is sustained, multiple lineages will fail to fully differentiate (Zhu, Wang et al. 2007).

### 1.1.2. Anatomy and physiology

The adenohypophysis and neurohypophysis formed during embryogenesis also serve as the two major anatomical divisions in the gland. The adenohypophysis is subdivided into the *pars distalis*, *pars tuberalis* and *pars intermedia*. The *pars distalis* occupies the anterior-most portion of the gland while the *pars tuberalis* wraps around the infundibulum; together, these two subdivisions form the anterior pituitary. Dorsal to the *pars distalis* is the *pars intermedia*, which contains a number of cysts amassing to form Rathke's cleft, an embryological remnant of the lumen of Rathke's pouch. The neurohypophysis occupies the posterior portion of the gland and is continuous cranially to the hypothalamus. It is divided to include the median eminence, the infundibulum and the *pars nervosa*, with the later being the sole component of the posterior pituitary gland (Mizeres 1981, Junqueira, Carneiro et al. 1986) (Figure 2).

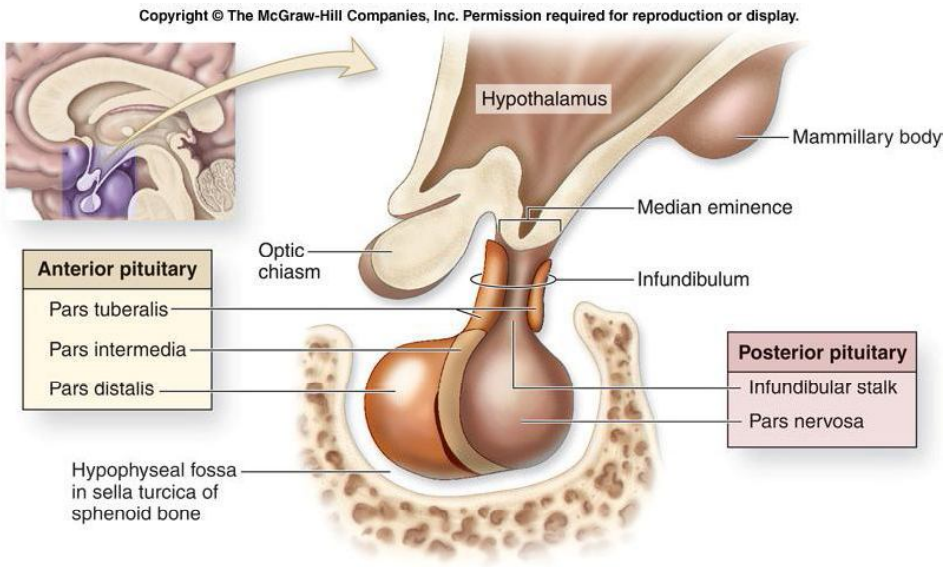


**Figure 2.** Pituitary gland anatomy and localization within the skull (McKinley and O'Loughlin 2012).

Being an endocrine organ, the vascularisation of the pituitary gland is essential for its functioning. The gland as a whole, receives its blood from the superior and the inferior hypophyseal arteries, the latter of which supply the neurohypophysis. The superior hypophyseal arteries feed the adenohypophysis and also form the hypophyseal-portal vascular system, a vascular network critical to the proper functioning of this portion of the gland. This system begins with the right and left superior hypophyseal arteries that will spread out to form the primary capillary plexus within the median eminence; a location where they are in close association with the axon terminals of the neuro-secretory parvicellular neurons. The capillaries form portal vessels that first run along the pituitary stalk then divide again a secondary capillary plexus within the anterior lobe (Junqueira, Carneiro et al. 1986). This provides a “natural” route for trophic/inhibitory hypothalamic hormones to be released into the primary plexus, travel down the portal vessels and arrive at the secondary plexus where the capillaries surround the target

endocrine cells. Ultimately, blood from both the adenohypophysis and neurohypophysis drains into dural sinuses via venous vessels (Junqueira, Carneiro et al. 1986).

The synthesis and release of the hormones, adrenocorticotropic hormone (ACTH), thyroid-stimulating hormone (TSH), follicle-stimulating hormone (FSH), lutenizing hormone (LH), growth hormone (GH) and prolactin (PRL), is the primary function of the anterior pituitary gland and is a process rigorously controlled by the hypothalamus and systemic factors. The neurosecretory neurons of the hypothalamus synthesize and release hypophysiotrophic hormones that will subsequently trigger or inhibit anterior pituitary hormone synthesis and secretion. This process begins with the synthesis and storage of hypophysiotrophic hormones by hypothalamic neurosecretory cells. Upon stimulation, these factors will be released from the axonal endings of the neurons in the median eminence into the primary capillary plexus of the hypophyseal-portal vascular system where they are carried to the secondary plexus in the *pars distalis*. Some hypophysiotrophic hormones are: thyrotropin-releasing hormone (TRH), dopamine, growth hormone-releasing hormone (GHRH), somatostatin, gonadotropin-releasing hormone (GnRH) and corticotropin-releasing hormone (CRH). Each physiotrophic hormone exerts a stimulatory or inhibitory effect on a specific hormone-secreting cell type in the anterior pituitary gland and several (TRH and GnRH) will affect more than one cell type (Brook and Marshall 2001) (Figure 3).

Feedback loops that ultimately directly or indirectly act on the anterior pituitary also modulate hormone synthesis and release in this gland. As a result of the action of anterior pituitary hormones, target glands will synthesize and secrete their own hormones that, apart from

exhibiting a primary physiological role, return to the hypothalamo-pituitary axis to reduce (negative feedback) or increase (positive feedback) the secretion of the hypothalamic or pituitary factor that initially resulted in their release. Thyroxine (T4) and triiodothyronine (T3) are synthesized and released by the thyroid gland in response to TSH. Once released into circulation, aside from their systemic effect on metabolism, T4 and T3 act in a negative feedback manner at the level of the hypothalamus by reducing the secretion of TRH. The thyroid hormones also act further down the hypothalamo-pituitary axis, by reducing the sensitivity of thyrotrophs to TRH, thereby decreasing the secretion of TSH (Brook and Marshall 2001, Rhoades and Bell 2009). An example of positive feedback can be observed in the female for a brief period just prior to ovulation. LH secretion from the anterior pituitary will result in an increased ovarian production of oestrogen that then influences the pituitary gonadotrophs by increasing production of LH. In this particular physiological state, LH stimulates its own production and secretion via the ovary and estrogen hormones (Heffner and Schust 2010).

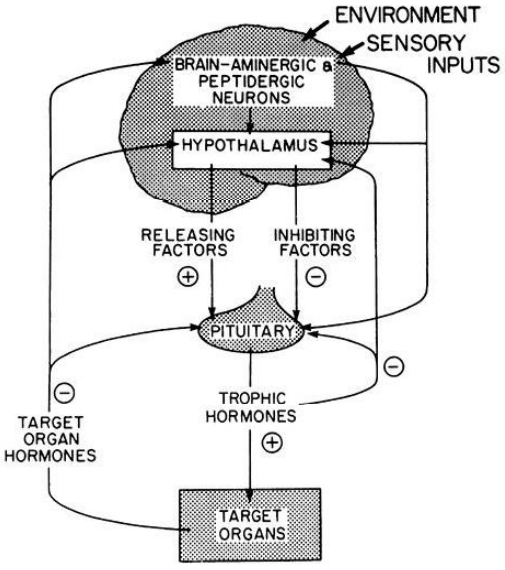


**Figure 3.** Illustration of positive and negative feedback mechanisms of target organ factors on the hypothalamic-pituitary axis (Rudolph 2011).

In addition to the hypophysiotrophic hormones, anterior pituitary secretory cells are also strongly influenced by a wide variety of paracrine messengers that are synthesized and secreted directly within the gland. These are present in a variety of chemical forms including: small molecules (Ex: nitric oxide (NO) and adenosine), and an assortment of proteins that include cleavage products (common α-subunit of glycoproteins LH, FSH and TSH) and peptides (follistatin and vasoactive intestinal peptide (VIP)). The general effect on hormone secretion of many of these paracrine messengers is similar to that of the hypophysiotrophic hormones, in that secretion is either decreased or increased in response to a particular messenger. For instance, adenosine (secreted by folliculo-stellate cells) has been shown to decrease FSH secretion from gonadotrophs (Yu, Kimura et al. 1998). Furthermore, paracrine messengers exert their effects on hormone secretion by other means including: increasing endocrine cell proliferation (mitogenic effect) (ex: insulin-like growth factor I (IGF-I) and basic fibroblast growth factor (bFGF)), hormone-secreting cell hyperplasia (galanin) and stimulation of endocrine cell differentiation (common α-subunit of glycoproteins LH, FSH and TSH). The fact that the production of these factors is assumed by the anterior pituitary hormone-secreting cells or the folliculo-stellate cells (to be discussed in subsequent sections), suggests a local control mechanism amongst adenohypophyseal endocrine cells (Schwartz 2000).

The secretion of the neurohypophyseal hormones oxytocin and vasopressin occurs through a mechanism different to that of the adenohypophysis. The cell bodies of the neurosecretory cells producing oxytocin and vasopressin are respectively located in the paraventricular and supraoptic nuclei of the hypothalamus, while their axons descend through the infundibulum into

the *pars nervosa*. After synthesis in the cell bodies, oxytocin and vasopressin will be stored in axonal vesicles awaiting their release triggered by specific stimuli (Brook and Marshall 2001).

### 1.1.3. Morphology of adenohypophyseal cells

The major cell types in the anterior pituitary are the granular, hormone secreting cells. Of these, the somatotrophs are the most abundant accounting for close to 50% of anterior pituitary cells. In humans, they are most abundant in the lateral portion of the anterior lobe, are of medium size and are spherical or oval in shape. Lactotrophs, which constitute 10 – 25% of anterior pituitary cells are scattered throughout the anterior lobe but are mostly concentrated in areas close to the posterior lobe. They are generally seen in two forms: angular or elongated of small to medium size, or large and of polyhedral shape. Corticotrophs are primarily located in the central region of the anterior lobe and overall represent 10 – 15% of anterior pituitary cells. They exhibit an oval shape and are of medium to large size. The thyrotropes are the least abundant cell type in the anterior pituitary, representing less than 10% of all cells in the gland; they are large and oval or irregular in shape and localize to the anteromedial area of the *pars distalis*. Gonadotrophs, accounting for 15 – 20% of anterior pituitary cells, can be found throughout the *pars distalis* where they adjoin capillaries and are frequently in close association with lactotrophs, furthermore, they also localize to the *pars tuberalis* (Imura 1985, Heaney and Melmed 2004). Another, non-endocrine cell type can also be found in the gland, the folliculo-stellate cells, which are the topic of the current study.

### 1.1.4. The folliculo-stellate (FS) cells

Initially described with the electron microscopy study by Rinehart and Farquhar (1953), the FS cells account for 5 – 10% of all anterior pituitary cells and are thoroughly distributed through the *pars distalis*. They are star-shaped (hence their name) with long cytoplasmic processes forming pseudo-follicles by surrounding endocrine cells. Unlike the hormone-secreting cells of the gland, FS cells are agranular. Other morphological aspects of these cells include the presence of an abundance of type-III vimentin intermediate filaments in their cytoplasm (Cardin, Carbajal et al. 2000). FS cells were initially believed to originate from the ectoderm of the oral cavity, implying that they are a derivative of Rathke's pouch cells and share a common progenitor with their endocrine hormone-secreting neighbours. However, it was later established that FS cells express the neuroglial cell-specific marker GFAP (Glial fibrillary acidic protein), implying a neuroectodermal origin to the FS cells (Inoue, Couch et al. 1999). Another marker that had facilitated the identification of FS cells is S-100, a calcium-binding protein not expressed by anterior pituitary endocrine cells but typically expressed by FS cells (Nakajima, Yamaguchi et al. 1980).

*In vivo*, FS cells have been shown to alter their morphology in response to different hormonal environments. Cardin et al, (2000) have described two distinct S-100 positive cell types (I and II) in the mink (*Mustela vison*) that are also suspected to carry out different physiological activities. The type-I cell was characterized by a stellate shape and were most prevalent during physiological periods characterized by high serum and anterior pituitary PRL levels and by low FSH and LH levels. The type-II cell typically lacked cytoplasmic projections and exhibited a rounded morphology. Furthermore, their presence was most noted during periods when serum

and anterior pituitary PRL levels were low and FSH and LH levels were high. It has been proposed that the endocrine milieu of the anterior pituitary could influence the transformation of one cell type to the other (Cardin, Carbajal et al. 2000). Similarly, studies of the equine anterior pituitary gland throughout its annual breeding cycle have confirmed a morphological change in the FS cells (Henderson, Hodson et al. 2008).

While the FS cells have a variety of functions in the anterior pituitary, it is largely accepted that they are responsible for the maintenance of the anterior pituitary microenvironment. FS cells were initially ascribed the function of pituitary scavengers involved in the phagocytosis and degradation of apoptotic cells and extracellular debris (Devnath and Inoue 2008). However, the major function of FS cells is the secretion of a variety of growth factors and cytokines that act in both autocrine and paracrine manners. These chemical messengers include bFGF, Vascular endothelial growth factor (VEGF), Interleukin-6 (IL-6) and IL-1 which mediate a plethora of functions ranging from immune system modulation to hormone gene regulation (Allaerts and Vankelecom 2005, Herkenham 2005).

In addition, several *potential* functions have also been attributed to FS cells. The first of these is based on the close physical association of FS cell extensions and pituitary capillaries and suggests that FS cells act as an intermediary in the transport of nutrients and oxygen from capillaries to endocrine cells, a function similar to that of astrocytes in the central nervous system (Inoue, Couch et al. 1999, Inoue, Mogi et al. 2002). Furthermore, FS cells were found to express Pitx-1, a transcription factor common to all pituitary cells. This discovery led to the hypothesis that FS cells may in fact be pituitary stem cells with the capacity to differentiate into endocrine

cells of the adenohypophysis (Tremblay, Marcil et al. 1999, Devnath and Inoue 2008, Drouin 2011). FS cells have also been shown to express adenohypophyseal-hormone receptors, specifically: the receptors for Thyroid-Stimulating Hormone ($TSH_R$), Growth Hormone ($GH_R$) and Adenocorticotropin ($ACTH_R$). This finding may further implicate the FS cells in a local, paracrine-driven control mechanism (Brokken, Leendertse et al. 2004).

The manner in which FS cells are organized within the anterior pituitary is also a critical feature with regard to intercellular communication throughout the gland. Studies of the gland by electron microscopy led to the initial proposal that the FS cells form an extensive 3-D (3-Dimensional) network throughout the anterior pituitary (Vila-Porcile 1972). This proposal has since been substantiated by confocal microscopy and electrophysiology (Fauquier, Lacampagne et al. 2002). The FS cells are arranged in a mesh-like fashion and it is within the confines of this mesh that the hormone-secreting endocrine cells dwell. Importantly, this FS cell network is physically continuous through connexin43-mediated (Cx43) gap junction channels (Morand, Fonlupt et al. 1996). Furthermore, at several points throughout this network, heterologous connections have been described between FS cells and lactotrophs (Morand, Fonlupt et al. 1996). Physiologically, the FS network plays the role of an information highway capable of rapidly transmitting chemical messages relatively long distances throughout the gland. Small signaling molecules such as cytokines, and growth and immune factors produced by FS cells, can be released and propagated locally through gap junctions. Alternatively, signalling in the form of a cytosolic increase in Calcium ion ($Ca^{2+}$) concentration has been shown to travel extensive distances (millimeters). FS cells are capable of spontaneously generating $Ca^{2+}$ signals that are subsequently propagated throughout the network in a regenerative, pulsatile fashion, as is seen

with action potentials (Fauquier, Guerineau et al. 2001). This spontaneous generation of $Ca^{2+}$ signals has been proposed to synchronize cellular activities within the anterior pituitary and to contribute to the autonomous, hypothalamus-independent functioning of the anterior pituitary (Devnath and Inoue 2008). Gap junctions have been shown to play an crucial and vital role in the formation of the FS cell network, especially in the transmission of $Ca^{2+}$ signals since their experimental blockage severely compromises signal transmission (Fauquier, Guerineau et al. 2001). Furthermore, Cx43-mediated gap junctions between FS cells have been shown to be highly responsive to FS cell-secreted growth factors and cytokines (Fortin, Pelletier et al. 2006, Meilleur, Akpovi et al. 2007).

## 1.2. Gap junctions

Gap junction channels result from the pairing of connexons/hemichannels, each being a contribution from adjacent cells. Each connexon/hemichannel is made up of connexin proteins, also known as the elemental structures of gap junction channels. Until now, both rodents and humans have been found to express approximately twenty connexin variants that can be classified into sub-groups based on amino acid sequence homology and oligomerization: α, β, γ and unclassified (Evans and Martin 2002) (Figure 4).

Table 1. Properties of mouse and human connexins subject to characterization. Other human connexin genomes recently identified include Cx25 (mol. mass 25, 892 D unclassified, Cx58 (mol. mass 58, 842 D unclassified) and Cx62 (mol. mass 61, 871 D, α-class). Cx26, 30 and 46 are located close together on chromosome 14; Cx40 and 50 are located on chromosome 3 (reproduced from Willecke *et al.* 2002).

| Connexin | Sub-group | Chromosome | mRNA [kb] | Protein [aa] | Cyt. Loop [aa] | C-Term. [aa] | Phosph. |
|---|---|---|---|---|---|---|---|
| Cx26 | β | 14 | 2.4 | 226 | 35 | 18 | – |
| Cx29 | | 5 | 4.4 | 258 | 30 | 50 | |
| Cx30 | β | 14 | 2.0, 2.3 | 261 | 35 | 55 | |
| Cx30.3 | β | 4 | 1.8, 3.2 | 266 | 30 | 65 | |
| Cx31 | β | 4 | 1.9, 2.3 | 270 | 30 | 65 | |
| Cx31.1 | β | 4 | 1.6 | 271 | 30 | 70 | |
| Cx32 | β | X | 1.6 | 283 | 35 | 75 | + |
| Cx33 | α | X | 2.3 | 286 | 55 | 60 | |
| Cx36 | | 2 | 2.9 | 321 | 100 | 50 | |
| Cx37 | α | 4 | 1.7 | 333 | 55 | 105 | + |
| Cx40 | α | 3 | 3.5 | 358 | 55 | 135 | + |
| Cx43 | α | 10 | 3.0 | 382 | 55 | 155 | + |
| Cx45 | γ | 11 | 2.2 | 396 | 80 | 150 | |
| Cx46 | α | 14 | 2.8 | 417 | 50 | 190 | + |
| Cx47 | γ | 11 | 2.5 | 437 | 105 | 155 | |
| Cx50 | α | 3 | 8.5 | 441 | 50 | 210 | + |
| Cx57 | α | 4 | 3.5 | 505 | 55 | 275 | |

**Figure 4.** Table of human and mouse connexin gene and protein information (Evans and Martin 2002).

### 1.2.1. Gap junction structure

The connexin proteins possess a highly conserved tertiary structure containing intracellular amino- (N) and carboxyl- (C) termini, joined by four transmembrane domains, which themselves are linked by a total of three loops, two being extracellular and one on the cytoplasmic side (Evans and Martin 2002) (Figure 5).

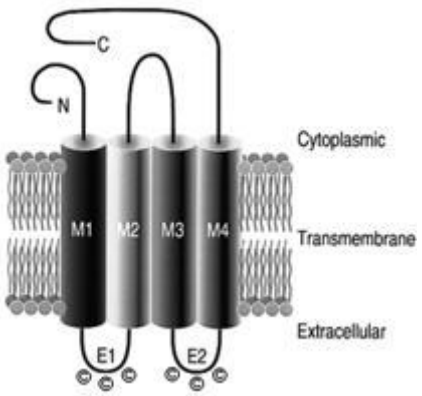


**Figure 5.** Schematic of connexin protein topology (Sohl and Willecke 2004).

Throughout the connexin family, the N-terminal is a conserved portion of the protein presenting little variation in both amino acid sequence and length. Functionally, this domain is important for the proper insertion of the protein into the membrane during translation; a role that is also shared by the first of the four transmembrane α helices (Evans and Martin 2002). The third transmembrane domain primarily serves a structural function and contributes to the wall of the connexon channel. In addition, the transmembrane domains have been suggested to be required for the oligomerization of individual connexin proteins during the formation of a connexon (Evans and Martin 2002). The extracellular loops are arranged as anti-parallel β-sheets, each containing three cysteine residues that form disulfide bridges between the two loops of a connexin protein. The loops are important for the docking process between one connexon and its pair in an adjacent cell (Evans and Martin 2002). The identity and distinctiveness of a connexin family member is derived primarily from its C-terminal and to a lesser degree, the cytoplasmic loop that shows the greatest variation in amino acid sequence and length (Mese, Richard et al. 2007). The C-terminal is also the portion of the protein that will undergo post-translational

modifications and processing in response to stimuli such as phosphorylation (Berthoud, Beyer et al. 1997).

The connexon/hemichannel is an assembly of six connexin proteins arranged in a cylinder with a hollow core. The completed connexon/hemichannels will be shipped to the membrane where it will eventually join another connexon/hemichannel from a neighbouring cell to form a gap junction channel or remain unpaired. Most cell types express more than one connexin member. Connexons can have a homomeric or heteromeric composition (Mese, Richard et al. 2007). Heteromeric connexons are composed of two different connexins of the same sub-group. Alternatively, a gap junction can be composed of two identical connexons, thereby making it homotypic (bearing in mind that these connexons may be heteromeric, although identical); or can be the product of two different connexons and therefore classifying it as heterotypic (Figure 6). Combining different connexins or connexons results in the formation of junctions with unique biochemical properties thus extending their functional capabilities (Jiang and Goodenough 1996).

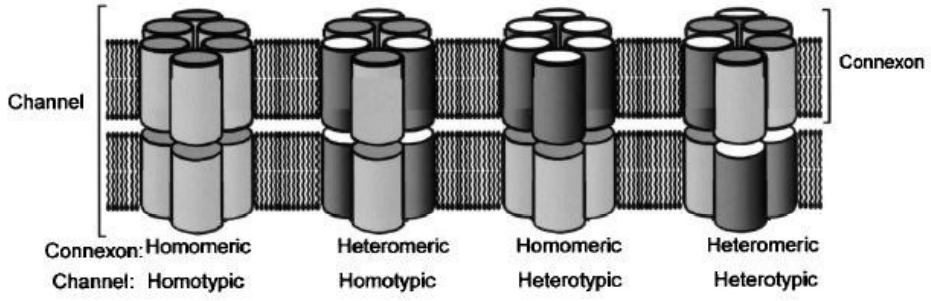


**Figure 6.** Diagram of homo- and heteromeric connexons and homo- and heterotypic gap junctions (Evans and Martin 2002).

### 1.2.2. Gap junction and connexon/hemichannel functions

Gap junctions connect the cytoplasms of two adjacent cells, through a tunnel formed by the individual joined connexons. The tunnels allow small molecules up to 1.5 kilo-Daltons (kDa) in size to passively travel from one cell to another (Kumar and Gilula 1996).

The permeability of gap junctions to small molecules was generally thought to be relatively non-selective whereby free passage would be granted to any ion or molecule equal to or smaller than 1 – 1.5 kDa (el-Fouly, Trosko et al. 1987). Although this has remained true to a certain extent, the varying permeability properties of different channels to metabolites and ions are increasingly apparent (Goldberg, Moreno et al. 2002). Of the metabolites and ions, one of the most studied is $Ca^{2+}$ (most likely due to their involvement in intracellular signalling), as well as several metabolites including Inositol triphosphate ($IP_3$, related to $Ca^{2+}$ signalling), signalling molecules: cyclic adenosine monophosphate (cAMP), and the cellular metabolites glucose and adenosine triphosphate (ATP) (Goldberg, Moreno et al. 2002, Medina and Tabernero 2005). Each ion and molecule endows individual gap junctions with a function more important than connecting two adjacent cells. The permeability of gap junctions to $Ca^{2+}$, $IP_3$ and other signalling molecules is strongly indicative of a role in the propagation of cellular messages including cell death and survival signals (Krysko, Leybaert et al. 2005). The passage of ATP, the currency of cellular energy, demonstrates a role of gap junctions in nutrient exchange. Gap junctions also couple cells electrically, allowing for such a signal to be disseminated considerable distances in relatively little time (Hestrin 2011). The selectivity of gap junctions composed of a particular connexin protein can also modulate gene expression post-transcriptionally between adjacent cells by means of their permeability to small interfering RNA (siRNA) molecules (Valiunas, Polosina

et al. 2005). In this context, siRNA molecules produced in one cell can travel within a group of cells to influence gene expression, provided the cells are joined by connexin-specific gap junctions.

Cell motility, especially with respect to development, and the cell transformation processes, has been shown to rely strongly on connexin expression (Li, Waldo et al. 2002). Specific connexin genes are expressed during precise periods of embryonic development and various studies have associated substantial defects with the perturbation of these genes. Embryonic expression of Cx43 by proepicardial progenitor cells, mediates (amongst other developmental events) the organized migration of these cells that will eventually differentiate to form critical coronary structures. In the absence of Cx43, the proepicardial progenitor cells were shown to have an altered directionality and motility (increased migrational velocity) that resulted in extensive structural defects in the coronary arteries and cardiac muscle (Li, Waldo et al. 2002, Rhee, Zhao et al. 2009).

Apoptosis and the regulation of cell death have been found to be influenced both by gap junctions and connexins. The "bystander effect" was a term introduced by Freeman et al. (Freeman, Abboud et al. 1993) used to describe a phenomenon whereby a cellular death signal (in this case a toxin) can spread from a small subset of cells to eventually encompass a larger cell mass, through gap junctions. This concept has since been extended to include any gap junction-permeable intermediates/second messengers that may trigger an apoptotic event including $Ca^{2+}$, $IP_3$ and cAMP. These factors, all released in abundant quantities during apoptosis, will passively travel through gap junctional channels into adjacent "bystander cells" effectively propagating an

apoptotic cascade (Krysko, Leybaert et al. 2005). Monomeric connexin proteins also appear to play a significant role in the signalling aspects of apoptosis, by direct interaction with apoptotic protein mediators. In human cancer cell lines, Cx26 and Cx43 have been co-localized with Bcl-2 proteins: Bak, Bcl-xL and Bax (Decrock, Vinken et al. 2009). Oddly, the transcriptional levels of both pro- and anti-apoptotic genes were affected in response to alterations in Cx43 expression (Decrock, Vinken et al. 2009). This contradictory observation makes it difficult to assign an inhibitory or inductive role to Cx43 with respect to programmed cell death.

Connexons/hemichannels, which remain unpaired, provide a gated passageway to the surrounding extracellular milieu and play several important cellular functions including the release of ATP and subsequent propagation of $Ca^{2+}$ waves. The mechanism for this process begins with an initial stimulus (a stressor) that causes the release of ATP. Extracellular ATP will then bind P2 purinergic receptors on a nearby cell that in turn, stimulates the production of $IP_3$ subsequently leading to the release of $Ca^{2+}$ from the endoplasmic reticulum (ER) (Lodish 2000). Changes in the intracellular $Ca^{2+}$ levels then lead to the opening of hemichannels and the ensuing release of ATP, allowing propagation of the signal (Goodenough and Paul 2003). This signalling has proven essential to a variety of physiological events ranging from neural development (Dale 2008) to cell division and differentiation in the retina (Pearson, Dale et al. 2005).

In addition to the communication roles attributed to gap junctions and connexon/hemichannels, there is experimental evidence demonstrating the involvement of connexon proteins in numerous non-conventional roles. The effect that specific connexin members have on cell growth and tumourgenicity is an example of this. Particularly, Cx32 and Cx43 have been reported to inhibit

cell growth and act as a tumour suppressor in a manner independent of hemichannel and gap junctional intercellular communication (Fujimoto, Sato et al. 2005, Jiang and Gu 2005, Langlois, Cowan et al. 2010). This has been supported by the fact that transformed cells were shown to have a decreased connexin expression and that cancer cell lines transfected with connexin genes exhibit a reduction in their growth rate and metastatic potential (Zhao, Han et al. 2011). Moreover, several of the connexins implicated in exhibiting these effects have been localized to the cell nucleus (Cx30 and Cx43) and were reported to be cleaved or truncated with the intent of isolating the C-terminal (Dang, Doble et al. 2003, Mennecier, Derangeon et al. 2008); a fact further supporting the claim that this phenomenon is not influenced by gap junctional communication. Under non-pathological conditions, connexin expression has been shown to promote mitosis. Cx50 is an example of this, whereby its expression during postnatal development is essential for ocular lens growth. The absence of Cx50 drastically reduces the mitotic index of developing lens cells resulting in micropthalmia (smaller eye and lens) (White, Goodenough et al. 1998, Sellitto, Li et al. 2003).

### 1.2.3. The life cycle of a gap junction

Connexins are relatively short-lived proteins with most having a half-life of around 1.5 – 5 hours (Laird 2005). Although the connexins follow a similar path from synthesis to degradation, variations in both the intermediate and ultimate fates of the proteins are known to exist.

The biosynthesis of connexin proteins commences in the rough endoplasmic reticulum (RER) where the protein is co-translationally inserted into the RER membrane (Mese, Richard et al. 2007). From this location to the *trans*-Golgi apparatus, there is a gradual oligomerization of

individual connexin proteins to form a connexon/hemichannel. In the case of homomeric channels, this process occurs spontaneously, whereas it is hypothesized that unidentified chaperone proteins are needed to oligomerize heteromeric connexins (Evans and Martin 2002). Connexons are then transported from the *trans*-Golgi in vesicles that travel along microtubules to eventually fuse with the plasma membrane. The connexon will diffuse laterally either towards an area of the plasma membrane unopposed by another cell where it will fulfill its functions as a connexon/hemichannel or towards a cell-cell contact area where it will dock with a compatible connexon/hemichannel in the adjacent cell forming a gap junction channel (Evans, De Vuyst et al. 2006). This pairing of connexons results in a 2 – 4 nanometres (nm) "gap" between the two cells visible by electron microscopy (Herr 1976). A newly formed gap junction will find itself on the outside of a gap junctional plaque. Gap junctional plaques are large aggregations of gap junction channels, where the "youngest" channels join the plaque at its periphery, gradually migrating to its centre. As younger channels join the plaque, the "older" ones are pushed to the centre where they are ultimately internalized into annular junctions (a type of vesicle) (Pelletier 1995, Jordan, Chodock et al. 2001). As opposed to the processes of assembly, gap junctions are not separated into connexons but rather, are entirely taken into annular junctions. Logically, this event indicates that annular junctions, also known as connexosomes, are composed not only of their own plasma membrane, but also of that of the adjacent cell to which they are joined (Leithe and Rivedal 2007). Annular junctions will either fuse directly with lysosmes or indirectly, by first maturing into early and late endosomes. Alternatively, certain connexins are ubiquitinated and degraded through the proteasomal pathway (Fortin, Pelletier et al. 2006, Leithe and Rivedal 2007). Autophagy, has also been shown to contribute to connexin and gap junction degradation,

specifically targeting connexin-containing vesicles from the secretory pathway or annular junctions from gap junctional plaques (Lichtenstein, Minogue et al. 2011) (Figure 7).

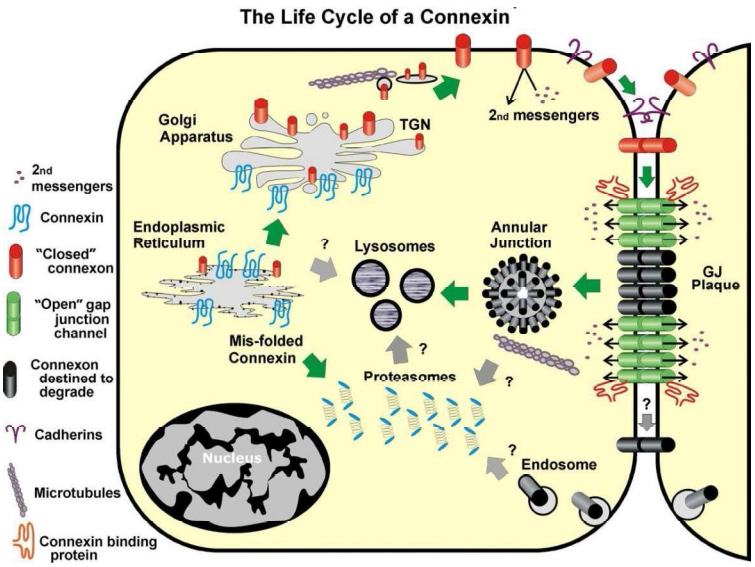


**Figure 7.** The life cycle of a connexin protein (Laird 2005).

Post-translational modifications represent a major event in the lifecycle of connexin proteins that serve to regulate various functional aspects of connexins and gap junctions. Turnover, coupling, conductance (gap junction channels), sub-cellular trafficking, degradation and assembly are all events that can be affected by post translational modifications targeting connexins and gap junctional channels. The phosphorylation status of connexin proteins is not only the most prevalent of modifications, but also serves as an indicator of physiological activity and localization (Fortin, Pelletier et al. 2006). Various stimuli, such as growth factors and cytokines, can significantly affect the phosphorylation status of a connexin by the addition or removal of a phosphate group via kinases and phosphatases, respectively (Meilleur, Akpovi et al. 2007). As previously mentioned, these actions occur predominantly on amino acid residues on the C-

terminal tail and intracellular loop. The functional consequences of a phosphorylation event are highly variable and are often specific to the phosphorylated residue, connexin family member and cell type. As will be discussed in subsequent sections (1.3.), an alteration in phosphorylation status is often a terminal event in a signaling cascade initiated by a stimulus. In addition to phosphorylation, intracellular loop and terminal amino acid residues on connexin proteins are also modified via nitrosylation and sumoylation (Straub, Billaud et al. 2011, Kjenseth, Fykerud et al. 2012). Nitrosylation, the attachement of a NO molecule to a cysteine amino acid, has been found to be especially relevant to endothelial and smooth muscle cell lines/tissue. In these settings, the permeability of Cx43 gap junctions has been shown to be altered in response to this particular covalent modification. Sumoylation, whereby a member of the small-ubiquitin like modifier (SUMO) protein family is attached to a lysine residue, has been often associated with nuclear proteins and that is linked to processes such as DNA repair and transcription. This post–translation modification, however, has also been documented to regulate Cx43 gap junctional channels and Cx43 protein levels (Kjenseth, Fykerud et al. 2012). As was seen with phosphorylation, nitrosylation and sumoylation can also bring about significant physiological changes via the modification of connexin proteins and gap junctional channels.

Not all connexins follow the above-described classical/conventional pathway. There exist alternative pathways as well as non-conventional functions that will localize connexins to unexpected parts of the cell. For example, Cx26, has been found to take a shortcut to the plasma membrane that completely bypasses the Golgi apparatus (Evans and Martin 2002). Furthermore, connexins do not always localize to the plasma membranes but have been unexpectedly located in a variety of cellular locations including the nucleus, where they are suspected to modulate

gene expression (Dang, Doble et al. 2003, Sanches, Pires et al. 2009). The inner mitochondrial membrane has also been found to house connexins (Cx43), more specifically, in the form of hemichannels/connexons that contribute to the uptake of potassium into the mitochondrial matrix in cardiomyocytes (Miro-Casas, Ruiz-Meana et al. 2009).

### 1.2.4. Connexin46 and connexin50

Cx46 and Cx50 are most notorious for their expression and importance in the ocular lens. Both connexins have been extensively studied with respect to the development of the lens and the maintenance of homeostasis. To date, Cx50 has not yet been described in other tissues of the body. Cx46 has been identified and studied in various other tissues including: cancerous breast epithelial cells, Schwann cells, bone osteoblastic cells and lung alveolar tissue (Chandross, Spray et al. 1996, Koval, Harley et al. 1997, Abraham, Chou et al. 1999, Banerjee, Gakhar et al. 2010).

The lens is an avascular, metabolically active organ that refracts light entering the eye onto the retina. It has three distinct regions: (1) a single layer of epithelial cells lining the anterior surface, (2) cortical fibre cells undergoing differentiation and (3) mature nuclear fibre cells. The cells in all three regions of the lens are connected by gap junctions. Cx43 is found between epithelial cells, Cx46 localizes to differentiating and mature fibre cells and Cx50 is expressed throughout both the lens epithelium and the lens fibre regions (Shakespeare, Sellitto et al. 2009). Together, these connexins allow the formation of an intercellular network that facilitates the uptake of nutrients from the surrounding aqueous humor and the elimination of waste products (Saleh, Takemoto et al. 2001). Mutations in Cx46 and Cx50 have been extensively documented especially with respect to ocular pathologies. Disruptions in the Cx46 gene have been shown to

result in the formation of nuclear cataracts (located in the central nucleus of the organ) (Gong, Li et al. 1997). Similar pathological features, pulverulent cataracts (literally meaning "dust-like"), have been noted following Cx50 mutations although these mutations are accompanied by microphthalmia (Dunia, Cibert et al. 2006). Although the cause for the later remains speculative (White, Goodenough et al. 1998, Gong, Cheng et al. 2007), apart from contributing to lens transparency Cx50 also plays a significant role in lens development.

The numerous studies on Cx46 and Cx50 in relation to ocular disease have revealed various aspects regarding their intracellular physiology.

Protein-protein interactions

Association of connexins with other proteins can reveal information on their post-translational status, cellular localization and involvement in signalling pathways. The connexin protein family bears a particular affinity for other cell junctions including claudins, occludins and cytoskeletal proteins including microtubules and catenins (Jiang and Gu 2005). While Cx46 and Cx50 have been found to interact with some of the "common connexin interactors", such as ZO-1 (Nielsen, Baruch et al. 2003), interactions with specific proteins differentiates Cx46 and Cx50 from each other and other members of the connexin family. Caveolin-1, a major constituent of caveolae and lipid rafts has been found to interact with Cx46, whereas Cx50's association with this protein remains a debated issue (Schubert, Schubert et al. 2002, Lin, Lobell et al. 2004). In the ocular lens, Cx46 and Cx50 interact with protein kinase C-γ (PKC-γ), causing a phosphorylation of the connexin proteins and alterations in the physical characteristics of the gap junctions (Saleh, Takemoto et al. 2001). These interactions and subsequent phosphorylation events are amplified

following oxidative stress (Lin, Lobell et al. 2004). Lastly, Cx46 and Cx50 can also interact with each other *in vivo,* an important fact especially during the formation of heteromeric connexins (Jiang and Goodenough 1996).

Post-translational modification and processing

Connexin phosphorylation represents one of the main manners that gap junction function is controlled. Cx46 and its homologues across several species are phosphorylated on threonine and serine residues on both their intracellular loop and C-terminal (Berthoud, Beyer et al. 1997, Wang and Schey 2009). Despite the fact that the exact phosphorylation sites remain putative and unconfirmed, bioinformatical analyses have revealed several consensus sequences throughout both aforementioned protein regions (Wang and Schey 2009). Casein kinases and protein-kinase C (PKC) isoforms have been shown to be responsible for these events (Saleh, Takemoto et al. 2001) that occur late in the life of the protein (Jiang, Paul et al. 1993). Furthermore, western blotting data from several rodent tissue and cell culture studies concur in reporting a Cx46 immuno-reactive band at 53 kDa and another at 68 kDA, corresponding to the non-phosphorylated and phosphorylated forms of the protein, respectively (Chandross, Kessler et al. 1996, Koval, Harley et al. 1997).

Connexin 50, also a phosphoprotein, is known to be phosphorylated on C-terminal serine and threonine residues in the lens by various kinases including PKC-γ, protein kinase A (PKA) and possibly, mitogen-activated protein kinase/ERK Kinase (MEK) (Lin, Lobell et al. 2004, Shakespeare, Sellitto et al. 2009, Liu, Ek Vitorin et al. 2011). Studies have reported various phosphorylation sites on the C-terminal (Wang and Schey 2009) and have indicated that serine-

395, a residue that is highly conserved in Cx50 proteins throughout several animal species has been confirmed to be phosphorylated by PKA *in vivo* (Liu, Ek Vitorin et al. 2011). These studies have shown that the physiological effects of Cx50 phosphorylation differ depending on the kinase responsible. Cx50 phosphorylation by PKC-γ resulted in an uncoupling of cortical fibre cells in the lens thereby reducing communication via Cx50 gap junctions between adjacent cells. In contrast, phosphorylation of Cx50 by PKA was found to enhance the permeability of gap junctions thereby promoting communication between adjacent cells in the lens (Liu, Ek Vitorin et al. 2011).

In addition to being phosphoproteins, Cx46 and Cx50 are also known to be truncated as part of their processing. Truncation occurs during the natural maturation of fibre cells of the ocular lens via calpain I and calpain II, two endogenous protein-processing proteases (Lin, Fitzgerald et al. 1997). Although the truncation sites and the localization of truncated connexins has been elucidated, the reasons for this specific form of processing remain unclear (Wang and Schey 2009).

## 1.3. Basic fibroblast growth factor

bFGF or fibroblast growth factor 2 (FGF-2) isolated in 1974 from pituitary and brain extracts and was initially described as a potent mitogen (Gospodarowicz 1974). It belongs to the FGF family comprising twenty-two members in mammals. FGF polypeptides function by binding to their receptors, which will initiate an intracellular signalling cascade via its intrinsic tyrosine kinase domain (Zhang, Ibrahimi et al. 2006) .

### 1.3.1. Ligand and receptor properties

The protein structure of bFGF contains various highly conserved domains, shared with other members of its family. Of these motifs is a highly conserved twenty-eight amino acid core that contains ten residues essential for the interaction of the peptide with its receptor (Ornitz and Itoh 2001). Heparin, needed for the efficient activation of the cascade, contains its own binding domain embedded within four of the receptor's twelve β-strands (Figure 8).

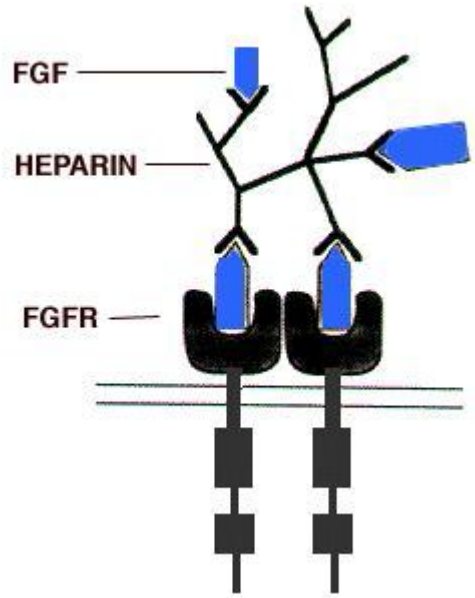


**Figure 8.** Illustration of FGF binding and receptor dimerization (Spivak-Kroizman, Lemmon et al. 1994).

Interestingly, unlike the other FGFs, bFGF does not contain an N-terminal signal sequence that would allow it to be actively secreted from the cell; nevertheless, it is found on the cell surface and in the extracellular matrix (Dvorak, Hampl et al. 1998). The exit of bFGF from the interior of the cell has been hypothesized to occur via several mechanisms including an alternative/non-classical exocytosis, through damaged plasma membranes and a mechanism mediated by ATP-binding cassette (ABC) transporters (Flieger, Engling et al. 2003). The "basic" component of its name derives from its basic isoelectric point (9.6) distinguishing it from its acidic counterpart, aFGF (acidic-FGF, also known as FGF-1) (Gospodarowicz, Ferrara et al. 1987).

Each of the five existing FGF receptors ($FGF_R$1-5) can be activated by different FGF peptides (Cotton, O'Bryan et al. 2008). Further adding to their diversity, $FGF_R$1-3 transcripts are subjected

to alternative splicing producing two isoforms of each of these receptors ($FGF_R$1- III b and c); ultimately, the result is a drastic change in affinity for a given FGF ligand (Ornitz and Itoh 2001).

The binding of bFGF to its receptor ($FGF_R$1-4) first requires the formation of a multimer comprising bFGF and heparin. As previously stated, heparin will bind both the ligand and receptor to stabilize the resulting structure (Dailey, Ambrosetti et al. 2005). Although binding of FGFs to $FGF_R$s may still occur in the absence of heparin, it does so at a drastically reduced and inefficient rate (Cotton, O'Bryan et al. 2008). The binding of the bFGF-heparin multimer to the $FGF_R$ is followed by the formation of receptor dimmers, which then leads to the activation of the tyrosine kinase domain. The activated tyrosine kinase phosphorylates various tyrosine residues on the $FGF_R$s, which allows for the recruitment of signal transducing proteins thus continuing the phosphorylation cascade. In most cell types, three key signal transduction pathways are activated: the phospholipase C-γ (PLC-γ) pathway, the phosphatidylinositol-3 (PI3) kinase pathway and the FRS2-Ras-MAP kinase pathway. Ultimately, these transduction cascades will affect the cell in several ways (Figure 9):

1. An activated form of PLC-γ hydrolyses phosphatidylnositol to generate the second messengers 1, 2-diacylglycerol (DAG) and $IP_3$. $IP_3$ then binds to $IP_3$-sensitive $Ca^{2+}$ channels on the ER membrane, causing the release of $Ca^{2+}$ into the cytosol. The resulting increase in cytosolic $Ca^{2+}$ concentration induces the recruitment conventional isoforms of PKC to the membrane where they are activated by DAG. Active PKC phosphorylates a range of proteins and modifies their activity. Many of the effects of an increased $Ca^{2+}$

concentration are mediated by calmodulin, a protein to which $Ca^{2+}$ ions bind. The $Ca^{2+}$-calmodulin complex can bind and activate a variety of different enzymes including myosin light-chain kinase, which ultimately brings about cytoskeletal changes (Lodish 2000).

2. The PI3 kinase pathway is initiated by activated membrane receptor regulatory subunits that recruit PI3 kinase. Once active, PI3 kinase phosphorylates phosphatidylinositol-4,5-bisphosphate to generate phosphatidylinositol-3,4,5-triphosphate ($PIP_3$). As its name implies, 2-phosphoinositide-dependent kinase relies on $PIP_3$ such that it may phosphorylate, and thus fully activate, protein kinase B (AKT/PKB). AKT/PKB will influence the activity of pro-apoptotic factors ultimately preventing the apoptotic cascade (Chalhoub and Baker 2009).

3. The FRS2 RAS-MAP kinase signaling pathway is initiated by FRS2 and its recruitment of a core signaling complex of proteins. Of these, the guanine nucleotide exchange factor: son of sevenless (SOS) activates RAS beginning a phosphorylation cascade resulting in the phosphorylation of proteins of the MAP kinase family such as: extracellular signal-regulated kinases (ERK1/2), P38 and c-Jun N-terminal kinases (JNK). Activated MAP kinases translocate to the nucleus and regulate the transcription factors of target genes via phosphorylation (Lodish 2000, Dailey, Ambrosetti et al. 2005) .

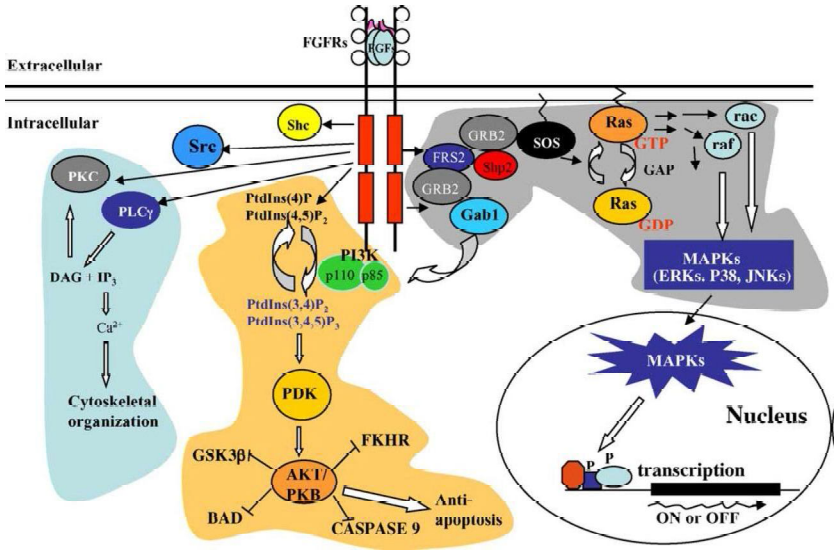


**Figure 9.** Intracellular signaling pathways activated by bFGF (Dailey, Ambrosetti et al. 2005).

## 1.3.2. Basic fibroblast growth factor in the anterior pituitary gland

The concentration of bFGF in the anterior pituitary is higher than that of any other tissue in the body and the FS cells of the gland the primary source of this growth factor (Chaidarun, Eggo et al. 1994, Vlotides, Cruz-Soto et al. 2006). The "release" of bFGF by FS cells can be triggered by several factors including transforming growth factor β 3 (TGF-β3), released by lactotrophs upon their stimulation by estrogen (Chaturvedi and Sarkar 2005). Once released, bFGF functions in an autocrine and paracrine manner exerting its effects on both FS and endocrine cells. In vitro experiments with an FS cell line, the TtT/GF folliculo-stellate cells, indicate a potent mitogenic action of bFGF on the very cell type from which it is secreted; an event that was later found to be mediated in part by the MAPKs: JNK (c-Jun N-terminal kinases) and ERK (extracellular signal-related kinases) (Vlotides, Chen et al. 2009). bFGF also induces bFGF gene transcription in TtT/GF folliculo-stellate cells (Vlotides, Chen et al. 2009). Both observations indicate that bFGF acts in a rather egocentric, autocrine function that is essentially self-promoting.

One paracrine property of bFGF in the anterior pituitary is that it functions as a potent mitogen of the assorted population of cells, as tested in primary cell culture (Chaidarun, Eggo et al. 1994, Vlotides, Chen et al. 2009). Its effects on the endocrine functions of the secretory cells of the gland appear to be restricted to lactotrophs and thyrotrophs, and only following a prolonged exposure to the growth factor (Chaidarun, Eggo et al. 1994). In primary cell cultures, a significant increase in the sensitivities of lactotrophs and thyrotrophs to their shared hypothalamic stimulating factor, TRH, was reported (Baird, Mormede et al. 1985). In addition, in the absence of stimulation from the hypothalamic factor, the basal secretion level of PRL (but not TSH) was also increased following a chronic exposure to bFGF (Baird, Mormede et al. 1985). Aside from increasing the sensitivity of lactotrophs to TRH, bFGF also antagonizes the effect of dopamine, the primary inhibitor of PRL secretion (Spuch, Diz-Chaves et al. 2006). On a molecular level, bFGF can also induce the transcription of PRL mRNA as was demonstrated in a lactotroph cell line (Mallo, Wilson et al. 1995). All aspects considered, bFGF plays a significant role in the local modulation of TSH and PRL synthesis and secretion.

The effects exerted on connexins and gap junctions by bFGF vary among cell types and depend on the connexin(s) being expressed. Normal neural development relies upon bFGF and its signalling cascades, which in turn modulate Cx43 expression and phosphorylation status. During neurogenesis in the telencephalic ventricular zones, bFGF induces gap junction formation that dictates the fate of neural progenitor cells (NPC). Removal of bFGF lowers Cx43 protein levels causing an uncoupling of NPC cells eventually resulting in their differentiation to more specialized cell types (Cheng, Tang et al. 2004). In the developing neocortex, bFGF has been

shown to increase cell coupling between cortical progenitor cells by increasing Cx43 mRNA and protein levels (Nadarajah, Makarenkova et al. 1998). Differential responses within the cells of the heart have been reported, cardiac fibroblasts respond to bFGF by increasing Cx43 mRNA and protein levels, resulting in increased coupling between cells (Doble and Kardami 1995). In contrast, cardiac myocytes respond to bFGF by phosphorylating Cx43, resulting in a decrease in cell coupling. In contrast to the occurrences in cardiac fibroblasts, mRNA and protein levels of the Cx43 were not altered in cardiac myocytes in response to bFGF (Doble, Chen et al. 1996). In the urinary bladder, an outlet blockage induces a pathological scenario whereby bladder smooth muscle cells increase bFGF production leading to an increase in Cx43 protein levels (Imamura, Negoro et al. 2009). A bladder smooth muscle cell line also exhibited an up-regulation in Cx43 accompanied by an increase in phosphorylation of the connexin (Imamura, Negoro et al. 2009). The main pathway responsible for the aforementioned effects was found to be the ERK1/2 pathway. Interestingly, the activation of the PKC variants: PKC-δ and PKC-ε have also been reported and held responsible for the phosphorylation of connexin proteins upon bFGF stimulation (Niger, Hebert et al. 2010). De Vuyst and colleagues (De Vuyst, Decrock et al. 2007) demonstrated the differential effect bFGF has on hemichannels and gap junctions composed of the same connexin in the same cell type. In a glioma cell line, bFGF was found to open Cx43 connexons/hemichannels (determined by ATP release into extracellular milieu) and close Cx43 gap junctions (De Vuyst, Decrock et al. 2007). The aforementioned results indicate that generalizations with regards to the effect of bFGF on gap junctions cannot be made. The effect on bFGF on connexins, gap junctions and gap junctional intercellular communication must be studied on a case-by-case basis; experimentally, these effects have yet to be investigated in the anterior pituitary.

## 1.4. Experimental Models

### 1.4.1. The TtT/GF folliculo-stellate cell line

The TtT/GF folliculo-stellate cell line was initially isolated from a radiothyrodectomy-induced pituitary thyrotropic tumour and bears many of the morphological and biochemical characteristics of normal FS cells (Inoue, Matsumoto et al. 1992). They display a stellate shape with long cytoplasmic processes and as with FS cells, express S-100 thus facilitating their identification and biochemical characterization (Inoue, Matsumoto et al. 1992). Similar to FS cells, the TtT/GF folliculo-stellate cells secrete a variety of chemical messengers including IL-6, bFGF and VEGF (Matsumoto, Koyama et al. 1993, Gloddek, Pagotto et al. 1999, Vlotides, Chen et al. 2009). In addition, the TtT/GF folliculo-stellate cell line is physiologically responsive to many systemic and local pituitary factors including: TGF-β and pituitary adenylate cyclase-activating peptide (PACAP) (Renner, Lohrer et al. 2002). Importantly, TtT/GF folliculo-stellate cells establish gap junctions and communicate amongst each other when in culture and their gap junctional channels remain responsive to changes in the chemical milieu (Fortin, Pelletier et al. 2006).

### 1.4.2. The mink as an animal model for research in endocrinology, reproduction and immunology

Bred for its fur coat, the mink has also proven a valuable animal model for the study of intercellular junction dynamics (Pelletier 1986, Pelletier 1988) and immunotolerance in the testis (Pelletier, Yoon et al. 2009). Mink are short day breeders, breeding during mid-March. As in all animals, their reproductive status is regulated by hormonal changes that in turn vary as a function of daylight (Sundqvist, Amador et al. 1989).

From birth, the juvenile mink will reach adulthood after a two-hundred-seventy day period (Pelletier, Akpovi et al. 2011). Mating takes place throughout the second and third weeks of March. The gestation period in mink vary due to a delayed implantation of the fertilized egg, although the duration of pregnancy lasts, on average, fifty-one days (Sundqvist, Amador et al. 1989). Parturition takes place from late April to mid-May (due to the delay of implantation) and generally produces five kits per litter (Sundqvist, Ellis et al. 1988, Peytevin, MassonPevet et al. 1997).

In the female, the ovaries remain small throughout anestrum and nearly double in size in time for the mating season. At the end of the mating season, there is a steep decline in the mass of the ovaries until late summer (Sundqvist, Amador et al. 1989). In the male, spermatogenesis is seasonally re-initiated in August (Pelletier, Yoon et al. 2009). The events occurring in female and male gonads stem initially from the pineal gland in response to changes in the photoperiod. The endocrine cells of the gland, the pinealocytes, synthesize and secrete melatonin that influences hormone release and other biological factors such as fur quality and metabolism (Sundqvist, Amador et al. 1989). Of the hormones affected by melatonin are those necessary for follicular maturation in females and spermatogenesis in males. It is the dynamic nature of the serum levels of these hormones that will in turn result in the yearly gonadal changes (DiGregorio, Gonzalez Reyna et al. 1994).

### 1.4.2. FS cells and intercellular communication in the mink anterior pituitary

Morphological differences of the FS cells in the mink anterior pituitary are reflective of the animal's hormonal status. The heterogeneous FS cell population changes throughout the reproductive cycle, with stellate-shaped type-I cells being more plentiful during high PRL periods, while rounded type-II cells increase in number in the winter when PRL levels are low (Cardin, Carbajal et al. 2000). FS cells express Cx43 dynamically throughout the reproductive cycle. Connexin protein expression correlates closely with that of PRL, whereby it is high during lactation and in spring. Consequently, Cx43 gap junctions are more abundant during phases of high PRL expression and are frequently observed between S-100 positive cells (Vitale, Cardin et al. 2001).

The dynamic nature of the mink anterior pituitary gland makes it an ideal model to study gap junction physiology. The changes that occur in the gland as a result of the annual mating cycle provide a *natural* environment where connexin modulation, including protein expression and post-translational modifications, can be investigated. Complementing the *in vitro* studies with an *in vivo* component will allow for an understanding of the influence of the physiological milieu (ex. other cell types) on connexin behaviour that would not have been seen in a cultured cell line.

## 1.5. Basis for our study

I. To date, only Cx43 has been identified and studied in the FS cells. Considering tissues generally express more than one connexin type, we sought to determine whether other connexin members are expressed by the FS cells and whether there could be a different modulation of these connexins.

II. We have chosen to investigate Cx46 and Cx50 for several reasons:

1. Cx43, Cx46 and Cx50 are co-expressed in the ocular lens (White, Bruzzone et al. 1994).
2. Cx43, Cx46 and Cx50 all belong to the α-connexin sub-type (Evans and Martin 2002) and therefore, can theoretically form heteromeric connexons amongst each other.
3. Cx46 and Cx50 have previously been shown to form heteromeric connexons in the lens (Jiang and Goodenough 1996).
4. Cx46 and Cx50 gap junctions are modulated by growth factors (bFGF and TGF-β) in the ocular lens (Shakespeare, Sellitto et al. 2009, Boswell, VanSlyke et al. 2010). These growth factors, also present in the anterior pituitary (Kabir, Chaturvedi et al. 2005), may affect Cx46 and Cx50 gap junctions in a similar or different manner.

# 2. Materials and Methods

## 2.1 Antibodies and probes for western blot and microscopy studies

The primary antibodies and probes used for the identification and characterization of Cx46 and Cx50 are listed in **Table 1** along with all pertinent information.

## 2.2. Cell Culture and Tissue Preparation

### 2.2.1. Cell lines and culture

The TtT/GF folliculo-stellate cell line was originally derived from a pituitary radiothyrodectomy-induced thyrotropic tumour (Inoue, Matsumoto et al. 1992). This cell line was obtained from Dr Ulrich Renner of the Max-Planck Institute in Munich, Germany. TtT/GF folliculo-stellate cells share many of the morphological and functional characteristics of FS cells. They are agranular, stellate-shapped with long cytoplasmic extensions and produce both bFGF and VEGF. Furthermore, these cells express S-100 and GFAP, both markers for FS cells in the anterior pituitary (Inoue, Matsumoto et al. 1992, Inoue, Couch et al. 1999). Wild type Mouse embryonic fibroblasts (MEF) were a gift from Dr Robert Adelstein of the National Heart, Lung and Blood Institute, Maryland, USA. The MEF cell line was used in this study because the TtT/GF folliculo-stellate cell line has been shown to be a fibroblast-like cell (Stilling, Bayliss et al. 2005). Thus, the MEF cells serve as a suitable model to compare results obtained in the TtT/GF folliculo-stellate cells. For instance, connexin physiology may prove to be cell-type dependent, whereby findings between the MEF and TtT/GF folliculo-stellate cell line would be similar. All cell lines were cultured at a temperature of 37°C, in a 95-5% air-$CO_2$ environment

and were grown in Dulbecco's modified eagle medium (DMEM): Nutrient Mixture F-12 from GIBCO-Invitrogen (Burlington, ON, Canada) to which was supplemented 0.1M sodium bicarbonate ($NaHCO_3$), 0.2 mg/ml penicillin G, 0.05 mg/ml streptomycin sulphate (all from Sigma, St. Louis, MO, USA) and 5% foetal bovine serum (GIBCO/Invitrogen, Burlington, ON, Canada). Prior to use, this mixture was brought to a pH of 7.2 then sterilized through a 0.10µm filter (Millipore, Billerica, MA, USA).

Certain experiments required the use of serum-free medium, which was prepared exactly as described above although without foetal bovine serum.

### 2.2.2. Basic fibroblast growth factor treatment of TtT/GF cells

TtT/GF cell cultures were treated with bFGF (Biosource, Camarillo, CA, USA) to study its effect on the protein expression of Cx46 and Cx50 over time. Cells were first put into culture and grown to near confluence. Prior to treatment, the cell cultures were rinsed twice with serum-free medium, then serum-starved for a period of twenty-four hours. On the day of the treatment, bFGF was diluted in serum-free medium to a concentration of 15 ng/ml and applied to the cells for incubation periods of 0, 0.5, 1, 2, 4 and 8 hours (37°C). Following treatment, cell cultures were prepared either for electrophoresis or immunofluorescence microscopy.

### 2.2.3. Preparation of cell homogenate

Cells were harvested once having reached 60 – 70% confluence (higher confluence would hinder visualization of cell-to-cell contacts). After being washed with cold phosphate buffered solution (PBS: 137mM NaCl, 3mM KCl, 8mM $Na_2HPO_4$ and 1.5mM $KH_2PO_4$, pH 7.4), they were

detached using a cell scraper and centrifuged at 2000 RPM for 5 minutes in a Beckman, GS-6R centrifuge with a GH 3.8 rotor (Beckman Coulter Canada Inc., Mississauga, ON, Canada). The cell pellet was resuspended in a protease phosphatase inhibitor cocktail made in PBS (4mM $Na_3VO_4$, 80mM NaF, 20mM $Na_4P_2O_7$, 2mM EGTA (pH 8.5), 10µM bpV-phen, 5µg/ml leupeptin and 5µg/ml aprotinin). The cell pellets were then sonicated at moderate intensity (Fisher Sonic Dismembranator Model 300) for 30 seconds.

### 2.2.4. Mouse ocular lens

Lenses excised from normal mouse eyes were briefly immersed into dry ice then fragmented. The fragments were allowed to thaw, then were homogenized in PBS-protease phosphatase inhibitor using a Polytron PT 3100 homogenizer (Kinematica, Lucerne, Switzerland). Aliquots of the total homogenate were stored at -80°C until use.

### 2.2.5. Preparation of mink and mouse anterior pituitary tissue

Mink tissue was prepared as described by Vitale, M.L. and colleagues (Vitale, Cardin et al. 2001). Mink were purchased from the *Visonnière St. Damase* mink farm, in St Damase, QC, Canada. Animals were anaesthetized using sodium pentobarbital (0.2 ml/kg), then decapitated. Anterior pituitaries were excised and placed in PBS-protease phosphatase inhibitor. The tissues were then sonicated and stored at -80°C until use.

Albino male mice obtained from Charles River (St Constant, Qc, Canada) were anaesthetized and decapitated as described by Vitale, M.L. and colleagues (Vitale, Akpovi et al. 2009). Anterior pituitary tissue was excised and placed in PBS-protease phosphatase inhibitor, sonicated

and stored at -80°C until use. This protocol was conducted in conformity with the *Université de Montréal* animal welfare mandate. The studies presented have been approved by *Le Comité de déontologie de l'expérimentation sur les animaux* (*Université de Montréal*).

## 2.3. Lipid raft isolation

Cells were grown to 60 – 70% confluence in standard conditions, washed with ice-cold PBS, then collected and centrifuged to isolate the cells in a pellet. After centrifugation, the PBS was removed and replaced with cold MBS 1% Triton X-100 (MES-buffered saline: 25mM MES (2-(*N*-morpholino) ethanesulfonic acid, pH 6.5) and 150nM NaCl. Cells were homogenized using a Dounce homogenizer (10 strokes) then combined with an equal volume of 80% sucrose in MBS solution, to attain a final 40% sucrose concentration. The homogenate-40% glucose mixture was then loaded into a 5 ml ultracentrifuge tube, then overlaid with 25%, 15% and 5% sucrose-MBS solutions forming a discontinuous gradient. These preparations were then loaded into a SW60 rotor (Beckman Coulter Canada Inc., Mississauga, ON, Canada) and spun in a Beckman XL-70 ultracentrifuge at 200,000g for 18 hours at 4°C.

Lateral illumination of the ultracentrifuge tubes revealed a single turbid band at the 25%-15% interface, representative of the Triton-insoluble fraction (Philippova, Bochkov et al. 1998). Post-centrifugation, the contents of the test tube were aspirated into fractions of equal volume beginning with the least dense material at the top of the tube. A total of 13 fractions were isolated including the pellet. It was noted that the aforementioned turbid band was aspirated in the $4^{th}$ and $5^{th}$ fractions. Each fraction was quantified for protein concentration using the Bradford method (Bradford 1976) and samples were prepared for western Blot.

Anti-Caveolin1 and anti-Flotillin1, were used as markers of caveolae and lipid rafts, respectively (refer to **Table 1** for concentrations).

## 2.4. Cell fractionation – Nuclear fraction isolation

This protocol was obtained from Drs Katherine Borden and Biljana Culjkovic from IRIC (Institute for Research in Immunology and Cancer), Montreal, QC, Canada (Culjkovic, Topisirovic et al. 2006).

### 2.4.1. Cell lysis

Six confluent 100mm dishes of cells were first washed twice in ice-cold PBS and cells were collected and pelleted as previously described. The pellet was resuspended using 1 ml of Lysis buffer-B (10mM Tris (pH 8.4), 140mM NaCl, 1.5mM $MgCl_2$, 0.5% NP 40 and 1mM DTT) and cells were lysed by pipetting up and down 50x.

### 2.4.2 Separation of nuclear fraction from cytoplasm and plasma membrane

The cell lysate was spun at 1000g (Beckman, GS-6R centrifuge), 4°C for 3 minutes. The "cytoplasmic/plasma membrane" fraction, contained in the supernatant was transferred to a separate tube and resuspended in 1 ml of PBS-protease phosphatase inhibitor solution. Intact nuclei forming the pellet were resuspended in 1 ml lysis buffer-B and transferred to a round bottom tube. Under slow vortexing, 100µl of Detergent stock (3.3% (w/v) sodium deoxycholate and 6.6% (v/v) Tween 40) was added to the resuspended pellet that was then incubated on ice for 5 minutes.

### 2.4.3. Isolation of post-nuclear fraction

Following incubation, the nuclear fraction was spun at 1000g, 4°C for 3 minutes (Beckman, GS-6R centrifuge). The supernatant, containing the post-nuclear fraction, was added to the

previously-isolated “cytoplasmic/plasma membrane” fraction. The pellet, containing a purified nuclear fraction, was rinsed in 1 ml of lysis buffer-B then spun at 1000g, 4°C for 3 minutes (Beckman, GS-6R centrifuge). The supernatant was discarded and the pellet, consisting of intact purified nuclei, was collected. Throughout the purification steps, preparations were visually assessed via light microscopy and images of the isolated nuclei were captured.

### 2.4.4. Lysing of nucleus and sample preparation

The intact nuclei were resuspended in a PBS-protease phosphatase inhibitor solution then lysed via sonication (30 seconds at moderate intensity). The protein content of the nuclear lysate was determined and samples were prepared for Sodium dodecyl sulfate polyacrylamide gel electrophoresis (SDS-PAGE) as previously described (Culjkovic, Topisirovic et al. 2006). The protein content of the cytoplasmic/plasma membrane fraction and of the whole cell lysate was also determined and prepared for SDS-PAGE.

## 2.5. Alkaline phosphatase treatment

Cell cultures were grown to confluency then pelleted as previously described (2-3 100mm dishes). Excess PBS was removed and cold digestion buffer was added to the pellet (10mM $MgCl_2$, 1mM $ZnCl_2$ 50mM Tris-HCl pH 8.0), which was resuspended, then sonicated. Homogenates were quantified according to protein content then divided into equal parts of 100µg total protein. Thirty units of Calf intestine alkaline phosphatase (Roche, Laval, QC, Canada) were added to each experimental sample, while equal volumes of digestion buffer were added to control samples. Samples were then incubated in a 37ºC water bath under gentle agitation for the desired time periods (i.e. 0, 30, 60 minutes). At the end of the reaction times, alkaline phosphatase activity was halted using PBS-protease phosphatase inhibitor, then placed on ice for 15 minutes. Each sample was brought to a final volume of 50µl with sample buffer, and then boiled for 3 minutes. Whole cell lysates, control and experimental samples were then subjected to SDS-PAGE (Sambrook, Fritsch et al. 1989).

## 2.6. Reverse transcriptase PCR and Southern blot

### 2.6.1. Primer design

PCR primers were designed using the *Mus musculus* mRNA sequences for Cx46 and Cx50, obtained on the NCBI Nucleotide Database (Accession numbers: NM_016975.2 and NM_008123.2, respectively) (Pruitt, Tatusova et al. 2005). The NCBI Primer BLAST tool (Altschul, Gish et al. 1990) was then used to generated primer pairs based on the aforementioned sequences. Of the numerous primers that were produced, three pairs (**Table 2**) were chosen for each gene primarily based on specificity and, in the case of Cx46, the annealing of the primer across an exon-exon border (Cx46 Primer Pair A). These primers were individually "BLASTed" to verify their specificity to the genes of interest. Additional primer sequences for Cx46 and Cx50 from published research were obtained from Anderson et al (Anderson, Zundel et al. 2005) and Das et al (Das, Wang et al. 2011). A primer pair against housekeeping gene Hypoxanthine phosphoribosyl transferase-1 (HPRT-1) was also employed as an internal control (Pelletier, Akpovi et al. 2011).

### 2.6.2. RNA isolation and complementary DNA synthesis

Total RNA was isolated from TtT/GF cells using the High Pure RNA Isolation Kit (Roche, Laval, QC, Canada). RNA quantity and quality was determined via photospectromeric readings at 260 and 280nm. Complementary DNA (cDNA) was generated by reverse transcription of mRNA using the M-MLV Reverse Transcriptase (Sigma, St. Louis, MO, USA) and oligo-dT primers (Sigma, St. Louis, MO, USA). In the initial reaction, the oligo-dT primers were annealed to mRNA strands within the following mixture: dNTP mix (10mM), oligo-dT primer (5μM), RNA template, and nuclease-free water; which was incubated at 70°C for 10 minutes. To extend

the oligo-dT primers, the following components were added: M-MLV Reverse Transcriptase Buffer (10x), M-MLV Reverse Transcriptase (200U/µl), RNase inhibitor (40U/µl) and nuclease-free water; incubated at 37°C for 50 minutes. A final incubation at 80°C for 10 minutes denatured the reverse transcriptase. "No reverse transcriptase" (No-RT) control reactions had the enzyme replaced by nuclease-free water and were subjected to identical conditions.

### 2.6.3. PCR and Southern blot

The PCR mixture included: *Taq* polymerase buffer (10x), primer pairs (10µM), dNTPs mix (10mM), cDNA, *Taq* polymerase (5 U/µl) and nuclease-free water. In the negative control mixtures, cDNA was replaced with nuclease-free water. The thermal cycler (T Gradient96, Biometra, Goettingen Germany) was programmed with the following steps: 1) 94°C – 5 minutes; 2) 94°C – 15 seconds; 3) 55°C – 30 seconds; 4) 72°C – 30 seconds. Steps 2) to 4) were cycled 40x. Final elongation was performed at: 5) 72°C – 7 minutes. PCR products were subjected to electrophoresis in a 2% agarose gel prepared in 1x TBE buffer (45 mM Tris-Borate and 1 mM EDTA). Gels were stained with ethidium bromide then visualized under a UV transilluminator (UVP, Upland, CA, USA).

## 2.7. Western blot

### 2.7.1. Protein dosage and sample preparation

Protein levels were measured according to the Bradford protein assay using the Protein assay dye reagent concentrate from Bio-Rad (Mississauga, ON, Canada) (Bradford 1976). Initially, a standard curve was established by performing the assay using known amounts of bovine serum albumin. This curve then served as a reference to determine the protein concentrations of our lysates based on a photospectromeric reading at 595nm. Samples for electrophoresis were prepared to a concentration of 2 µg/µl using a 2x loading buffer (8M urea, 3% SDS, 5% β-mercaptoethanol, 0.005% bromophenol blue and 70 mM Tris-HCl (pH 7.6)).

### 2.7.2. SDS-PAGE

Gels of 10% and 12% acrylamide were made according to the following recipe: 0.2M Tris-0.1M glycine, 0.4% SDS, 4mM EDTA (pH 6.7), 5% glycerol and 10% or 12% acrylamide. These were then topped with a 4% stacking gel (70mM Tris-HCl (pH 6.7), 0.4% SDS, 4mM EDTA (pH 6.7), 5% glycerol and 4% acrylamide). Samples that had been previously quantified and prepared in loading buffer were loaded into the gel, placed into the electrophoresis apparatus that was then filled with electrophoresis buffer (0.1M Tris, 0.15M glycine and 0.1% SDS). The migration was programmed at 80 volts for 30 minutes to allow all samples to clear the stacking gel, and then increased to 120 volts for a period of 2-4 hours.

### 2.7.3. Transfer onto nitrocellulose membrane

Following the migration, the proteins in the polyacrylamide gel were transferred onto a 0.45µm nitrocellulose membrane (Bio-Rad, Mississauga, ON, Canada). The transfer was performed in a

transfer buffer (25mM Tris (pH 8.3), 15mM Glycine and 20% Methanol) at 4°C for a period of 1.5 hours at 0.300 amperes and 200 volts. The success of the transfer was evaluated by staining the membrane with Ponceau red (0.2% ponceau in 3% trichloroacetic acid); readily removed via a quick wash in PBS.

### 2.7.4. Blocking of non-specific sites and antibody incubation

Nitrocellulose membranes were blocked with 5% skim milk made in PBS Tween-20 (0.05%) at 37°C for 1 hour. Membranes were then probed with the primary antibody diluted in 5% milk and left overnight on a rotating drum at 4°C. The following day, membranes were washed 3x in PBS Tween-20 (0.05%) for 10 minutes on a rotating mixer. The peroxidase (POD)-conjugated secondary antibody, also diluted in 5% milk, was then applied to the membrane at room temperature for 1 hour on a rotating mixer (**Table 3**). The membranes were then washed 3x in PBS Tween-20 (0.05%) for 10 minutes.

Washed membranes were placed in a chemiluminescent POD-substrate (Roche, Laval, QC, Canada) to reveal antigen-antibody complexes. The emitted light was captured on x-ray film (AGFA Radiomat B Plus, Mortsel, Belgium) that were then developed.

### 2.7.5. Densitometry of bands obtained in western blot

Quantification of the band signal intensity obtained on the film, densitometry, allowed for the determination of the relative protein quantities in each of the samples used. To arrive at a numerical value for the bands obtained, the x-ray films were first digitized using an Epson perfection 3200 photo scanner along with Epson scan software (Epson, Markham, ON, Canada).

Digital images were then processed using Scion Image (Scion Corporation, Bethesda, MA, USA), which served to measure the intensities of the bands and assign a numerical value to individual bands based on their density.

## 2.8. Immunofluorescence

### 2.8.1. Preparation of cells

Cells were put into culture on sterilized 22x22mm glass coverslips (No. 0 and 1 thickness) placed within 35mm Petri dishes. After leaving the cells overnight at 37 °C and 5% $CO_2$, the cultures either underwent a specific treatment (serum starvation and growth factor, refer to **2.2.2.**), or were directly fixed and permeabilized.

### 2.8.2. Fixation and permeabilization

Cells were fixed and permeabilized using one of three methods (Sambrook, Fritsch et al. 1989):

Method 1. Formaldehyde fixation and acetone permeabilization

Cell cultures on glass coverslips were first washed with PBS then fixed using 3.7% formaldehyde made in PBS for 20 minutes at room temperature. Next, cells were washed several times with PBS then permeabilized in 3 successive ice-cold acetone baths of 50% (diluted in distilled water), 100% and 50% for 5 minutes each.

Method 2. Methanol fixation and permeabilization.

With this method, cell cultures grown on coverslips were washed with cold PBS then immersed into a -20°C methanol bath for a period of 10 minutes. The methanol treatment served to both fix and permeabilize the cells.

Method 3. Formaldehyde fixation and methanol permeabilization

This method was used to better visualize nuclear proteins. Cells were first fixed in 3.7% formaldehyde made in PBS for 20 minutes then permeabilized in a -20°C methanol bath for 10 minutes.

### 2.8.3. Blocking and incubation with antibodies

Prior to blocking, cells were washed several times with PBS to remove any residual acetone or methanol. Non-specific binding sites were blocked using 3% skim milk (made in PBS Tween-20 (0.05%)) for 1 hour at room temperature. Cell cultures were then incubated at 37°C for 1 hour with primary antibodies diluted in 1% skim milk (made in PBS Tween-20 (0.05%)) according to their respective concentrations (refer to **Table 1**). Following the binding of the primary antibodies, cells were washed with PBS and probed with Fluorescein-5-isothiocyanate (FITC)- or Tetramethylrhodamineisothiocyanate (TRITC)-conjugated secondary antibodies (refer to **Table 4**) diluted in 1% skim milk for 1 hour at 37°C.

Double-labelling was achieved by combining primary antibodies at their respective concentrations in 1% skim milk and applying the mixture to the fixed and permeabilized cells. FITC- and TRITC-conjugated secondary antibodies were also combined at their respective concentrations in 1% milk and applied to the cells as described above. Care was taken to ensure that double-labelling experiments were performed with primary antibodies of different isotypes to avoid non-specific reactions of the FITC and TRITC-conjugated secondary antibodies.

### 2.8.4. Mounting and observation

The coverslips were mounted onto glass slides using Mowiol® (EMD Biosciences, San Diego, CA, USA) (For 60 ml: 8 g polyvinyl alcohol, 40 ml 0.2M Tris-HCl (pH 8.5), 20ml glycerol, 1% DABCO). Visualization of labelled cells and image capture was performed using a Zeiss Axioskop 2 fluorescence microscope (Carl Zeizz Canada Ltd, Toronto, ON, Canada) and a Leica DM IRB confocal microscope (Leica Microsystems Inc., Richmond Hill, ON, Canada). Image

capture of fluorescently labelled cells was carried out via Northern Eclipse (Empix Imaging Inc., Mississauga, ON, Canada) and Leica Confocal software.

**Table 1.** Primary antibodies used in western blot and immunofluorescence

| Antibody/Probe | Isotype | Associated sub-cellular structure | Optimal concentration (ratio) | | Manufacturer |
|---|---|---|---|---|---|
| | | | Western Blot | Immuno-fluorescence | |
| Calnexin | Rabbit, polyclonal, IgG | Endoplasmic reticulum | N/A | 1 : 250 | Calbiochem (San Diego,CA, USA) |
| Caveolin-1 | Rabbit, polyclonal , IgG | Lipid rafts/caveoles | 1:5000 | 1 : 50 | Santa Cruz Biotechnology (Santa Cruz, CA, USA) |
| Concanavalin A | Probe | Endoplasmic reticulum | N/A | 1 : 150 | Molecular Probes (Eugene, OR, USA) |
| EEA-1 - Early Endosome Antigen-1 | Goat, polyclonal, IgG | Early endosomes | N/A | 1 : 5 | Santa Cruz Biotechnology, Inc (Santa Cruz, CA, USA) |
| Flotillin-1 | Mouse, polyclonal, IgG | Lipid rafts | 1:500 | 1 : 3 | BD Transduction Laboratories (Missisauga, ON, Canada) |
| GM-130 – Golgi Matrix | Mouse, monoclonal, IgG | *cis*-Golgi | N/A | 1 : 25 | BD Transduction Laboratories (Missisauga, ON, Canada) |
| LAMP-1– Lysosomal Associated Membrane Protein-1 | Rat, monoclonal, IgG2a | Lysosomes | N/A | 1 : 20 | J. Thomas August, Johns Hopkins University School of Medicine (Baltimore, MD, USA) |
| TGN 38 - *Trans*-Golgi Network 38 | Mouse, monoclonal, IgG | *trans*-Golgi | N/A | 1 : 10 | Affinity Bioreagents (Golden, CO, USA) |
| WGA - Wheat Germ Aglutinin | Probe | *trans*-Golgi | N/A | 1 : 60 | Molecular Probes(Eugene, OR, USA) |
| | | | | | |
| Connexin 46 | Rabbit, polyclonal, IgG | N/A | 1:250 | 1 : 5 | Invitrogen Canada Inc. (Burlington, ON, Canada) |
| | Rabbit, polyclonal, IgG | N/A | 1:250 | N/A | Alpha Diagnostic International Inc. (San Antonio, TX, USA) |
| | Rabbit, polyclonal, IgG | N/A | 1: 150 | N/A | U.S. Biologicals (Salem, MA, USA) |
| Connexin 50 | Mouse, monoclonal, IgM | N/A | 1:1000 | 1 : 10 | Invitrogen Canada Inc. (Burlington, ON, Canada) |
| | Rabbit, polyclonal, IgG | N/A | 1:500 | N/A | Alpha Diagnostic International Inc. (San Antonio, TX, USA) |
| Connexin 43 (Pan) | Mouse, monoclonal, IgG | N/A | N/A | 1 : 7 | Millipore (Billerica, MA, USA) |
| | Rabbit, polyclonal, IgG | N/A | 1:18,000 | 1:100 | Sigma (St. Louis, MO, USA) |

**Table 1.** Primary antibodies used in western blot and immunofluorescence (continued)

| Antibody/Probe | Isotype | Associated sub-cellular structure | Optimal concentration (ratio) | | Manufacturer |
|---|---|---|---|---|---|
| | | | Western Blot | Immuno-fluorescence | |
| PML | Mouse, monoclonal, IgG | PML (Promyelocytic Leukemia) Bodies | 1:2000 | 1 : 150 | Millipore |
| NOPP-140 | Rabbit, polyclonal, IgG | Intermediate between Nucleolus and Cajal bodies | 1:1000 | 1 : 100 | Unknown |
| NOPP-140 | Mouse, monoclonal, IgG | Intermediate between Nucleolus and Cajal bodies | 1:250 | 1:2 | Santa Cruz Biotechnology |
| Coilin/p80 | Mouse, monoclonal, IgG | Main component of Cajal/Coiled bodies | 1:250 | 1:2 | Santa Cruz Biotechnology |
| Glyceraldehyde-3-Phosphate Dehydrogenase | Rabbit, polyclonal, IgG | Glycolytic pathway | 1:1000 | N/A | Abcam |

**Table 2.** PCR primer pairs – Nucleotide sequence and product information

| Primer Pair - Identity | Nucleotide Sequence | | Expected Product/Amplicon Side (bp) | Sequence Design |
|---|---|---|---|---|
| | Forward (5' – 3') | Reverse (5' – 3') | | |
| Cx46 A | CCCCAGACGGGACCCGGTTA | GTCCGATTGCTCGTCGCCCC | 186 | Vitale-Garcia |
| Cx46 B | CGCGATGACCGTGGCAAGGT | CCAGCGGTCGCAGCGGTAAA | 156 | Vitale-Garcia |
| Cx46 C | CGTCTGCTACGACCGCGCTT | ACCTTGCCACGGTCATCGCG | 246 | Vitale-Garcia |
| Cx50 A | TCGGGACAGCAGCGGAGTTTG | TACCGCGTGCCCCACGTACAT | 182 | Vitale-Garcia |
| Cx50 B | CGGTACACCACGTTCGCATGGAG | GCGATAGAGGGGCAGGATGCG | 281 | Vitale-Garcia |
| Cx50 C | GGGACAGCAGCGGAGTTTGTGT | TGTACCGCGTGCCCCACGTAC | 182 | Vitale-Garcia |
| HPRT-1 | TGACACTGGCAAAACAATGCA | GGTCCTTTTCACCAGCAAGCT | 93 | (Pelletier, Akpovi et al. 2011) |
| Cx46D | AATCGGACTTCACCTGCAAC | TGCTGAGGGTTGTCTCTCCT | 217 | Chen, Pelletier Unpublished |
| Cx50D | CTGCCCCAATGTGGTAGACT | AGTGGAGGGACTTCTCAGCA | 200 | Chen, Pelletier Unpublished |
| Cx46E | GGTTAGCTGTTGGGAGCAAT | CAGAATGCGGAAGATGAACA | 123 | (Das, Wang et al. 2011) |
| Cx50E | CGGAGCAGCAAGAGAGAAAG | TGCTCATTCACCTCTTCCAA | 112 | (Das, Wang et al. 2011) |
| Cx46F1 | TGAGAGAGCCCGGACGAG | GAATGCGGAAGATGAACAG | Unknown | (Anderson, Zundel et al. 2005) |
| Cx46F2 | ACGAGTAAAGAGGGAGCC | X | Unknown | (Anderson, Zundel et al. 2005) |

**Table 3.** Peroxidase-conjugated secondary antibodies used in Western blot

| Antibody | Host Animal | Optimal Concentration | Manufacturer |
|---|---|---|---|
| Anti-mouse IgM (μ-chain specific) | Goat | 1:2000 | Sigma (St. Louis, MO, USA) |
| Anti-mouse IgG (H+L) | Donkey | 1:2000 | Jackson Immunoresearch Laboratories Inc (West Grove, PA, USA) |
| Anti-rabbit IgG (H+L) | Goat | 1:2000 | Jackson Immunoresearch Laboratories Inc (West Grove, PA, USA) |

**Table 4.** FITC- and TRITC-conjugated secondary antibodies used in immunofluorescence

| Antibody | Host Animal | Fluorophore* | Optimal Concentration | Manufacturer |
|---|---|---|---|---|
| Anti-mouse IgM (μ-chain specific) | Goat | FITC | 1:200 | Sigma (St. Louis, MO, USA) |
| | Donkey | FITC | 1:200 | Jackson Immunoresearch Laboratories Inc(West Grove, PA, USA) |
| Anti-mouse IgG (subclasses 1+2a+2b+3) | Goat | FITC | 1:200 | Jackson Immunoresearch Laboratories Inc (West Grove, PA, USA) |
| Anti-mouse IgG (H+L) | Donkey | TRITC | 1:200 | Jackson Immunoresearch Laboratories Inc (West Grove, PA, USA) |
| Anti-rabbit IgG (H+L) | Donkey | FITC | 1:200 | Jackson Immunoresearch Laboratories Inc (West Grove, PA, USA) |
| | Donkey | TRITC | 1:200 | Jackson Immunoresearch Laboratories Inc (West Grove, PA, USA) |
| Anti-rat IgG (H+L) | Donkey | FITC | 1:200 | Jackson Immunoresearch Laboratories Inc (West Grove, PA, USA) |
| Anti-goat IgG (H+L) | Donkey | FITC | 1:200 | Jackson Immunoresearch Laboratories Inc(West Grove, PA, USA) |

*FITC, Fluorescein-5-isothiocyanate; TRITC, Tetramethylrhodamineisothiocyanate

# 3. Results

## 3.1. Identification of Cx46 and Cx50 in the TtT/GF folliculo-stellate cell line and mouse anterior pituitary

Our lab has previously shown the expression of Cx43 in the folliculo-stellate cells of the anterior pituitary (Vitale, Cardin et al. 2001) and has characterized its function in the TtT/GF folliculo-stellate cell line (Fortin, Pelletier et al. 2006, Meilleur, Akpovi et al. 2007). Based on the aforementioned findings and the fact that most cell types express more than one connexin type (Simon and Goodenough 1998), we therefore investigated whether other connexins besides Cx43 are expressed in the folliculo-stellate cells. We first tested for the expression of Cx46 and Cx50. The co-expression and physiological co-operation of Cx43, Cx46 and Cx50 within the lens (Jiang and Goodenough 1996) prompted us to investigate the possibility that the later two of these connexins are expressed and play a functional role in the anterior pituitary gland. Furthermore, these three connexins belong to the α-connexin family, and thus, can theoretically form heteromeric connexons with one another (Evans and Martin 2002). Firstly, we sought to analyse the presence of both Cx46 and Cx50 at the level of the transcript (mRNA) through PCR and at the protein level through Western blot and immunofluorescence microscopy. We used the TtT/GF folliculo-stellate cell line since they possess many of the morphological and physiological characteristics of FS cells (Inoue, Matsumoto et al. 1992)

### 3.1.1. Expression of Cx46 and Cx50 mRNA by the TtT/GF folliculo-stellate cell line

Detecting Cx46 and Cx50 at the level of the transcript in the TtT/GF cell line involved extracting the mRNA that was then used as a template to synthesize cDNA via a reverse transcription reaction. Specifically designed primer pairs (**Table 2**) were then used to probe the cDNA and amplify specific sequences in a thermal cycler. Of all the PCR primers designed specifically for Cx46 (**Table 2**), primer pair Cx46E (Das, Wang et al. 2011) provided the best results. **Figure 10A** shows this primer pair generated a major amplification product at 133 bp and two less prominent products at 290 bp and 450 bp in the TtT/GF cells. The expected product size in the lens, according to those who had designed the primers, was 123 bp (Das, Wang et al. 2011). Amplification products were not noted in the No-RT and $H_2O$ control lanes of the gel.

All primer pairs designed for Cx50 were assayed and it was determined that primer pair Cx50E (Das, Wang et al. 2011) provided the best results (**Table 2**). Of the products generated by this primer pair, major amplification products measuring 310 bp and 114 bp were generated when applied to the TtT/GF folliculo-stellate cells. In addition to these products, another less prominent amplification product was also detected at 190 bp. In lens, an amplification product of 112 bp was expected (Das, Wang et al. 2011). The No-RT and $H_2O$ control lanes did not reveal amplification products in the form of bands but did contain low molecular weight smears (**Figure 10B**).

The procedure was verified through a housekeeping gene, HPRT-1. This primer pair generated a single 104 bp band when used to probe TtT/GF folliculo-stellate cell cDNA (**Figure 10C**). The

effectiveness of this primer pair has previously been demonstrated whereby it had generated an amplification product of 93 bp (Pelletier, Akpovi et al. 2011). The No-RT and H2O control lanes were free of amplification products in the form of bands and smears (**Figure 10C**).

### 3.1.2. Protein expression of Cx46 and Cx50 in the TtT/GF folliculo-stellate cell line and mouse anterior pituitary

After having confirmed the expression of Cx46 and Cx50 at the transcript level, we next determined whether Cx46 and Cx50 were expressed at the protein level. To achieve this, we performed western blots using three Cx46 antibodies, two recognizing epitopes on the C-terminal (Invitrogen and Alpha-Diagnostics) and one that recognized an internal epitope (U.S. Biologicals). Both Cx50 antibodies that we used were generated against C-terminal epitopes (Invitrogen and Alpha-Diagnostics).

Proteins from mouse lens (control) probed with antibodies against Cx46 generated three immunoreactive bands: a doublet with bands at 48 and 49 kDa, and a single band at 68 kDa (**Figure 10D**). TtT/GF cells showed the same 48, 49 and 68 kDa bands when probed with Cx46-specific antibodies. A Western blot of mouse anterior pituitary revealed the 48 and 49 kDa doublet but lacked the 68 kDa band found in the lens tissue and TtT/GF folliculo-stellate cells (**Figure 10D**). In the TtT/GF folliculo-stellate cells both the Invitrogen and Alpha-Diagnostics generated similar results and revealed the aforementioned bands. For Western blots, we preferred using the Alpha-Diagnostics anti-Cx46 as it produced more consistent results compared to the Invitrogen anti-Cx46.

Western blots performed with antibodies against Cx50 revealed two bands in the membrane containing proteins from the ocular lens: one at 52 kDa and another at 61 kDa. Western blots of the TtT/GF folliculo-stellate cell line also demonstrated the 52 kDa band and upon prolonged exposure of the membrane, an additional band at 65 kDa was detected. Western blots of the anterior pituitary only revealed the 52 kDa band (**Figure 10E**). While both Cx50 antibodies revealed these bands, the polyclonal Alpha-Diagnostics anti-Cx50 produced several additional bands when used to probe TtT/GF folliculo-stellate cells.

### 3.1.3. Expression of Cx46 and Cx50 in mouse embryonic fibroblasts

We further investigated the expression of Cx46 and Cx50 proteins in two other cell lines: a wild-type mouse embryonic fibroblast (MEF) cell line (WT) and in a MEF cell line where the myosin heavy chain IIB gene had been deleted (MHCB-/-). Immunoblots of WT and MHCB-/- MEFs probed for Cx46 showed a large band at 49 kDa in the WT and MHCB-/- cells that had only become visible after a prolonged exposure (**Figure 10F**). Membranes probed with antibodies against Cx50 presented strikingly different results: the WT cells showed two bands, an intense band at 47 kDa and a weaker one at 52 kDa. The lane with proteins from the MHCB-/- cells revealed a strong band at 54 kDa and two weaker bands at 50 and 49 kDa (**Figure 10G**).

### 3.1.4. Phosphorylation status of Cx46 in the TtT/GF folliculo-stellate cell line

The constant observation of multiple bands in Western blots of Cx46 in the TtT/GF folliculo-stellate cells led us to test for a post-translation modification that affected the migration of the protein in a polyacrylamide gel. Based on the information that phosphorylation represents one of the most relevant modifications connexin proteins undergo with regard to life-cycle and

physiological function (Johnstone, Billaud et al. 2012), we investigated as to whether Cx46 was phosphorylated using alkaline phosphatase.

**Figure 10H** shows a representative result from the alkaline phosphatase experiment: the control (0 minute incubation, no enzyme) showed the characteristic bands of Cx46 at 49 and 68 kDa and a weak band at 56 kDa. These same immunoreactive bands were present in another control where the cell lysate was incubated for 30 minutes but in the absence of the enzyme (30m-Ø). When the cell lysate was treated with the alkaline phosphatase (30m-A.P.), the intensity of the 68 kDa band was greatly reduced and the 56 kDa band disappeared entirely. The 49 kDa band, however, remained (**Figure 10H**).

### 3.1.5. Distribution of Cx46 and Cx50 in the TtT/GF folliculo-stellate cell line

We next investigated the intracellular distribution of Cx46 and Cx50 in the TtT/GF folliculo-stellate cell line. To accomplish this, we performed immunofluorescent labelling using antibodies against Cx46 and Cx50. As shown in **Figure 10I**, the immunofluorescent labelling in cells probed for Cx46 was punctate and primarily concentrated in the perinuclear area. Labelling in cytoplasmic projections was very faint and cell-to-cell contact areas did not consistently demonstrate concentrated areas of fluorescence. Occasionally, TtT/GF folliculo-stellate cells displayed nuclear labelling of Cx46 as is shown in the insert of **Figure 10I**. This observation was confirmed by confocal microscopy (see **Figure 11C** for examples of Cx46 nuclear labelling).

Immunofluorescent labelling of TtT/GF folliculo-stellate cells for Cx50 produced a punctate pattern that was uniform through the cytoplasm of the cells including cytoplasmic projections

(**Figure 10J**). Labelling for Cx50 was absent in the nucleus (confirmed by confocal microscopy, as seen in **Figure 12**).

**Figure 10.** Studies on the presence of Cx46 and Cx50 in the TtT/GF folliculo-stellate cell line and in the anterior pituitary

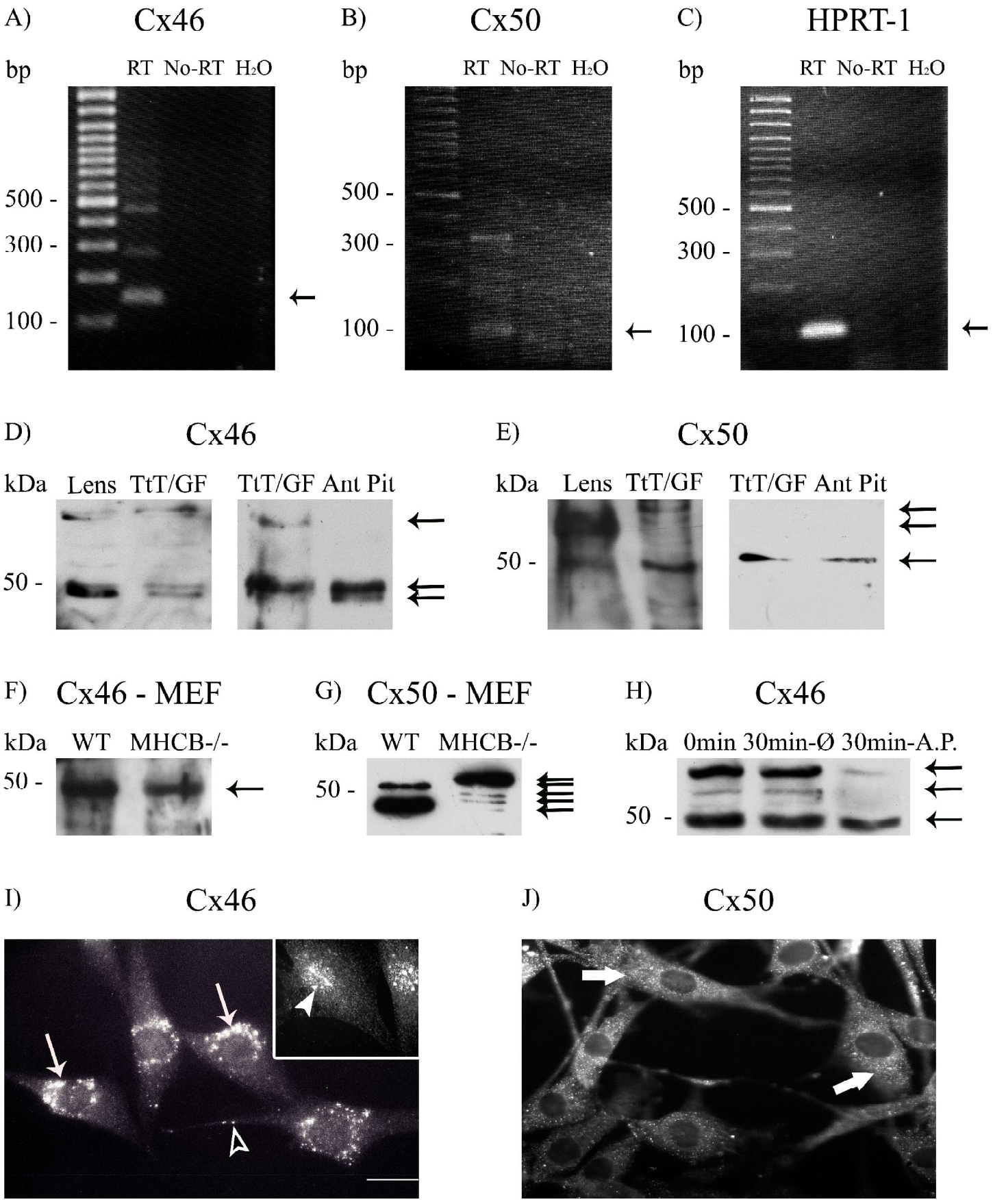

**Figure 10.** Studies on the presence of Cx46 and Cx50 in the TtT/GF folliculo-stellate cell line and in the mouse anterior pituitary

**A – C)** The expression of mRNA coding for Cx46 and Cx50 was evaluated using reverse-transcription PCR. TtT/GF folliculo-stellate cells were lysed and total RNA extracted. From the total RNA, mRNA was reverse transcribed into cDNA, probed using Cx46- and Cx50-specific primers then amplified in a thermocycler. Amplification products (RT) were run on an agarose gel alongside negative controls (No-RT: No reverse transcriptase enzyme; $H_20$: distilled water used in place of cDNA) and a molecular weight marker to calculate band size in base pairs (bp). **A)** Cx46-specific primers generated several amplification products, including one represented by a prominent 133 bp band (**arrow**). **B)** Cx50-specific primers also generated several amplification products including a noteworthy 114 bp band (**arrow**). **C)** Primers specific for HPRT-1 produced a single 104 bp band (**arrow**). Figures are representative of three independent Northern blot experiments.

**D and E)** Western blot was used to evaluate Cx46 and Cx50 protein expression in both the TtT/GF folliculo-stellate cells and mouse anterior pituitary (Ant Pit) against a control tissue (mouse ocular lens). Cell and tissue lysates were migrated on a polyacrylamide gel and proteins were transferred to a nitrocellulose membrane. Proteins were then probed with antibodies specific to Cx46 (Alpha Diagnostic) and Cx50 (Invitrogen). **D)** Membranes incubated with Cx46-specific antibodies revealed three bands in the lens tissue at 48, 49 and 68 kDa, three bands at 48, 49 and 68 kDa in the TtT/GF folliculo-stellate cell line and two bands at 48 and 49 kDa in the anterior pituitary lysate (**arrows**). **E)** Probing with Cx50-specific antibodies revealed two

separate bands at 52 and 61 kDa in the lens tissue homogenate and a single immunoreactive 52 kDa band in the TtT/GF folliculo-stellate cells and anterior pituitary (**arrows**). Prolonged exposure of membranes containing the TtT/GF folliculo-stellate cell lysate revealed the presence of an additional band at 65 kDa. Figures are representative of three independent experiments.

**F and G)** Cx46 and Cx50 protein expression was also investigated in a Wild Type (WT) Mouse Embryonic Fibroblast (MEF) cell line and a MEF cell line lacking the heavy chain of Myosin IIB (MHCB-/-). Cell lysates were subjected to SDS-PAGE then proteins were transferred onto nitrocellulose membranes, which were probed with Cx46 (Alpha Diagnostic) and Cx50 (Invitrogen) antibodies. **F)** Membranes probed for Cx46 generated an immunoreactive band at 49 kDa in WT and MHCB-/- cell lysates (**arrow**). **G)** Membranes probed with Cx50-specific antibodies generated two bands in the WT MEF sample: a relatively less reactive band at 52 kDa and a stronger band at 47 kDa. The MHCB-/- MEF lysate revealed a strongly reactive band at 54 kDa and two relatively weaker immunoreactive bands at 50 and 49 kDa (**arrows**). Figures are representative of three independent experiments.

**H)** The phosphorylation status of Cx46 was verified using alkaline phosphatase. TtT/GF folliculo-stellate cell lysates were incubated in the presence of the enzyme for a period of 30 minutes (30min-A.P.), control experiments were incubated without the enzyme (0min and 30min-Ø). The lysates were subjected to SDS-PAGE, proteins were transferred onto nitrocellulose membrane that was probed with an antibody against Cx46 (Alpha Diagnostic). Both controls showed two strongly reactive bands at 49 and 68 kDa, and a less reactive band at 56 kDa (**arrows**). In the sample incubated with the phosphatase, the 49 kDa band remained, the

56 kDa band disappeared and the 68 kDa band was of much lesser intensity with respect to controls (**arrows**). Figures are representative of three independent experiments.

**I and J)** Cx46 and Cx50 protein distribution was visualized using immunofluorescence microscopy: TtT/GF folliculo-stellate cells were grown on glass coverslips, fixed, permeabilized and probed with Cx46 (Invitrogen) and Cx50 (Invitrogen) primary antibodies followed by fluorophore-conjugated secondary antibodies. **I)** Cx46-specific antibodies demonstrated a perinuclear distribution (**arrows**) in the TtT/GF cells, although a nuclear distribution (**arrowheads**) was also observed (**insert**). Some labelling was associated with the plasma membrane (**arrowhead outline**). **J)** Cx50 labelling showed a uniform cytoplasmic distribution of (arrows). Bar = 20 μm.

## 3.2. Association of Cx46 and Cx50 with cellular organelles in the TtT/GF folliculo-stellate cell line

Given the intracellular distributions of Cx46 and Cx50 seen in **Figures 10I** and **10J**, we next sought to determine the cellular organelles associated with these connexins. This information can provide an insight as to their intracellular trafficking routes and compartmentalization. To achieve this, TtT/GF folliculo-stellate cells were double labelled with either Cx46 or Cx50 and one of several cellular organelle markers (see **Table 1**). Preparations were viewed under a confocal microscope to assess co-localization of the connexin and a particular organelle marker.

### 3.2.1. Association of Cx46 with cellular organelles in TtT/GF folliculo-stellate cells

The isotype of the Cx46 antibody used in our experiments restricted us from double labelling cells with markers of identical isotypes (IgG, made in rabbit). The fluorescent pattern displayed by Cx46 remained rather constant: the labelling was punctate, the distribution was both cytoplasmic and nuclear and in several instances, fluorescence was concentrated in the perinuclear area (**Figure 11**).

**Figure 11A** shows the results from a double labelling of TtT/GF cells for Cx46 and the ER marker, concanavalin A. Concanavalin A produced a fluorescent pattern that was cytoplasmic but that did not extend to the periphery of the cell. Furthermore, the structures labelled by concanavalin A were of an irregular shape. While an initial merge of the individual images did generate a yellow coloration, a closer inspection confirmed the separate localization of Cx46 and

concanavalin A labelling. The *trans*-Golgi was labelled using Wheat germ agglutinin (WGA), which produced a cytoplasmic vesicular-like staining pattern that was concentrated in an area near to the nucleus (**Figure 11B**). A merged image of Cx46 and WGA showed co-localization in the perinuclear area (**Figure 11B, arrows**). The *trans*-Golgi was also labelled with the antibodies against TGN-38, generating a punctate cytoplasmic pattern that was seen around the nuclear area and that did not extend into cytoplasmic projetions (**Figure 11C**). Merging the TGN-38 and Cx46 images showed a partial co-localization in the perinuclear area (**Figure 11C, arrow**).

Early endosomes were labelled with the EEA-1 antibody and displayed vesicular-like structures in the cytoplasm with a greater concentration in the perinuclear area (**Figure 11D**). Cx46 and EEA-1 co-localization was observed in the perinuclear area (**Figure 11D, arrows**). **Figure 11E** shows the labelling of lysosomes with antibodies against the protein LAMP-1 that uncovered round or elongated-shaped structures that were mostly located in the perinuclear area. Cx46 and LAMP-1 co-localizated in some structures in the perinuclear areas (**Figure 11E, arrow**). The co-localization of Cx46 with nuclear structures is presented in section **3.4.2.**.

### 3.2.2. Association of Cx50 with cellular organelles in TtT/GF cells

Given that the Cx50 antibody isotype used in our experiments was IgM, we were able to double label Cx50 with a greater variety of organelle markers than in the case of Cx46. Cx50 displayed an even distribution throughout the cytoplasm, including cellular projections. We did not note any labelling in the nuclei of TtT/GF folliculo-stellate cells (**Figure 12**).

**Figure 12A** shows the distribution of Cx50 and the *trans*-Golgi marker, WGA; the merged image did not uncover any indication of co-localization. Double labelling with TGN-38 (**Figure 12B**) also failed to reveal co-localization with Cx50 in the merged image. **Figure 12C** displays the results from the Cx50 and LAMP-1 double labelling experiments. Despite the similarity of their fluorescent labelling patterns, co-localization between Cx50 and LAMP-1 was not observed in the merged images.

As is seen in **Figure 12D**, the labelling pattern of the ER marker, calnexin, is punctate and irregularly distributed throughout the cytoplasm. Labelling is slightly more concentrated in areas closer to the nucleus. A merged image of Cx50 and calnexin shows partial co-localization in cytoplasmic regions of the cell (**Figure 12D, arrows**). These results were confirmed using another ER marker, concanavalin A, which also demonstrated co-localization in a merged image with Cx50 (**Figure 12E, arrows**). The *cis*-Golgi marker GM-130 labelled vesicles that were organized in a narrow perinuclear area. Faint, punctate labelling was seen towards the periphery of the cell. The merged image of Cx50 and GM-130 showed partial co-localization in the narrow perinuclear area that can be seen in the merged image (**Figure 12F**). **Figure 12G** shows the results obtained from a Cx50 and EEA-1 labelling experiment; we noted a significant amount of co-localization (**Figure 12G, arrows**) with respect to experiments performed with other markers. The areas of co-localization were more prevalent in the perinuclear areas of the two cells pictured. Despite the abundant yellow labelling, the merged image still displayed green and red fluorescence from the individual markers.

**Figure 11.** Confocal microscopy studies on the co-localization of Cx46 and cell organelles in TtT/GF folliculo-stellate cells

A)

Cx46 | Concanavalin A | Merge

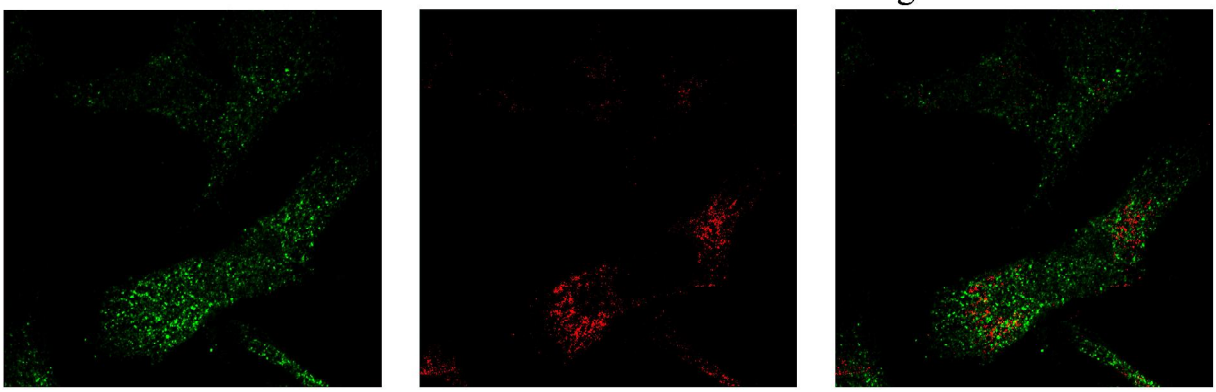

B)

Cx46 | WGA | Merge

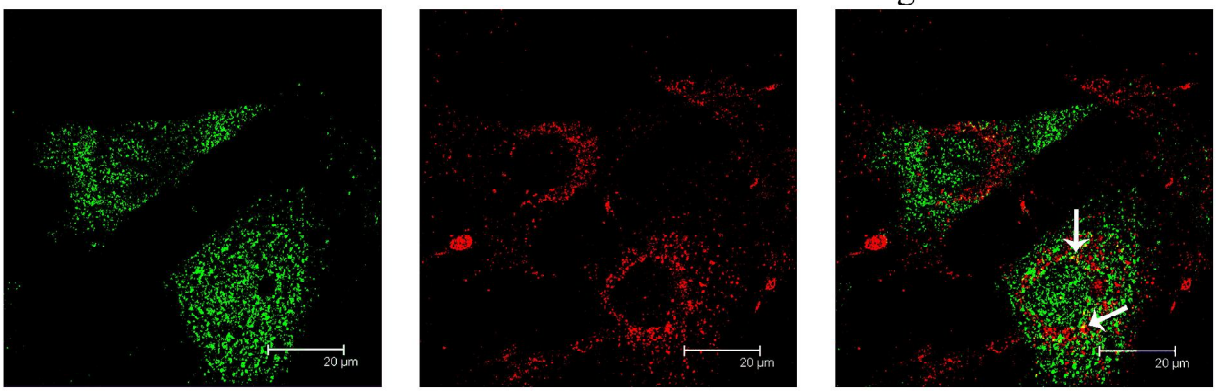


C)

Cx46 | TGN-38 | Merge

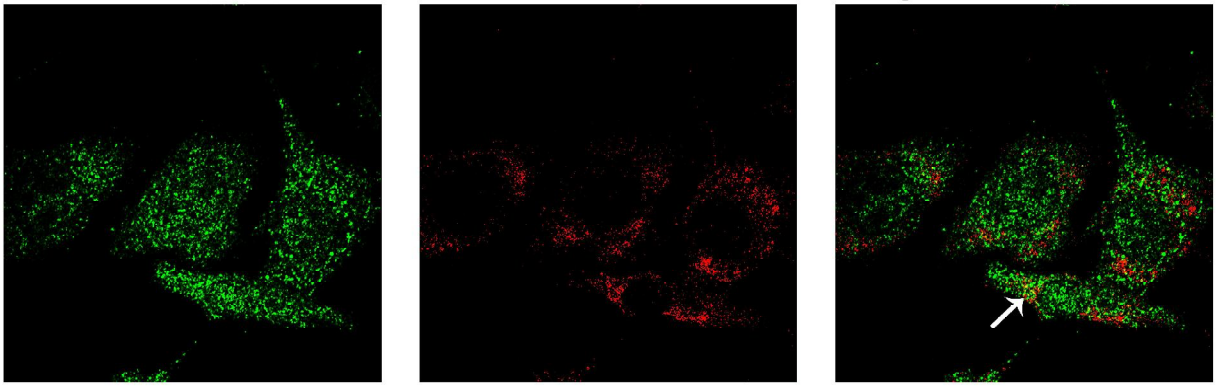

**Figure 11.** Confocal microscopy studies on the co-localization of Cx46 and cell organelles in TtT/GF folliculo-stellate cells

D)

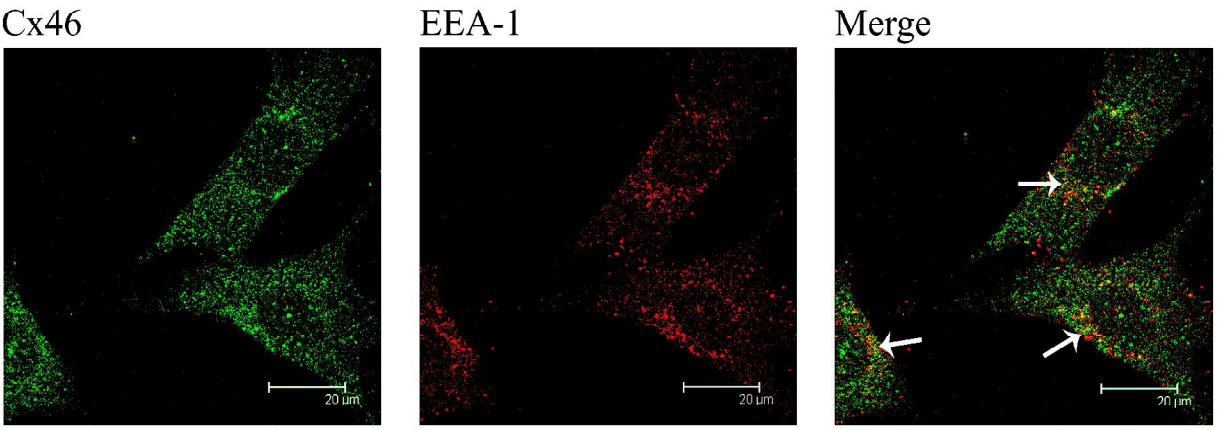


E)

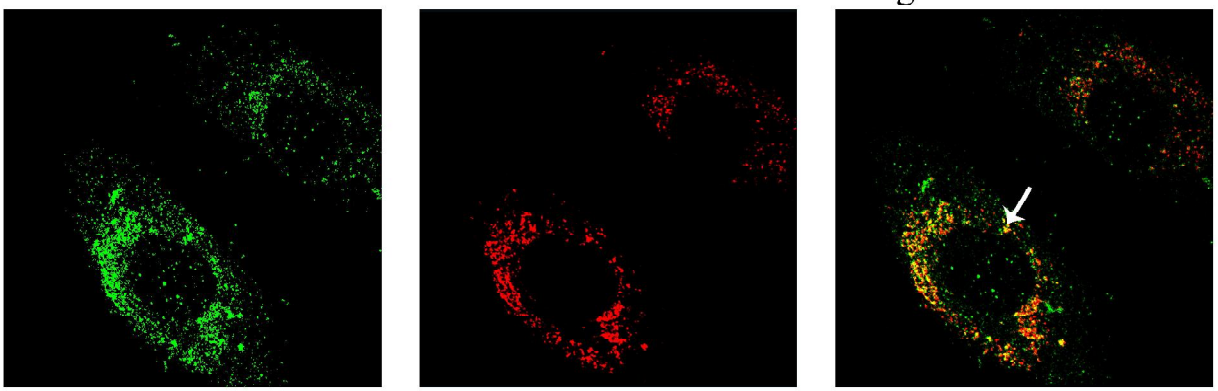

**Figure 11.** Confocal microscopy studies on the co-localization of Cx46 and cell organelles in TtT/GF folliculo-stellate cells.

TtT/GF folliculo-stellate cells were grown on glass coverslips, next they were fixed, permeabilized and double-stained with antibodies against Cx46 (Invitrogen) and an organelle marker (antibody or probe). Preparations were then incubated with FITC- and TRITC-conjugated secondary antibodies or PBS in the case of a probe. Mounted preparations were visualized in successive sections throughout the Z-plane of the cell under a confocal microscope and images were captured. Bar = 20μm.

**A)** Double labelling for Cx46 and concanavalin A (endoplasmic reticulum marker) did not reveal any colocalization.

**B, C, D, E)** Co-localization, indicated by a yellow colouration in the merged image, was observed for experiments labelling cells for Cx46 and for the markers of either: the *trans*-Golgi (WGA and TGN-38), early endosomes (EEA-1) or lysosomes (LAMP-1) (**arrows**).

**Figure 12.** Confocal microscopy studies on the co-localization of Cx50 and cell organelles in TtT/GF folliculo-stellate cells

A)

Cx50 WGA Merge

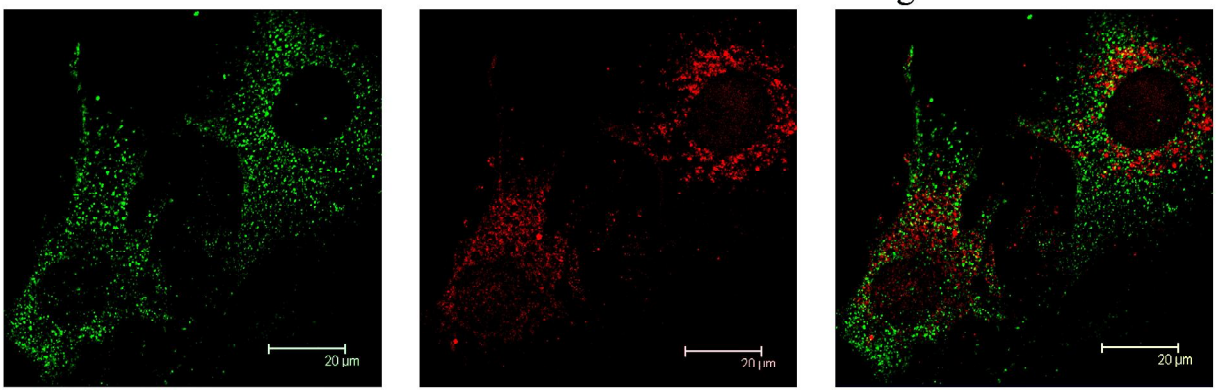


B)

Cx50 TGN-38 Merge

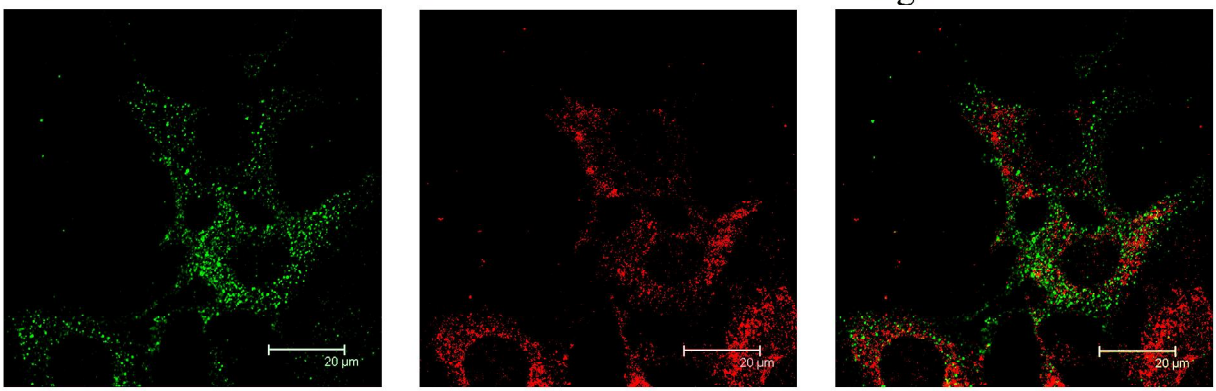


C)

Cx50 LAMP-1 Merge

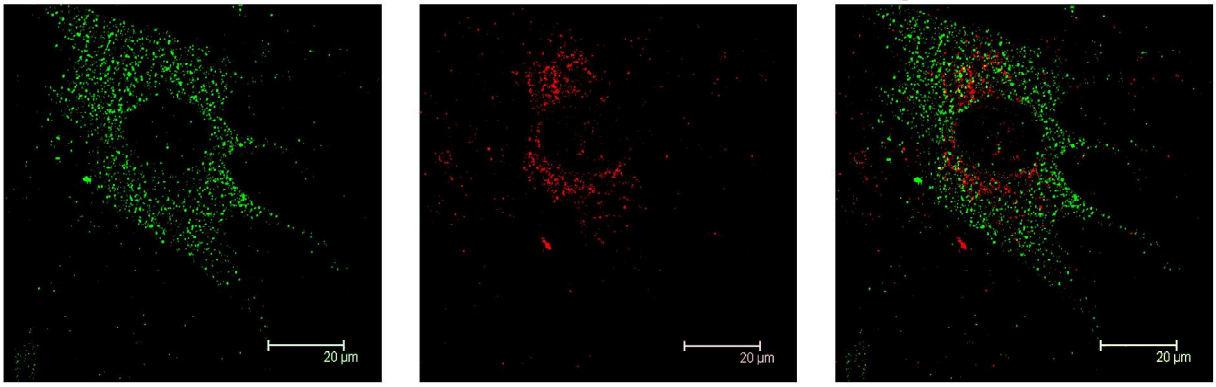

Figure 12. Confocal microscopy studies on the co-localization of Cx50 and cell organelles in TtT/GF folliculo-stellate cells

D)

Cx50 | Calnexin | Merge

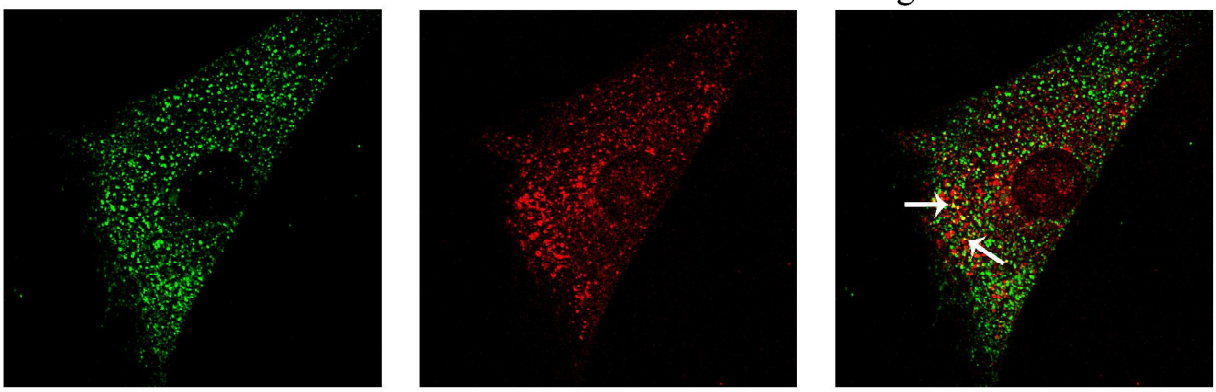

E)

Cx50 | Concanavalin A | Merge

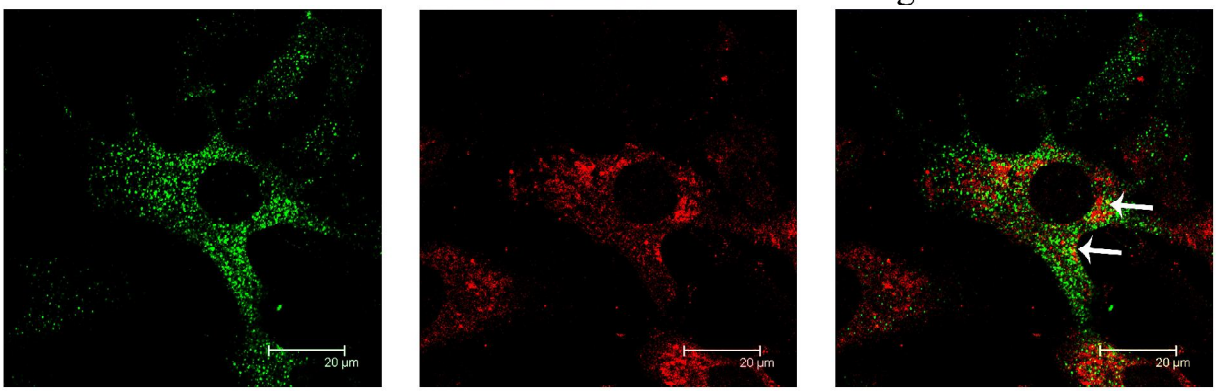


F)

Cx50 | GM-130 | Merge

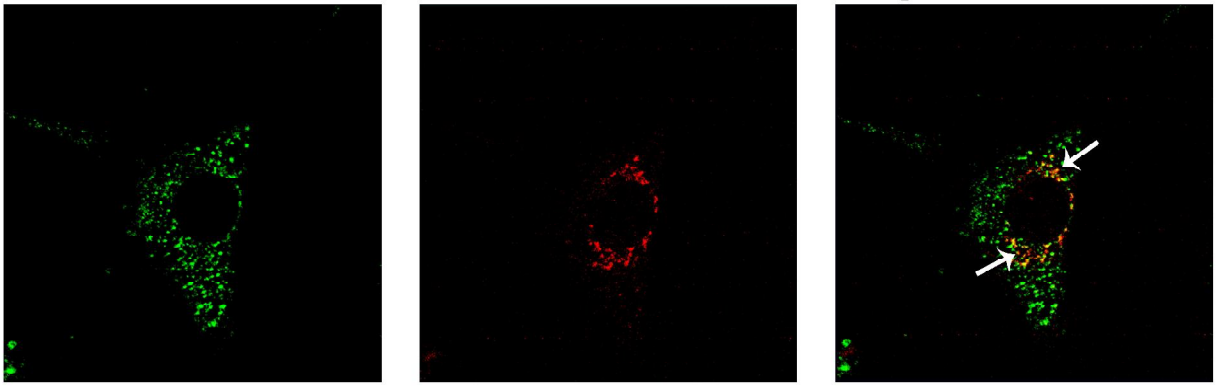

**Figure 12.** Confocal microscopy studies on the co-localization of Cx50 and cell organelles in TtT/GF folliculo-stellate cells

G)

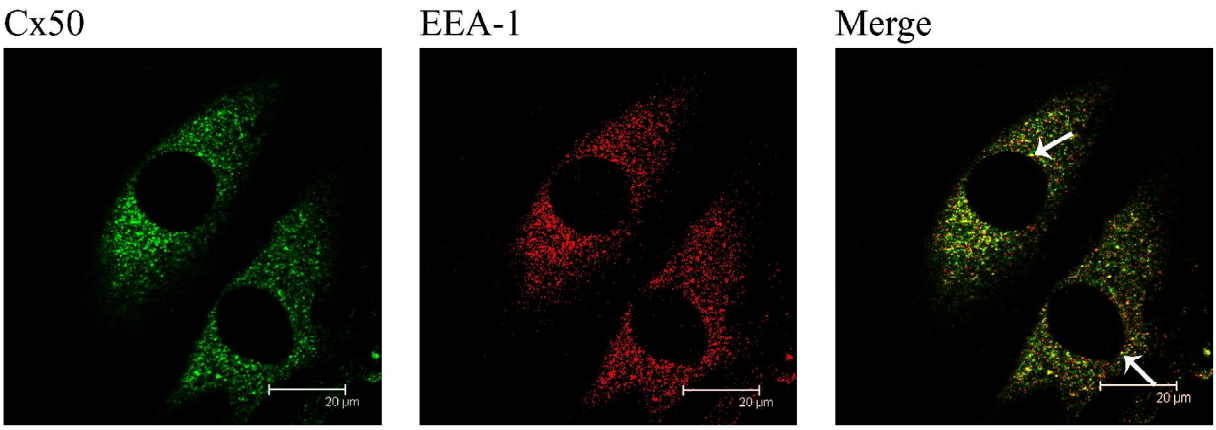

**Figure 12.** Confocal microscopy studies on the co-localization of Cx50 and cell organelles in TtT/GF folliculo-stellate cells

TtT/GF folliculo-stellate cells were grown on glass coverslips, next they were fixed, permeabilized and double-stained with a Cx50 antibody (Invitrogen) and an organelle marker (antibody or probe). Preparations were then incubated with FITC- and TRITC-conjugated secondary antibodies or with PBS in the case of probes. Mounted preparations were visualized in successive sections throughout the Z-plane of the cell under a confocal microscope and images were captured. Bar = 20μm.

**A, B, C)** Experiments labelling Cx50 and either the *trans*-Golgi (WGA and TGN-38) or lysosomes (LAMP-1) did not reveal any co-localization.

**D, E, F, G)** Double labelling experiments with Cx50 and markers for either: the endoplasmic reticulum (calnexin and concanavalin A), *cis*-Golgi (GM-130) or the early endosomes (EEA-1) revealed yellow colouration in merged images, indicating co-localization (**arrows**).

| Cellular Domain | Markers | Cx46 | Cx50 |
|---|---|---|---|
| Endoplasmic reticulum | Calnexin | N/A | ✓ |
| Endoplasmic reticulum | Concanavalin A | X | ✓ |
| *Cis*-Golgi | GM-130 | N/A | ✓ |
| *Trans*-Golgi | TGN-38 | ✓ | X |
| *Trans*-Golgi | WGA | ✓ | X |
| Early endosomes | EEA-1 | ✓ | ✓ |
| Lysosomes | LAMP-1 | ✓ | X |

**Table 5.** Summary of co-localization studies between Cx46 and Cx50 with markers of cellular organelles. X denotes no co-localization was observed, ✓ denotes that co-localization was observed, N/A denotes an experiment that has not been performed due to a common isotype between the Cx46 antibody and the probe.

## 3.3. Characterization of Cx46 and Cx50. Presence within membrane domains: lipid rafts and caveolae, of TtT/GF folliculo-stellate cells

After having investigated the intracellular distribution of Cx46 and Cx50, we proceeded to further characterize the localization of these two connexins in the TtT/GF folliculo-stellate cells by examining their association with lipid rafts and caveolae. Previous studies have described the importance of lipid rafts and caveolae with respect to the physiological function of connexins (Langlois, Cowan et al. 2008). Furthermore, the association of Cx46 and Cx50 to lipid rafts and caveolae is a topic that has previously been investigated in the ocular lens (Schubert, Schubert et al. 2002, Lin, Lobell et al. 2004). Despite the fact that we observed very little fluorescent labelling of Cx46 and Cx50 at the cell membrane, we nevertheless investigated whether Cx46 and Cx50 could be associated with lipid rafts and/or caveolae in the TtT/GF folliculo-stellate cells. Also, our immunolabelling method may have not been sensitive enough to detect membrane-bound Cx46 and Cx50. To accomplish this, we subjected TtT/GF folliculo-stellate cell lysates to ultracentrifugation in a discontinuous sucrose gradient to isolate cell fractions insoluble in a Triton X-100 solution. Following ultracentrifugation, a single turbid band representing the Detergent-insoluble glycolipid (DIG) fraction was visible close to where the border of the 15% and 5% sucrose-MBS solutions. Equal volume fractions (1 – 11) were successively taken from the ultracentrifuge tube, the turbid band was taken into the third and fourth fractions. Fractions were dosed for protein concentration then subjected to SDS-PAGE. Proteins were transferred to a nitrocellulose membrane then incubated with antibodies.

### 3.3.1. Identifying the Detergent-insoluble glycolipid fractions isolated from TtT/GF folliculo-stellate cells via the presence of flotillin-1 and caveolin-1

As a control we characterized the presence of lipid rafts and caveolae, by probing all eleven fractions, the pellet (fraction 12) and a whole cell lysate (L) with antibodies against flotillin-1 (lipid raft marker) and caveolin-1 (caveolae marker) by Western blotting.

As shown in **Figure 13A**, the lipid raft marker flotillin-1 was found as a 47 kDa immunoreactive band in the DIG fractions (3 and 4) and throughout fractions 7 to 11, representing the denser portions of the preparation. The pellet (fraction 12) contained ample amounts of flotillin-1, and the whole cell lysate (L) revealed the presence of flotillin-1. The 22 kDa immunoreactive band corresponding to caveolin-1, the marker for caveolae, was found in the DIG fractions and in varying quantities in fractions 6 through 11. Its presence was also noted in the pellet (fraction 12) and in the whole cell lysate (L). We also employed the *cis*-Golgi marker, GM-130 as a negative control to ensure that our DIG fractions were not contaminated with fragments of the *cis*-Golgi (**Figure 13B**). The immunoreactive doublet at 130 kDa was found only in fractions 8 through 11, in the pellet (fraction 12) and in the whole cell lysate (L). Prolonged exposure of the membrane did not show any immunoreactive bands in fractions 1 to 7.

We also determined if Cx43 was present in the DIG fractions as evidence of this had previously been documented in other cell types (Langlois, Cowan et al. 2008). As shown in **Figure 13C**, prolonged exposure of the membrane probed with antibodies against all isoforms of Cx43 (pan-Cx43) revealed the presence of a 37 kDa band (one of the Cx43 isoforms) in the DIG fractions.

A series of different immunoreactive bands representing different forms of Cx43 were also detected in greater quantities in fractions 6 to 11, in the pellet (fraction 12) and in the whole cell lysate (L).

### 3.3.2. Association of Cx46 and Cx50 with lipid raft and caeolae markers

**Figure 13C** shows that nitrocellulose membranes probed for Cx46 generated an immunoreactive band (49 kDa) in the pellet fraction (12) and whole cell lysate (L). Probing membranes for Cx50 produced an immunoreactive signal (52 kDa) in the pellet fraction (fraction 12) and in the whole cell lysate fraction (L) (**Figure 13C**). Extended exposure times of the Cx46 and Cx50 membranes did not reveal immunoreactive bands in any of the other fractions.

To confirm our results from the previously presented isolation study, we labelled cells with Cx46 or Cx50 along with the lipid raft and caveolae markers flotillin-1 and caveolin-1. Preparations from this double-labelling immunofluorescence experiment were then viewed under the confocal microscope where images were captured and co-localization was assessed.

Throughout the experiment, labelling for Cx46 was punctate and present throughout the nucleus and cytoplasm, but rarely extending into cytoplasmic projections. At times, fluorescence was also found to be concentrated in the perinuclear area. Flotillin-1 demonstrated a thorough, uniform labelling throughout the nucleus and cytoplasm, even extending into cellular projections (**Figure 14A**). Labelling for flotillin-1 did not generate concentrated areas of fluorescence around the periphery of the cells. Merging the Cx46 and flotillin-1 images did not reveal any co-

localization. Due to the isotype of caveolin-1 (IgG, made in rabbit), a double labelling experiment with Cx46 could not be performed.

As seen in **Figure 14B**, labelling for Cx50 was as previously seen: punctate and evenly distributed throughout the cytoplasm while absent in the nucleus. Caveolin-1 revealed a non-uniform blurred labelling throughout the cytoplasm and nucleus. Fluorescence for the caveolae marker was seen to be concentrated at the periphery of the cells in several locations. When merged, images of Cx50 and caveolin-1 did not reveal any co-localization. Flotillin-1 displayed a punctate labelling that was evenly spread through the cytoplasm (**Figure 14C**). In addition, fluorescence for the lipid raft marker was also seen in the nucleus, although to a lesser extent. The periphery of the cell did not display any concentrated areas of fluorescence. Merging the individual Cx50 and flotillin-1 images results in substantial co-localization (**Figure 14C, arrows**). In addition, similarities in the labeling patterns between the two markers were noted upon closer analysis of the individual images.

**Figure 13.** Studies on the presence of Cx 46 and Cx50 in lipid rafts and caveolae in TtT/GF folliculo-stellate cells

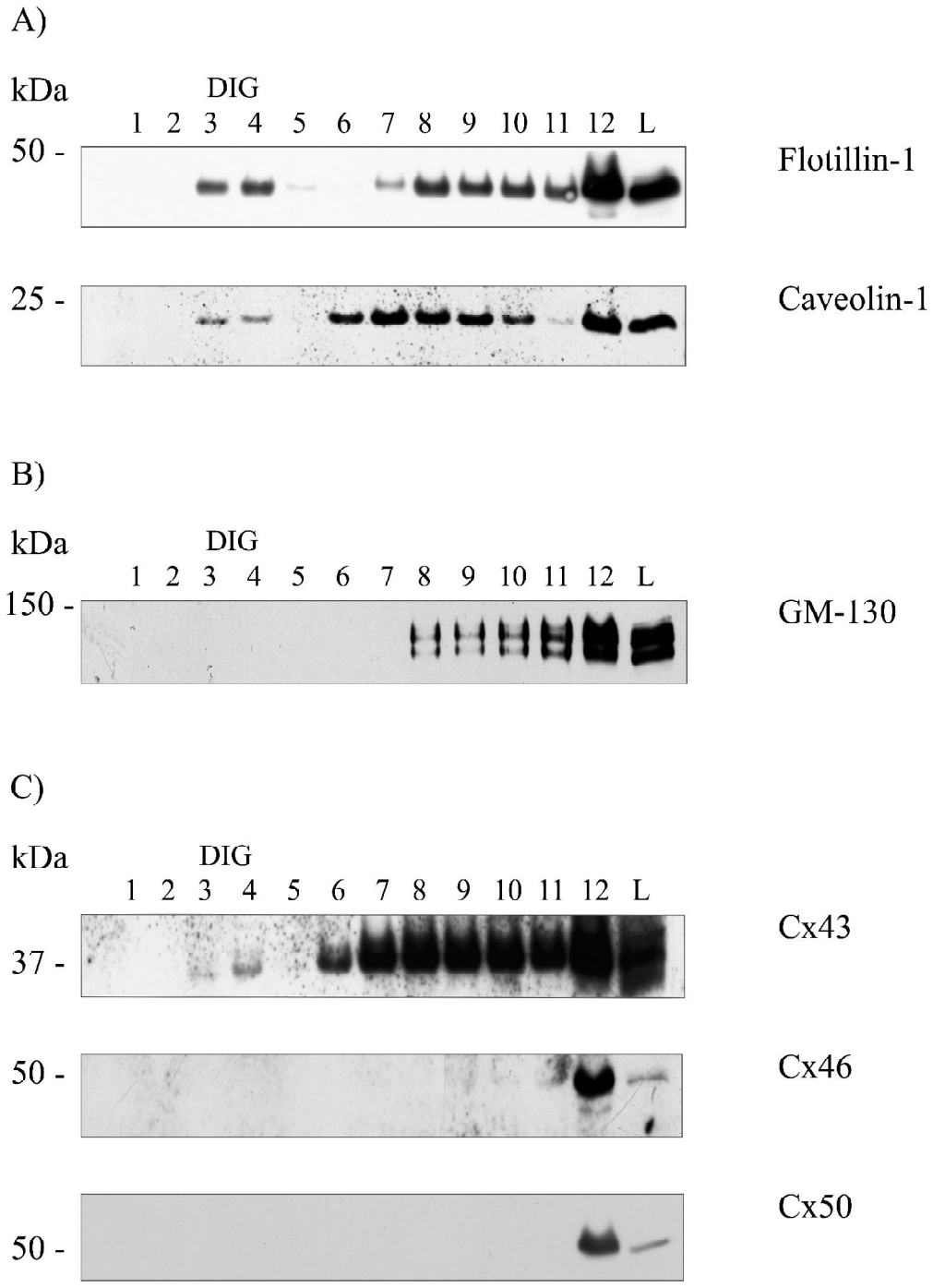

**Figure 13.** Studies on the presence of Cx46 and Cx50 in lipid rafts and caveolae in TtT/GF folliculo-stellate cells.

To determine the presence of Cx46 and Cx50 in TtT/GF folliculo-stellate cell lipid rafts and caveolae, cells were homogenated in a non-ionic detergent, then separated through ultracentrifugation at 200,000g (18 hours, 4°C) on a discontinuous 5%, 15% and 25% sucrose gradient. Post-centrifugation, a turbid white band was visible close to where the 5% and 15% sucrose border was located. Fractions of the preparation were extracted, with the turbid band being present in the third and fourth fractions. In total, eleven equal volume fractions of the gradient (1 – 11), the pellet (12) and whole cell lysate (L) were subjected to SDS-PAGE, transferred onto a nitrocellulose membrane and probed with markers for: lipid rafts (flotillin-1), caveolae (caveolin-1), and the *cis*-Golgi-apparatus (GM-130). Preparations were also probed with antibodies against Cx43 (Sigma), Cx46 (Alpha Diagnostic) and Cx50 (Invitrogen).

**A)** Flotillin-1 was detected through the denser fractions and pellet but also in the Detergent-insoluble glycolipid (DIG) fractions (3$^{rd}$ and 4$^{th}$ fractions). Similarly, caveolin-1 was distributed in the denser fractions and in the DIG fractions.

**B)** The *cis*-Golgi marker, GM-130, was only detected in denser fractions and in the pellet.

**C)** Cx43 was found in denser fractions and upon prolonged exposure was also found to be in the

DIG fractions. Cx46 and Cx50 were only detected in the pellet (12) and whole cell lysate (L). Despite prolonged exposure and repeated experiments, Cx46 and Cx50 were not detected in the DIG fractions of TtT/GF folliculo-stellate cells.

Figures are representative of three independent experiments.

**Figure 14.** Confocal microscopy studies on the co-localization of Cx46 and Cx50 with lipid raft and caveolae markers in TtT/GF folliculo-stellate cells

A)

Cx46 | Flotillin-1 | Merge

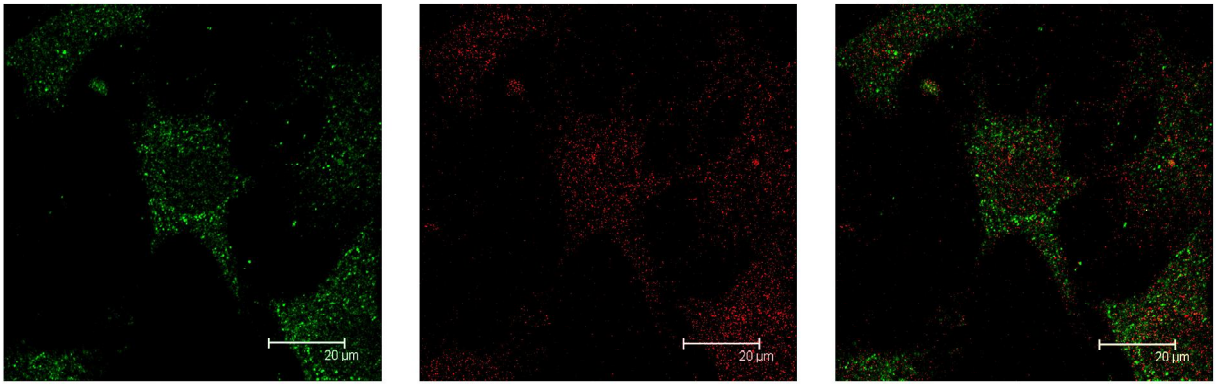


B)

Cx50 | Caveolin-1 | Merge

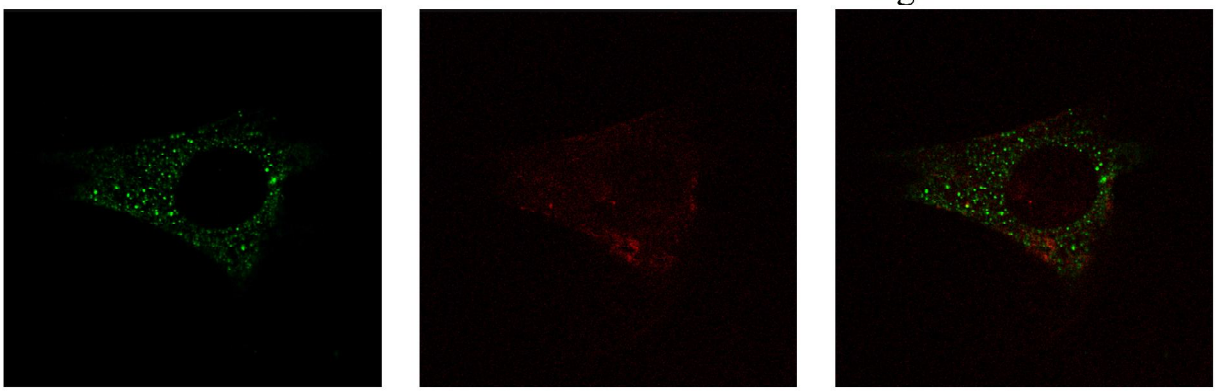

C)

Cx50 | Flotillin-1 | Merge

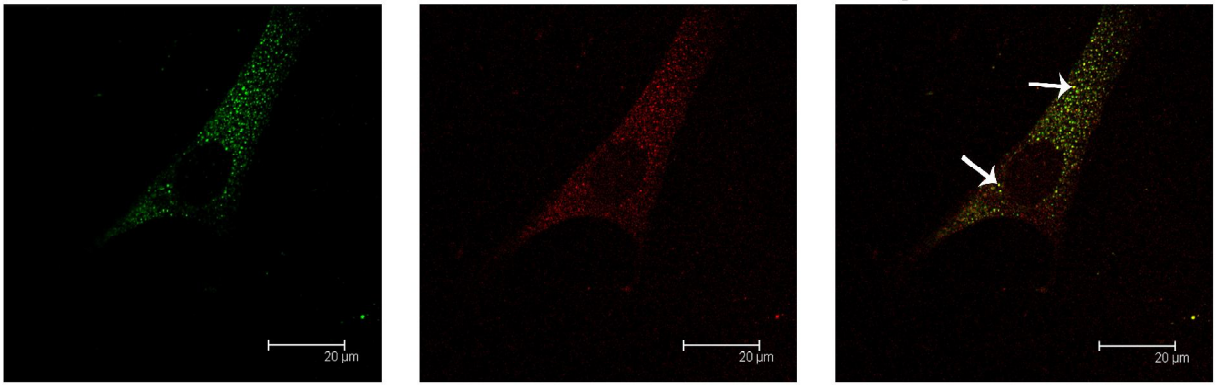

**Figure 14.** Immunofluorescence studies on the co-localization of Cx46 and Cx50 with lipid raft and caveolae markers in TtT/GF folliculo-stellate cells

TtT/GF folliculo-stellate cells were grown on glass coverslips, fixed, permeabilized and double-stained with a Cx46 (Invitrogen) or Cx50 (Alpha Diagnostic) antibody and a lipid raft/caveolae marker. Preparations were then incubated with FITC- and TRITC-conjugated secondary antibodies. Mounted preparations were visualized in successive sections throughout the Z-plane of the cell under a confocal microscope and images were captured. Bar = 20μm.

**A)** Double labelling with Cx46 and flotillin-1 (lipid raft marker) did not reveal any co-localization.

**B)** Labelling for Cx50 and caveolin-1 (caveolae marker) did not result in any indication of co-localization.

**C)** Double labelling for Cx50 and flotillin-1 did show co-localization in the cytoplasm (arrows). Figures are representative of three independent experiments.

## 3.4. Investigation of the nuclear labelling of Cx46 in TtT/GF folliculo-stellate cells

We have investigated the intracellular cytoplasmic localization of Cx46 with regard to organelles (**Figure 11**) and lipid rafts and caveolae (**Figure 13**, **Figure 14**). In addition, as is shown in insert of **Figure 10I**, immunofluorescent labelling of TtT/GF folliculo-stellate cells for Cx46 occasionally displayed a nuclear distribution, an observation that was later confirmed by confocal microscopy (**Figure 11**). We pursued the investigation of this finding by characterizing the nature of the nuclear Cx46 by studying whether nuclear Cx46 co-localized with a variety of markers of major sub-nuclear structures.

### 3.4.1. Separation of different Cx46 immunoreactive bands by fractionation / nuclear isolation of TtT/GF folliculo-stellate cells

TtT/GF folliculo-stellate cells were lysed and fractionated by successive rounds of centrifugation and resuspension in an NP-40 solution. Proteins in the nuclear (N), post-nuclear (PN) and whole cell lysate (L) were separated by SDS-PAGE, followed by transfer onto a nitrocellulose membrane. The purity of the fractions was assessed by probing the membranes with antibodies against the sub-nuclear structures: NOPP-140 – labelling a protein travelling between the nucleolus and coiled bodies (Isaac, Yang et al. 1998), PML – labelling promyelocytic leukemia nuclear bodies, also known as nuclear dots (Borden and Culjkovic 2009) and coilin/p80 – labelling coiled bodies, also known as Cajal bodies (Andrade, Chan et al. 1991) (**Figure 15A**). Fractions were also characterized using antibodies against markers of cytoplasmic organelles: GM-130 – *cis*-Golgi and calnexin – ER; membrane domains: flotillin-1 – lipid rafts and

caveolin-1 – caveolae; and cytoplasmic proteins: GAPDH – Glyceraldehyde-3-phosphate dehydrogenase (**Figure 15B**).

**Figure 15A** shows representative western blots of the characterization of the subcellular fractionation. Membranes probed for NOPP-140 displayed a band at 142 kDa and another at 110 kDa. The band at 142 kDa was present only in the nuclear and whole cell lysate fractions (**Figure 15A, arrowhead**). Moreover, this particular band was enriched in the nuclear fraction when compared to the whole cell lysate fraction (which presented a faint band). The 110 kDa band was seen throughout the three fractions and a review of the literature revealed it to be a non-phosphorylated version of the NOPP-140 present in both the cytoplasm and nucleus (Li, Meier et al. 1997). PML presented an immunoreactive doublet at 97 and 96 kDa. The doublet was present only in the whole cell lysate and nuclear fractions and was concentrated in the later fraction. The high intensity of the bands in the nuclear fraction made it difficult to distinguish as a doublet. Membranes probed for coilin/p80 revealed a single, 80 kDa band present only in the whole lysate and nuclear fractions. Immunoreactivity for coilin/p80 was stronger in the nuclear fraction (**Figure 15A**).

**Figure 15B** shows the results from membranes probed with different cytoplasmic markers: GM-130, calnexin and GAPDH. GM-130 displayed a 130 kDa doublet (previously seen in **Figure 13B**) in both the lysate and post-nuclear fractions. The intensity of the doublet is greater in the post-nuclear fraction. Calnexin produced a relatively intense 90 kDa band in the whole cell lysate and post-nuclear fraction. This band was also noted in the nuclear fraction although at a much lesser intensity. Membranes probed for GAPDH revealed a 37 kDa band in the whole cell

lysate and post-nuclear fractions; an immunoreactive signal was not seen in the nuclear fraction for this marker. Membranes were also probed with antibodies against the lipid raft and caveolae markers: flotillin-1 and caveolin-1 (**Figure 15B**). Flotillin-1 (47 kDa) was present throughout the post-nuclear and nuclear fractions as well as the whole cell lysate. Immunoreactivity for flotillin-1 was relatively less in the post-nuclear fraction. Similarly, caveolin-1 (22 kDa) was found in the post-nuclear and nuclear fractions and whole cell lysate, and the relative immunoreactive intensity of the marker was less in the post-nuclear fraction.

**Figure 15C** displays the immunoreactive bands that appear upon probing the subcellular fractions for Cx46. The 68 kDa band, corresponding to phosphorylated Cx46 was present in the whole cell lysate and post-nuclear fraction. The nuclear fraction did not reveal the presence of this band. A 56 kDa band, also a phophorylated version of Cx46, was observed in the nuclear fraction; however, corresponding bands were not found in the whole cell lysate nor in the post-nuclear fraction; rather, diffuse smears of a similar molecular mass were found. A relatively strong immunoreactive band was found in the whole cell lysate spanning across the 48 and 49 kDa area. In the post-nuclear fraction, a less intense 48 kDa band was identified and in the nuclear fraction, a moderately intense 49 kDa immunoreactive band was seen. The nuclear fractions revealed the presence of a 25 kDa band that was not present in either the lysate or post-nuclear fractions. A faint 14 kDa immunorective band was also noticed in the whole cell lysate. This band did not appear in the post-nuclear fraction but displayed strong reactivity in the nuclear fraction.

### 3.4.2. Association of nuclear Cx46 with the nuclear protein markers in the TtT/GF folliculo-stellate cells

After having determined that certain isoforms or cleaved products of Cx46 are found in the nucleus (**Figure 15C**) and taking into account the complex organization of the eukaryotic cell nucleus, we looked to uncover the specific regions of the nucleus to which Cx46 localized. To achieve this, we double labelled TtT/GF folliculo-stellate cells for Cx46 and markers of major sub-nuclear structures: coilin/p80, PML and NOPP-140. Preparations were viewed by confocal microscopy and images were captured to assess the co-localization of markers. Throughout these immunofluoresce microscopy experiments, the nuclear labelling of Cx46 was predominantly seen as irregularly shaped aggregations scattered throughout the nucleus.

**Figure 16A** displays the immunofluorescent labelling for Cx46 and coilin/p80. When contrasted to Cx46, the labelling of coilin/p80 is clearly in the nucleus but also appears sparsely distributed in the cytoplasm. This result was not expected as we did not observe an immunoreactive band(s) in the post-nuclear fraction that would support this result (**Figure 15A**). The merging of the individual images of Cx46 and coilin/p80 did not reveal any co-localization either in the nucleus or cytoplasm. Probing TtT/GF folliculo-stellate cells for PML clearly showed rounded, well defined structures that were evenly distributed within the nucleus (**Figure 16B**). Fluorescence for PML was not seen elsewhere in the cell. Merging the images of Cx46 and PML did not show any co-localization. Furthermore, a closer inspection of the distribution pattern did not reveal any similarities between the two. **Figure 16C** shows the immunolabelling of NOPP-140 that highlighted within the nucleus, irregularly-shaped structures showing a greater degree of fluorescence. Fluorescence for NOPP-140 in the cytoplasm was weak, although thorough, even

extending to cellular elongations. The immunolabelling of NOPP-140 in the cytoplasm of TtT/GF folliculo-stellate cells also served to confirm the presence of the non-phosphorylated form of NOPP-140 in the post-nuclear fraction of the cell fractionation/nuclear isolation experiment (**Figure 15A**). The merged images of Cx46 and NOPP-140 indicated a partial co-localization (**Figure 16C, arrow**) in the nucleus; furthermore, the irregularly-shaped structure containing punctate fluorescent spots was common to both individual images.

**Figure 15.** Studies on the presence of Cx46 isoforms in the nucleus of TtT/GF folliculo-stellate cells

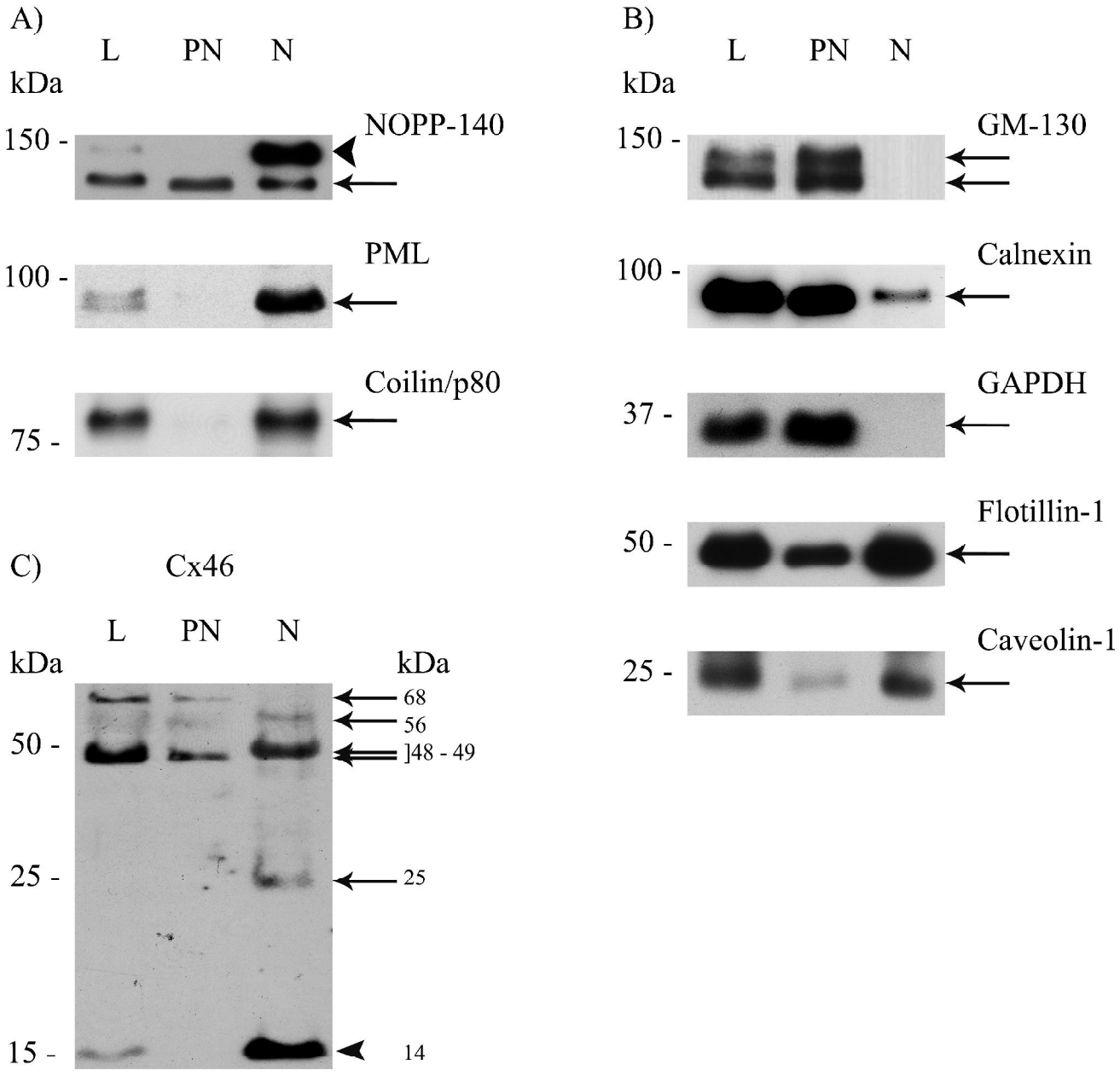

**Figure 15.** Studies on the presence of Cx46 isoforms in the nucleus of TtT/GF folliculo-stelate cells

TtT/GF folliculo-stellate cells were lysed in the presence of NP-40 then centrifuged to recover the nuclei. The supernatant was kept and constituted the post-nuclear fraction. The isolated nuclei (N), post-nuclear fractions (PN) and a whole cell lysate (L) were subjected to SDS-PAGE followed by a transfer of the proteins onto nitrocellulose membranes. **A)** Membranes were probed with antibodies targeting the following nuclear structures: the nucleolus and coiled bodies (NOPP-140), promyelocytic leukemia nuclear bodies (PML) and Cajal bodies (coilin/p80). **B)** Membranes were also probed with markers for the following cytoplasmic and membrane domains: *cis*-Golgi (GM-130), endoplasmic reticulum (calnexin), a cytosolic marker (glyceraldehyde 3-phosphate dehydrogenase – GAPDH), lipid rafts (flotillin-1) and caveolae (caveolin-1). **C)** Membranes were incubated with an antibody against Cx46 (Alpha Diagnostic). The figure shows Western blots representative of three independent experiments.

**A)** The nuclear marker NOPP-140 showed two immunoreactive bands at 140 (arrowhead) and 110 kDa (arrow). The 142 kDa band was restricted to the whole cell lysate and nuclear fraction where it was enriched, while the 110 kDa band was present across the three fractions. The other nuclear markers: PML and coilin/p80 were detected in the nuclear fraction and in the whole cell lysate, while they were absent from the post-nuclear fraction.

**B)** GM-130 and GAPDH were only detected in the whole cell lysate and post-nuclear fractions. Calnexin was detected in the whole cell lysate and post-nuclear fractions and exhibited a

relatively weak signal in the nuclear fraction. The membrane domain markers, flotillin-1 and caveolin-1 were found throughout the three fractions.

**C)** The 68 kDa immunoreactive band that corresponded to the phosphorylated form of Cx46 was found in the post-nuclear fraction and whole cell lysate (**arrow**), but was not recovered in the nuclear fraction. The 56 kDa band also corresponding to a phosphorylated form of Cx46 was detected in the nuclear fraction (**arrow**). A broad band spanning between 49 and 48 kDa was seen in the lysate, while a single 48 kDa band was seen in the post-nuclear fractions and a 49 kDa band was noted in the nuclear fraction (**arrows**). A single band was detected in the nuclear fraction at 25 kDa, but not in the lysate or post-nuclear fraction (**arrow**). A band seen at 14 kDa in the whole cell lysate was found to be enriched in the nuclear fraction but absent in the post-nuclear fraction (**arrowhead**).

**Figure 16.** Confocal microscopy studies on the co-localization of Cx46 and nuclear markers in TtT/GF folliculo-stellate cells

A)

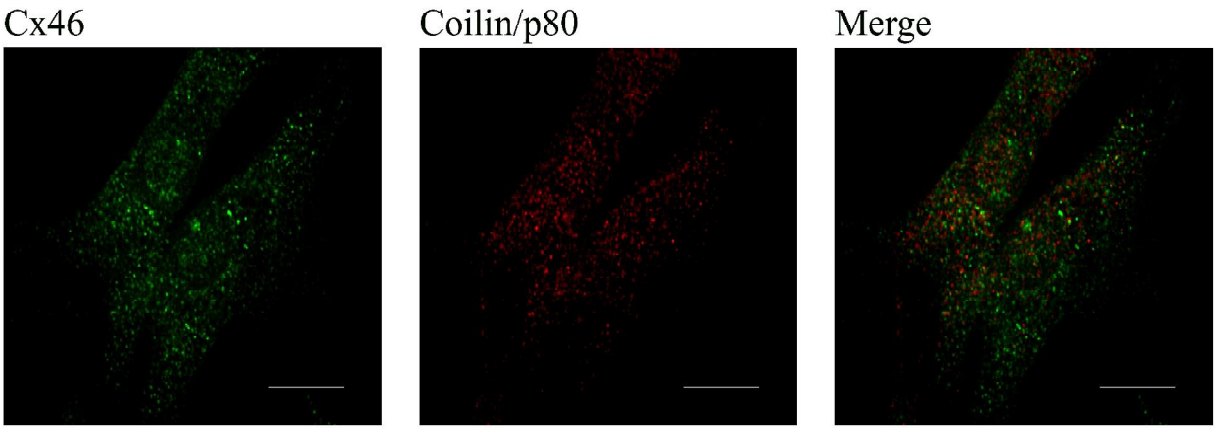


B)

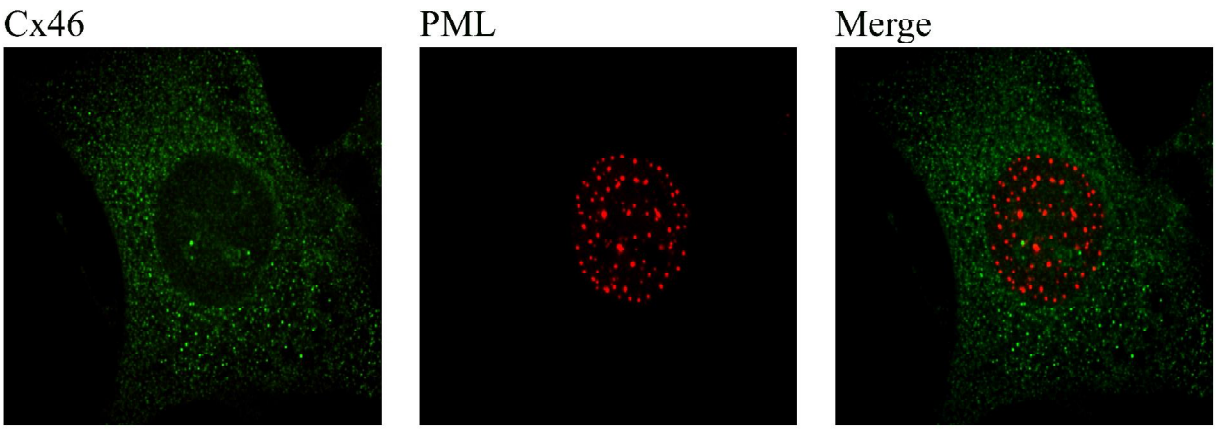


C)

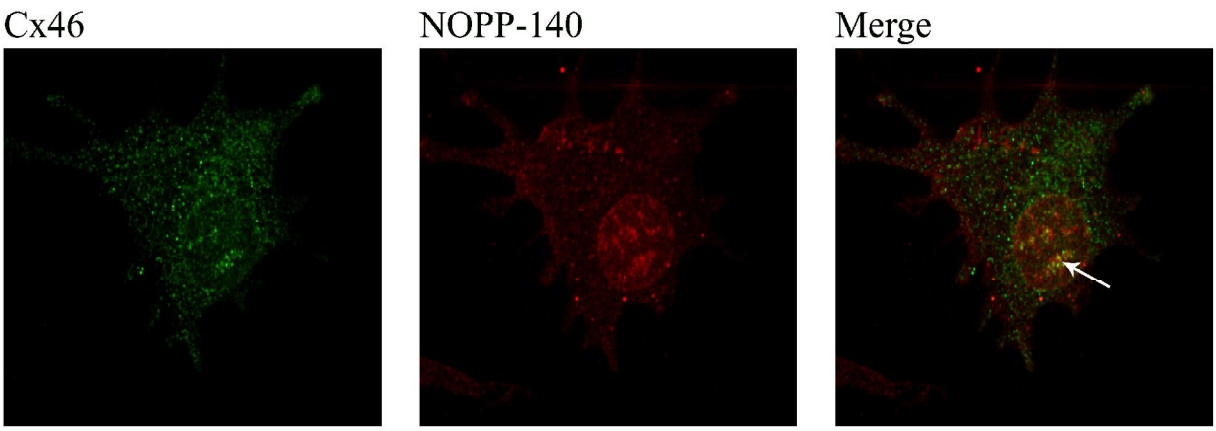

**Figure 16.** Confocal microscopy studies on the co-localization of Cx46 and nuclear markers in TtT/GF folliculo-stelate cells

TtT/GF folliculo-stellate cells grown on glass coverslips were fixed, permeabilized and probed with antibodies against Cx46 (Invitrogen) and markers of the following nuclear structures: Cajal bodies (coilin/p80), nucleolus-coiled bodies (NOPP-140) and promyelocytic leukemia nuclear bodies (PML), followed by fluorophore-conjugated secondary antibodies. Cells were visualized using confocal microscopy and images were captured at regular intervals throughout the Z plane/thickness of the cells. Figures are representative of three independent immune-labelling experiments. Bar = 20 μm.

**A)** Labelling of the TtT/GF folliculo-stellate cells for Cx46 and coilin/p80 did not reveal any co-localization.

**B)** Labelling for Cx46 and PML did not indicate any co-localization within the cell nucleus.

**C)** Immuno-staining for Cx46 and NOPP-140 revealed yellow colouration of irregularly shaped aggregations in the nucleus indicating co-localization (**arrow**).

## 3.5. Studies on the protein expression profiles of Cx46 and Cx50 in the TtT/GF folliculo-stellate cell line in response to bFGF treatment

In the previous sections, we identified and characterized Cx46 and Cx50 in the stable TtT/GF folliculo-stellate cell line. In a series of preliminary studies, whereby our objective was to understand the role of Cx46 and Cx50 in the anterior pituitary gland, we treated serum-starved TtT/GF folliculo-stellate cells with bFGF and observed the effects of the growth factor on the protein levels of Cx46 and Cx50 over time. We chose bFGF as a cellular stimulant for several reasons:

1. The anterior pituitary gland contains the highest concentration of bFGF as compared to other tissues (Chaidarun, Eggo et al. 1994).
2. The effect of bFGF on Cx43 in various other tissues has been previously documented (Chaidarun, Eggo et al. 1994, Doble and Kardami 1995).

Relative protein levels are expressed as a function of their fold change over the value obtained for time 0 minutes.

### 3.5.1. Protein expression profile of Cx46 in response of bFGF treatment of TtT/GF folliculo-stellate cells

In the experiments investigating the effects of bFGF on Cx46 protein levels over an eight hour time span, we consistently observed at 8 hours treatment, a decrease in the levels of Cx46 (40%). However, the time course for the inhibitory effect of bFGF on Cx46 expression differed in both trials (**Figure 17A**).

### 3.5.2. Protein expression profile of Cx50 in response of bFGF treatment of TtT/GF cells

Experiments investigating the expression profile of Cx50 were initially conducted over an 8 hour period; after observing visibly evident changes in protein relative quantity, it was decided to extend the treatment time to 24 hours (**Figure 17B**). All experiments produced a single immunoreactive band at 52 kDa. Changes in the protein quantities in response to bFGF was evident although occurred at different times throughout the trials. All experiments showed a transient increase in Cx50 expression following treatment with bFGF.

**Figure 17.** Preliminary studies: Expression profiles of Cx46 and Cx50 in response to bFGF treatment

A) Cx46

Trial 1

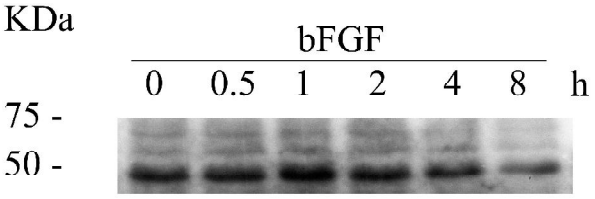


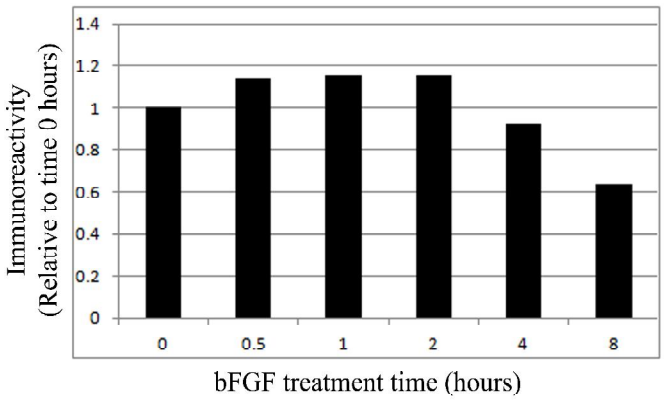


Trial 2

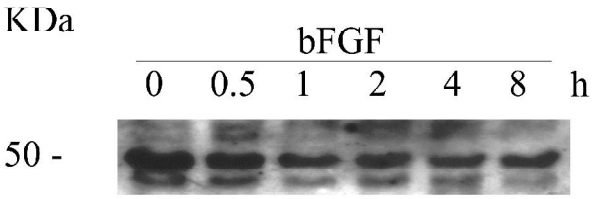


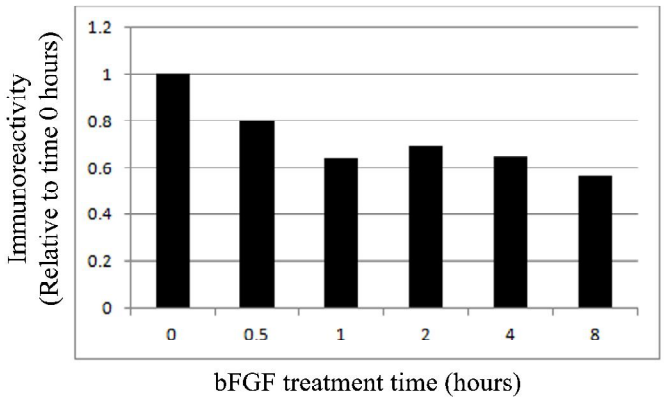

**Figure 17.** Preliminary studies: Expression profiles of Cx46 and Cx50 in response to bFGF treatment

B) Cx50

Trial 1

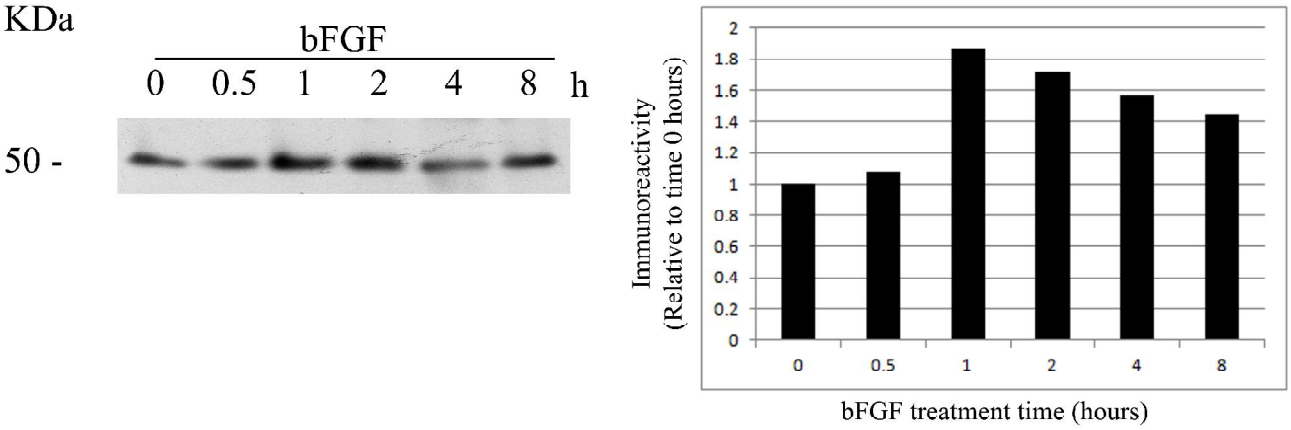


Trial 2

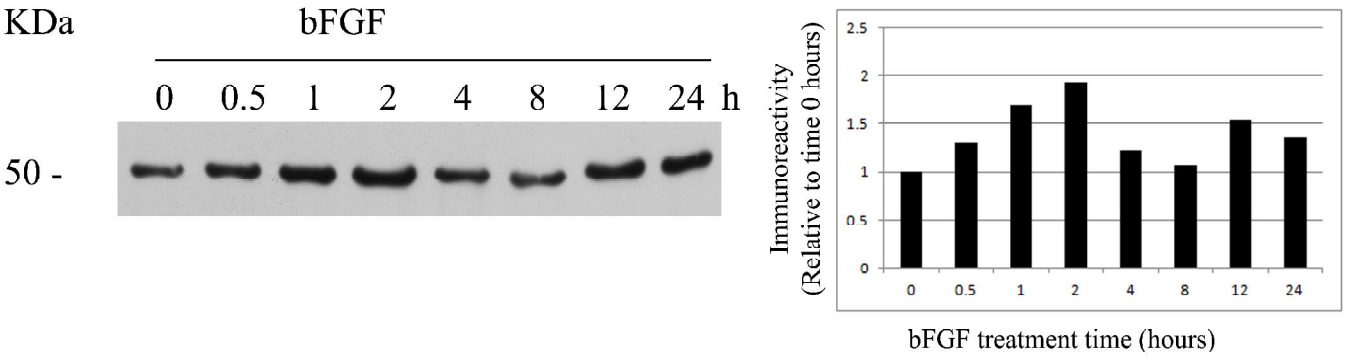


Trial 3

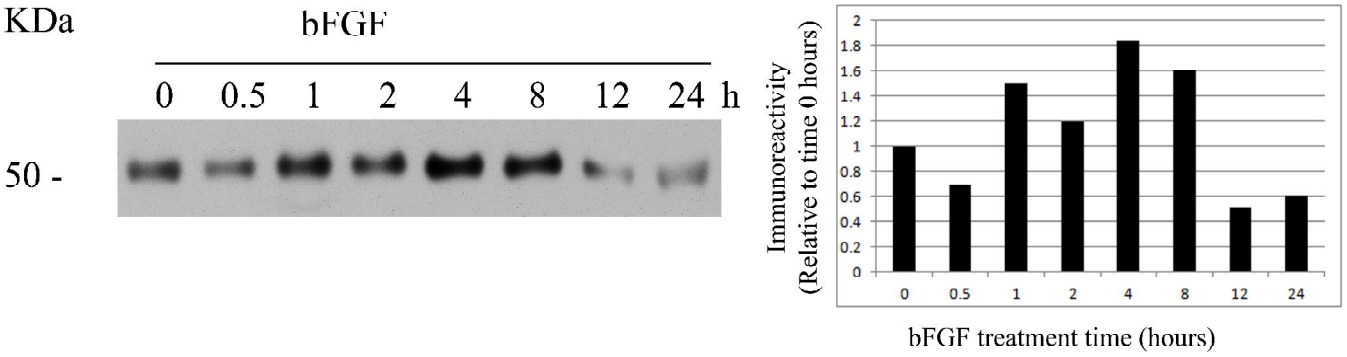

**Figure 17.** Expression profiles of Cx46 and Cx50 in the TtT/GF folliculo-stellate cells in response to bFGF treatment

TtT/GF cells were serum starved for twenty four hours to remove residual growth factors and cytokines present in fetal bovine serum. Cell cultures were then treated with bFGF diluted into serum-free medium (15 ng/ml) and incubated over varying time periods. After treatment, cells were collected and prepared for Western blotting. Cx46 (Alpha Diagnostics) and Cx50 (Invitrogen) antibodies were used to probe membranes. Bands obtained from Western blot were quantified to determine relative immunoreactivity and graphed as a function of time. Changes in protein expression are expressed in terms of the fold change as compared to time 0 hour.

**A)** The treatment with bFGF resulted in a gradual decrease of Cx46 protein levels.

**B)** The experiments investigating the protein expression profiles of Cx50 in response to bFGF showed a transient increase in the levels of Cx50.

## 3.6. Studies on the protein expression profiles of Cx46 and Cx50 in the anterior pituitary of male and female mink throughout the annual reproductive cycle

After having identified and characterized Cx46 and Cx50 in the TtT/GF folliculo-stellate cell line (*in vitro*), we next looked to investigate whether the expression profile of these two connexins were affected by the hormonal milieu of the anterior pituitary. For that purpose, we used the mink anterior pituitary gland. The mink anterior pituitary gland provided an interesting model to study Cx46 and Cx50 for several reasons:

1. Previous studies have demonstrated a variation in the expression levels of Cx43 in the anterior pituitaries of mink at different points throughout the reproductive cycle (Vitale, Cardin et al. 2001);
2. The mink anterior pituitary contains a heterogeneous and dynamic FS cell population that undergoes changes throughout the reproductive cycle (Cardin, Carbajal et al. 2000).

In the present studies, we determined if changes in the protein expression of Cx46 and Cx50 occurred in animals at different moments in the reproductive cycle. To accomplish this, the anterior pituitary glands were isolated from normal, adult female and male mink at different time periods in the reproductive cycle. The periods were chosen in function of significant hormonal changes that occur during these months (Cardin, Carbajal et al. 2000, Vitale, Cardin et al. 2001, Kabbaj, Yoon et al. 2003). Homogenates of the glands were subjected to SDS-PAGE, transferred to nitrocellulose membranes and probed with antibodies against Cx46 and Cx50.

### 3.6.1. Expression patterns of Cx46 and Cx50 in the female mink anterior pituitary gland

**Figures 18A** and **B** show the results from the Western blots of three different female mink anterior pituitaries probed for Cx46 and Cx50, which include May-L – lactating animals from the month of May, May-NL – non-lactating animals of the same month and Nov – animals from November (months when animals were euthanized). Western blotting with anti-Cx46 indicated the presence of a doublet with bands at 50 and 49 kDa in the May-L and May-NL samples, while the Nov samples presented a triplet with bands at 50, 49 and 48 kDa (**Figure 18A**). With regard to immunoreactivity for the Cx46 protein, the signal was strongest in lactating animals euthanized in the month of May (May-L), non-lactating animals of the same month (May-NL) showed a decrease in the level of immunoreactivity for Cx46 and November animals (Nov) displayed an intermediate intensity of reactivity. The 50 kDa band of the Nov sample was clearly less strong than the 49 and 48 kDa bands of the same sample.

Probing the same samples for Cx50 revealed a single immunoreactive band at 54 kDa (**Figure 18B**). Similar to the pattern seen when probing for Cx46, lactating animals from May showed the strongest immunoreactivity. The immunoreactive signal in non-lactating animals from May (May-NL) was barely present and the signal from November (Nov) animals was lower than the signal observed in lactating animals from the month of May, but higher than that of the May-NL sample.

### 3.6.2. Expression patterns of Cx46 and Cx50 in the male mink anterior pituitary gland

**Figures 18C** and **D** show images of the Western blots from five different male mink anterior pituitaries probed for Cx46 and Cx50, including: Jan – January, Feb – February, May, July and Nov – November. As shown in **Figure 18C**, adult male mink samples probed with antibodies against Cx46 show a doublet with bands at 50 and 49 kDa. The intensity of the bands was low in January animals and gradually increased in February until reaching its maximum reactivity in May animals. From the peak levels of immunoreactiviy seen in May animals, there was a gradual decrease of the signal in animals euthanized in July and November. When the same samples were probed for Cx50, a single immunoreactive band was detected at 54 kDa (**Figure 18D**). The intensity of the bands was greatest in animals euthanized during the month of January. Following this, samples from the months of February, May and July displayed greatly reduced intensity. The signals from November samples were barely visible.

### 3.6.3. Variations in the mink serum levels of the anterior pituitary hormones: PRL, FSH and LH

To facilitate the discussion of the variation of Cx46 and Cx50 expression in mink anterior pituitary, we reproduce here the levels of several of the anterior pituitary hormones obtained from our lab and having previously been published (Vitale, Cardin et al. 2001, Kabbaj, Yoon et al. 2003).

**Figure 18E** indicates relative PRL, GH and FSH content within the female pituitary gland during autumn/winter (Nov – Dec), spring (May) and the lactation period (May). PRL levels are

at their lowest during autumn/winter and increase throughout spring until the lactation period. GH levels are similar during autumn/winter and spring but decrease during the lactation period. FSH levels are elevated in autumn/winter but are found to be decreased in spring and during the lactation period (Vitale, Cardin et al. 2001). **Figure 18F** indicates that PRL concentration gradually increases from the month of February to reach a peak level in May. From May, there is a gradual decrease until August. **Figure 18G** shows a relatively higher concentration of FSH from February to May followed by a decrease in the months of June to August. Levels of LH are on a decreasing trend from February to April (**Figure 18H**), followed by an increase in the concentration until June followed by another decrease until August (Kabbaj, Yoon et al. 2003).

**Figure 18.** Preliminary studies: Expression profiles of Cx46 and Cx50 in female and male mink anterior pituitary glands throughout the annual reproductive cycle

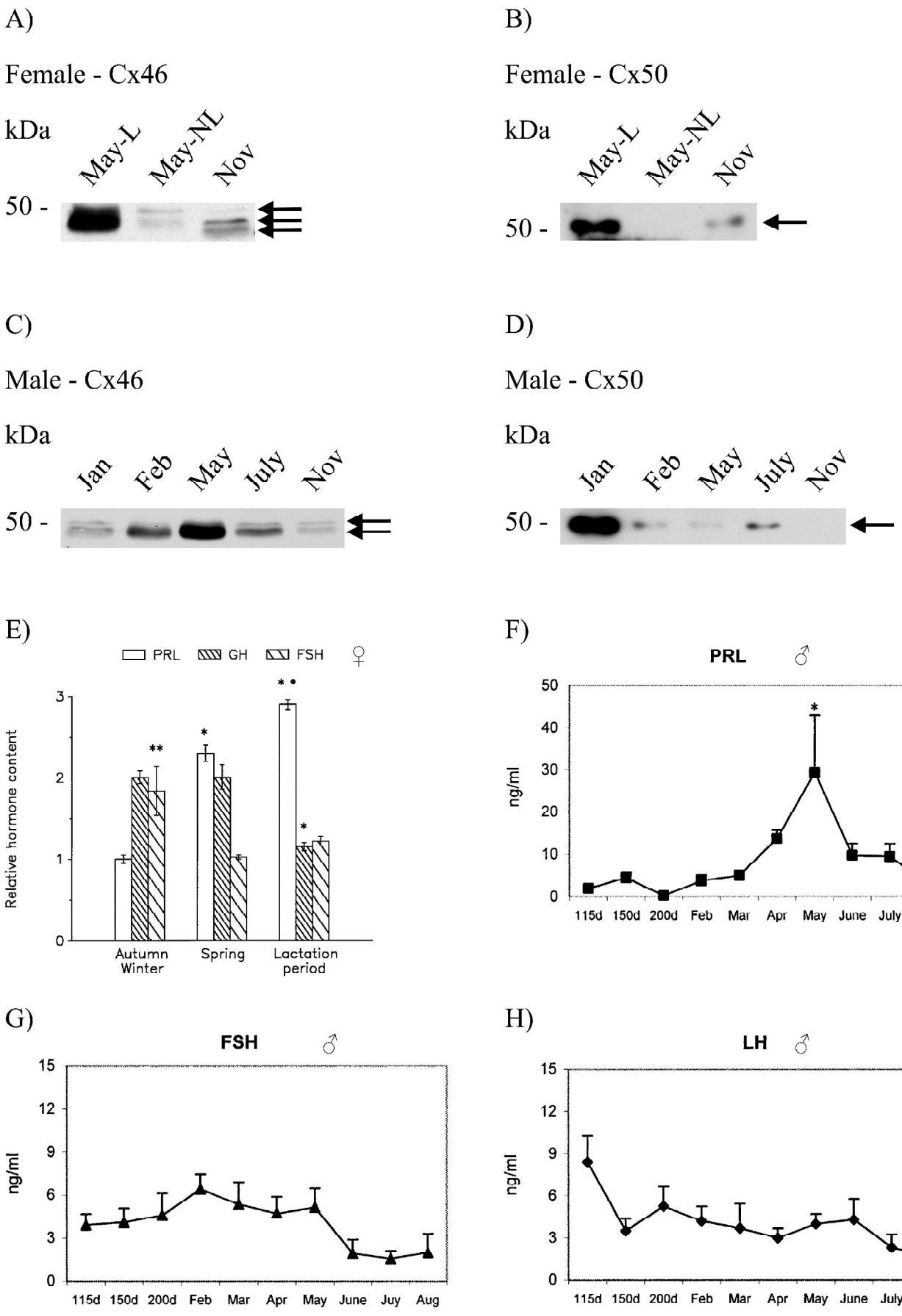

**Figure 18.** Preliminary studies: Expression profiles of Cx46 and Cx50 in female and male mink anterior pituitary glands throughout the annual reproductive cycle

**A – D)** Fertile female and male adult mink were euthanized at the following stages of the reproductive cycle: Female: May – Lactating (May-L), May – Non-Lactating (May-NL) and November (Nov); Male: January (Jan), February (Feb), May, July and November (Nov). Anterior pituitary glands were excised from the animals, homogenized and loaded into a polyacrylamide gel where proteins migrated prior to being transferred to a nitrocellulose membrane. Lastly, Cx46 (Alpha Diagnostic) and Cx50 (Invitrogen) antibodies were used to probe the membranes.

**A)** Membranes probed with a Cx46-specific antibody revealed a doublet with bands at 49 and 50 kDa in May-L and May-NL samples. Nov samples showed three bands at 48, 49 and 50 kDa (**arrows**). Immunoreactivity was stronger in May-L samples with respect to May-NL and Nov samples whereas Nov samples produced a signal slightly stronger than that of the May-NL sample.

**B)** Membranes probed with Cx50-specific antibodies produced a single 54 kDa band (**arrow**). The immunoreactive signal was strongest in the May-L sample when compared to May-NL and Nov samples. The intensity of bands produced by the Nov sample was slightly higher than the May-NL sample.

**C)** Male samples probed with Cx46 antibodies produced two bands at 49 and 50 kDa (arrows). The immunoreactive signal increased gradually from Jan to May, where the signal was strongest. Signal intensity then gradually decreased from May to Nov.

**D)** In the male samples probed with antibodies against Cx50, a 54 kDa band was detected. The immunoreactive signal was strongest in Jan and much weaker in Feb, May, July and Nov.

**E – H)** To aid in the discussion of the afore-presented results, here we reproduce the changes in the anterior pituitary hormone concentration taken from results previously published by our lab (Vitale, Cardin et al. 2001, Kabbaj, Yoon et al. 2003). These previous studies investigated the relative anterior pituitary hormone content of prolactin (PRL), growth hormone (GH) and Follicle-Stimulating Hormone (FSH) during development and throughout the adult reproductive cycle in female animals (Vitale, Cardin et al. 2001); and the serum concentrations of PRL, FSH and LH (Luteinizing Hormone) in male animals (Kabbaj, Yoon et al. 2003).

# 4. Discussion

The FS cells are organized to form a 3-dimensional network throughout the anterior pituitary gland (Vila-Porcile 1972). Gap junctional channels connect the cytoplasms of FS cells thereby allowing the passage of small molecular messengers throughout the network (Morand, Fonlupt et al. 1996). Gap junctional channels also connect the FS network to endocrine cells, more specifically, lactotrophs and gonadotrophs (Yamamoto, Hossain et al. 1993, Morand, Fonlupt et al. 1996). Thus far, only Cx43 has been identified and studied in the formation of this cellular network (Vitale, Cardin et al. 2001, Lewis, Pexa et al. 2006). In the present study, we used mouse and mink anterior pituitary homogenates to evaluated Cx46 and Cx50 protein expression. We then used the TtT/GF folliculo-stellate cell line to identify Cx46 and Cx50 using PCR and western blot. Furthermore, using cytochemical and biochemical approaches, we characterized Cx46 and Cx50 in the TtT/GF folliculo-stellate cells with regard to several properties including: intracellular distribution, association with organelles and cellular domains, and presence within lipid rafts and caveolae. We also performed *in vivo* studies to investigate how Cx46 and/or Cx50 are influenced by cytokines/growth factors or by the hormonal milieu of the anterior pituitary gland.

Beginning with an identification of the transcripts of Cx46 and Cx50, reverse-transcriptase PCR show the presence of both connexins in the TtT/GF folliculo-stellate cell line. Experiments with Cx46 showed multiple immunoreactive bands in western blots and a cytoplasmic and nuclear localization in confocal microscopy studies. We determined that Cx46 is present in non-phosphorylated and phosphorylated forms in the TtT/GF folliculo-stellate cells. We showed that different isoforms of the protein are present in the TtT/GF folliculo-stellate cells, including one

that is predominantly located within the nucleus where it is associated to NOPP-140. Experiments with Cx50 generated results suggesting a single form of the protein but we cannot disregard that this band may represent multiple forms of Cx50 with the same electrophoretic behavior (Krauchunas, Horner et al. 2012), expressed by the TtT/GF folliculo-stellate cells. The distribution of Cx50 was consistently cytoplasmic and was found to be associated with several cytoplasmic organelles. The results presented here indicate that both Cx46 and Cx50 have different biochemical, morphological and physiological characteristics. We showed opposing effects of bFGF on the protein expression of Cx46 and Cx50 on the TtT/GF folliculo-stellate cells. The expression profiles of Cx46 and Cx50 in the mink anterior pituitary gland revealed marked changes in the expression of both proteins during the male and female mink reproductive cycles.

## 4.1. Presence of Cx46 and Cx50 in the TtT/GF folliculo-stellate cells of the anterior pituitary gland

While most cells generally express more than one connexin species, we began our study by investigating the presence of Cx46 and Cx50 in the TtT/GF folliculo-stellate cells. Our reasoning for specifically studying the aforementioned connexins was that they are known to be co-expressed with Cx43 in the ocular lens (White, Bruzzone et al. 1994). Furthermore, Cx43, Cx46 and Cx50 all belong to the α-connexin family and can thus oligomerize to form heteromeric connexons (Evans and Martin 2002). Initially, we sought to identify Cx46 and Cx50 at the level of the transcript. For both Cx46 and Cx50, results from the PCR and Northern blot experiments showed several amplification products. The calculated sizes of the major bands from our experiments (Cx46: 133 bp, Cx50: 114 bp, HPRT-1: 104 bp) were comparable to those cited in

the literature from which the primer sequences were taken (Das, Wang et al. 2011, Pelletier, Akpovi et al. 2011). Minor differences could be attributed to discrepancies in the measuring of the band sizes. Despite finding bands that corresponded to the expected sizes of the PCR products, the Northern blot experiments for Cx46 and Cx50 both produced additional bands that were found at higher molecular weights. Generally, the intensity of these bands was also lesser than that of the band found at the expected sizes. The additional bands could be the products of non-specific binding of the primers that were amplified along with the intended target during PCR cycles. Considering the additional PCR products were noted well above 100 bp, primer dimers were eliminated as a possibility as these by-products are usually detected around 20 – 50 bp. The fact that bands were not observed in any of the control lanes indicates that our preparations were not contaminated with genomic DNA (No-RT control) but also indicated that our samples were devoid of any other genetic material other than the cDNA template ($H_2O$ control).

After having identified Cx46 and Cx50 at the level of the transcript, we proceeded with identifying the protein products of these genes. Western blots carried out with different Cx46 antibodies presented strong evidence that this connexin is expressed in the TtT/GF folliculo-stellate cells and in the mouse and mink anterior pituitary glands. Interestingly, TtT/GF folliculo-stellate cells presented the same bands of Cx46 as those observed in the mouse ocular lens: a doublet at 48 and 49 kDa and a higher molecular weight band at 68 kDa. Using alkaline phosphatase, we showed that the 68 kDa band represents a phosphorylated form of Cx46. The 68 kDa band however, was not detected in the mouse anterior pituitary and the presence of this band has yet to be explored in the mink anterior pituitary. Although this may indicate that this isoform

of the protein is not present in the mouse anterior pituitary, the methods employed may have lacked the sensitivity needed to detect low levels of the phosphorylated protein. Considering the TtT/GF folliculo-stellate cell line was isolated from the mouse anterior pituitary, differences in the expression of Cx46 between the two may be attributed to the physiological characteristics of a cell line versus that of a tissue. The influence of other cell types (hormone secreting cells, smooth muscle vascular cells, endothelial cells, fibroblasts) of the anterior pituitary may affect the phosphorylation status of Cx46, whereas this effect is not seen in a stable cell line. Similarly, systemic factors that normally exert feedback effects on the anterior pituitary gland may also affect the phosphorylation status of Cx46 in such a way that is not observed in the TtT/GF folliculo-stellate cell line. As previously mentioned, it must be kept in mind that the mouse anterior pituitary gland contains a variety of cell types other than the FS cells and therefore, the observed expression of Cx46 may be due to expression of the protein by some of the aforementioned cells in addition to the FS cells; although, we do not know whether the other cells present in the anterior pituitary express Cx46. WT and MHCB-/- fibroblasts were both found to express a 49 kDa version of Cx46, suggesting a similar processing of the protein in fibroblasts.

Of the two bands seen in the Cx50 Western blots of mouse lens tissue (Molecular weight: 52 and 61 kDa), it was only the 52 kDa band that was consistently detected in the TtT/GF folliculo-stellate cells and the mouse anterior pituitary. Previous studies performed in the mouse ocular lens indicate a 50 kDa band as being a non-phosphorylated version of Cx50, which was also observed as being less abundant that it's phosphorylated counterpart seen at approximately 60 kDa (Gong, Baldo et al. 1998, Xia, Cheung et al. 2006). Given the similarity in the molecular

weight of the immunoreactive band uncovered in the aforementioned study (50 kDa) to what was seen in our experiments (52 kDa), we suspect the band found in the TtT/GF folliculo-stellate cells and anterior pituitary to represent a non-phosphorylated version of Cx50.

While our intentions were firstly to identify Cx50 in the TtT/GF folliculo-stellate cell line and mouse anterior pituitary, they have also served to shed light on the physiological process taking place in the aforementioned tissues in comparison to the lens. Our results indicate that phosphorylation events affecting Cx50 in the lens are much more prevalent as compared to those in the TtT/GF folliculo-stellate cells and anterior pituitary. The non-phosphorylated status of Cx50 in the TtT/GF folliculo-stellate cells may suggest that kinases that are usually responsible for the phosphorylation of Cx50 are inactive, despite the fact that their expression has been confirmed in this cell line (Vlotides, Zitzmann et al. 2004). Observing the non-phosphorylated Cx50 in both a cell line and tissue raises the question as to whether Cx50 is phosphorylated at some point in the anterior pituitary. If so, under what cellular stimulus and importantly, what are the consequences with respect to the physiology of the cell or tissue? Drawing conclusions based on studies performed in the lens has proven difficult due to the different physiological effects of Cx50 phosphorylation previously observed. In the lens, PKC-γ phosphorylates Cx50 resulting in the disassembly of Cx50 channels and consequent uncoupling of cortical fibre cells (Zampighi, Planells et al. 2005); whereas phosphorylation of Cx50 by PKA increased gap junctional communication by promoting channel permeability (Liu, Ek Vitorin et al. 2011). Considering that the non-phosphorylated form was consistently observed in the TtT/GF folliculo-stellate cells and anterior pituitary, we suspect that Cx50 accomplishes its functions in the anterior pituitary gland without being phosphorylated or under non-stimulated conditions. However, it could be

possible that the phosphorylation of Cx50 in the TtT/GF folliculo-stellate cells and anterior pituitary may take place, but at residues that will not ultimately affect the electrophoretic migration of the protein. Furthermore, our results showed different immunoreactive bands for Cx50 in WT and MIIB-/- fibroblasts indicating that this connexin may be processed differently according to the cell/tissue environment.

Immunfluorescent labeling of TtT/GF folliculo-stellate cells for Cx46 and Cx50 allowed for interesting observations on the distribution of these proteins. Firstly, the punctate labeling displayed by Cx46 and Cx50 in the TtT/GF folliculo-stellate cells supports the notion of the expression of these connexins by these cells, as connexins characteristically show this type of labeling. Intriguingly, both Cx46 and Cx50 appeared to be predominantly distributed intracellularly and did not appear to be present at the plasma membrane. This result suggests that under basal conditions, Cx46 and Cx50 levels in the plasma membrane are too low to contribute to gap junction formation between adjoining TtT/GF folliculo-stellate cells or even to form hemi-channels. It may also be possible that neither Cx46 nor Cx50 are sent to the plasma membrane or that the transit of Cx46 and Cx50 from the cytoplasm to the plasma membrane and back occurs so rapidly that the concentration of Cx46 and Cx50 at the membrane is too low to be detected by our immunofluorescent methods. The latter possibility is supported by our studies on the co-localization of Cx46 and Cx50 with subcellular domains, particularly with respect to the presence of these connexins in early endosomes (section **4.2.**).

In addition to lacking an observable presence at the cell membrane, Cx46 and Cx50 labeling did not show punctate fluorescence at cell-cell contact areas as had been previously seen for Cx43

(Fortin, Pelletier et al. 2006). These large spots are indicative of gap junctional plaques present at cell-cell contact areas and has been noted to occur between the cellular projections of both, cultured FS cells (Vitale, Cardin et al. 2001) and TtT/GF folliculo-stellate cells (Fortin, Pelletier et al. 2006). Hence, this observation suggests that Cx46 and Cx50 do not contribute to direct intercellular communication between TtT/GF folliculo-stellate cells at least under basal conditions. In the case of Cx46, another surprising observation was that some cells showed a perinuclear distribution and other cells showed both nuclear and perinuclear labelling, without any alterations to culture conditions. This observation may suggest that, despite being under basal conditions, Cx46 is undergoing dynamic processes that result in a change of its cellular distribution. As opposed to the dynamic distribution seen with Cx46, Cx50 was distributed evenly throughout the cytoplasm, perhaps suggesting more stable intracellular processing.

## 4.2. Intracellular trafficking of Cx46 and Cx50 in the TtT/GF folliculo-stellate cells

In an effort to further characterize the intracellular distribution of Cx46 and Cx50, each connexin was co-labeled with markers for organelles and membrane domains. This series of experiments served to provide insight with regard to the intracellular trafficking and lifecycle characteristics (degradation pathways, for example) of the proteins. Connexin hemichannel assembly involves several subcellular compartments such as the ER, the ER-Golgi intermediate compartment (ERGIC), and the *cis*- and *trans*-Golgi (Koval 2006).

Cx46, failed to co-localize with the ER marker, concanavalin A. The apparent absence from the ER may suggest that Cx46 proteins are rapidly transferred to the Golgi apparatus, such that they go undetected by our method. If this is the case, Cx46 exits the ER in its monomeric form, as oligomerization generally begins to occur in the ERGIC or in the *trans*-Golgi network (Koval 2006). The co-localization of Cx46 with the *trans*-Golgi markers TGN-38 and WGA is strong evidence that this organelle is involved in the processing of Cx46. Given the implication of the *trans*-Golgi in the later stages of connexin oligomerization (Koval 2006, Laird 2006), our result may indicate that Cx46 monomers are actively being oligomerized into connexons at this stage of their life cycle. An alternative interpretation to this result is that Cx46 was being retained in the *trans*-Golgi in its monomeric form, as shown in previous studies conducted in osteoblastic cells (Koval, Harley et al. 1997). The co-localization of Cx46 and EEA-1 suggests that at one point during its lifecycle, Cx46 undergoes endocytosis and hence, is present, at least temporarily, at the plasma membrane. Although we did not detect Cx46 along the plasma membrane, or at cell-cell contact areas, it remains a possibility that Cx46 is incorporated into the plasma

membrane and internalized at such a rapid rate that it goes undetected by conventional immuno-labeling methods, a phenomenon that had previously been seen with the protein furin (Molloy, Thomas et al. 1994). Co-localization with the lysosomal marker LAMP-1, suggests that Cx46 undergoes degradation via the lysosome. The degradation of connexins has been found to occur through both pathways, individually and concurrently (Laing, Tadros et al. 1997). Therefore, the possibility that the protein is also degraded by the proteosomal pathway must not be disregarded and remains to be verified through the use of proteosomal inhibitors.

The co-localization of Cx50 with both ER markers: calnexin and concanavalin A may suggest that in addition to protein synthesis, stringent quality control mechanisms ensuring proper tertiary folding are exerted upon Cx50, as these are events that have been shown to occur in the ER with regard to connexins (Koval 2006, Laird 2006). Following this, our immunofluorescence microscopy studies results indicate the presence of Cx50 in the *cis*-Golgi, which may indicate that Cx50 monomers have started to oligomerize at this level. Although the exact location of connexin oligomerization is often debated (Laird 2006), what remains clear is that this process is often specific to the connexin and cell/tissue type. Furthermore, this process may also be dependent on the expression quantity of the connexin: highly expressed connexins may oligomerize earlier in the pathway (ER), whereas connexins expressed is lesser quantities oligomerize in distal organelles such as the *trans*-Golgi (Koval 2006). Cx50 was not found to co-localize with either TGN-38 or WGA, which strongly indicates that the *trans*-Golgi is bypassed by Cx50 during its processing or that Cx50 rapidly passes through this compartment. The co-localization of Cx50 with the early endosome marker EEA-1 suggests that at some point during its lifecycle, Cx50 undergoes endocytosis and consequently, could be found at the plasma

membrane. However, concentrated areas of fluorescence were not noted along the periphery of the cell, nor at cell-cell contact areas. Nevertheless, as we have suggested in the case of Cx46, migration to the membrane and subsequent internalization may occur so rapidly that our immunolabeling methods are unable to detect such an event, as has previously been reported with another protein (Molloy, Thomas et al. 1994). The observation of Cx50 not co-localizing with LAMP-1 suggests that this particular connexin is likely not degraded via the lysosomal pathway. Hence, there is a strong possibility that the degradation of Cx50 occurs through the proteosomal pathway, although this fact would need to be verified using proteosomal inhibitors.

## 4.3. Presence of Cx46 and Cx50 within the lipid rafts and caveolae of TtT/GF folliculo-stellate cells

Lipid rafts are specialized, small microdomains within a cell's plasma membrane containing a concentration of sphingolipids and cholesterol. As a result of their particular lipid composition, lipid rafts are targets for specific proteins that have a tendency to accumulate in these microdomains. Many of the proteins isolated from lipid rafts have been found to be implicated in cellular signaling pathways, including the IgE receptor (FcεR1) in mast cells and basophils (Brown and London 1998). Caveolae are small flask-shaped invaginations within the plasma membrane that, similar to lipid rafts, are enriched in cholesterol, sphingomyelin and glycosphingolipids. The lipid composition of caveolae allow them to resists solubilisation by certain detergents, thereby allowing for their experimental isolation. The principal protein component of caveolae is the caveolin-1 protein, which plays a structural role in lining the cytoplasmic side of the invagination and also serves to anchor the actin cytoskeleton (van Deurs, Roepstorff et al. 2003). Many of the functions of caveolae are mediated through the caveolin-1 protein and include: endocytosis, cell-signaling and structural scaffolding (Bender, Montoya et al. 2002). Given the implication of lipid rafts and caveolae in the aforementioned cellular processes, the localization of connexins in these membrane domains suggests functional roles of the connexins or connexons beyond that of gap junction proteins. For example, Cx43 has been shown to be associated with caveolin and to localize to caveolae in cardiac cells (Schubert, Schubert et al. 2002), thus, we investigated whether Cx46 and Cx50 were associated with these domains in the TtT/GF folliculo-stellate cells despite the fact that we did not find these particular connexins at the plasma membrane. Determining if Cx46 and Cx50 were localized to lipid rafts and/or caveolae was done through a lipid raft isolation method and by double labelling of

TtT/GF folliculo-stellate cells with the markers for lipid rafts and caveolae: flotillin-1 and caveolin-1.

To be able to draw conclusions from our isolation procedure, it was imperative that we first ensure the purity of the DIG fraction. Visually identifying the white turbid band was the first indication that the methods employed isolated a portion of the cell lysate that was abundant in lipids resistant to non-ionic detergents (i.e. cholesterol, sphingolipids). Confirming through Western blot that the markers flotillin-1 and caveolin-1 were present in the fractions corresponding to this white turbid band gives support to the idea that the DIG fraction contained lipid rafts and caveolae of TtT/GF folliculo-stellate cells. It was also evident that flotillin-1 and caveolin-1 were distributed to parts of the cell other than the aforementioned membrane domains, although this result was expected considering the path these proteins follow prior to reaching the plasma membrane: Flotillin-1 has been found to follow several cytoplasmic pathways prior to reaching the plasma mebrane (Morrow, Rea et al. 2002) and caveolin-1 monomers oligomerize during cytoplasmic transport (Tagawa, Mezzacasa et al. 2005). In addition, the absence of the *cis*-Golgi marker, GM-130 in fractions one through seven (inclusively) indicated that portions of this organelle and its contents did not contaminate the DIG fractions.

The complete absence of Cx46 and Cx50 in the DIG fraction despite prolonged exposure of the membrane during the Western blot indicates that these connexins are likely not found in lipid rafts and caveolae of TtT/GF folliculo-stellate cells. Cx43 was only observed in the DIG fractions after a prolonged exposure of the membranes. With regard to the aforementioned

results, it must be indicated that previous studies have localized Cx43 to the plasma membrane of TtT/GF folliculo-stellate cells (Fortin, Pelletier et al. 2006). These results further suggest that under the conditions tested, Cx46 and Cx50 are not directly implicated in functions that are occurring in lipid rafts and caveolae. Contrary to what we found in the TtT/GF folliculo-stellate cell line, previous studies report that both Cx46 and Cx50 localize to caveolae in the ocular lens (Lin, Lobell et al. 2004), other studies have shown Cx46 to be present in lipid rafts while Cx50 was absent from the same microdomains (Schubert, Schubert et al. 2002). This once again raises the issue that connexins must be studied with respect to their physical and physiological settings but may also indicate that the tissue environment may affect certain physiological characteristics of the connexin proteins. Importantly, the caveolae and lipid raft isolation method is another factor that must be considered when discussing the presence of Cx46 and Cx50 in caveolae and lipid rafts. For example, lipid rafts and caveolae with a lesser concentration of cholesterol and sphingolipids may be less resistant to the detergent and thus more susceptible to solubilisation. Hence, the possibility of Cx46 and Cx50 localizing to lipid rafts and caveolae to exert a particular function must not be negated based on these findings.

Our immunofluorescence microscopy studies showed that Cx46 did not co-localize with flotillin-1 and that Cx50 did not co-localize with caveolin-1, thereby supporting the results from the lipid raft and caveolae isolation studies. However, we did find co-localization of Cx50 with flotillin-1 in the cytoplasm of TtT/GF folliculo-stellate cells. Taken together, results from the double-labelling experiment of Cx50 and flotillin-1 and the lipid raft isolation studies indicate that Cx50 and flotillin-1 do interact in the TtT/GF folliculo-stellate cells, although this interaction in limited to the cytoplasm and does not extend to the lipid rafts. These results led us to question as

to why this interaction remains cytoplasmic but does not extend to the periphery of the cell. Our observations show that Cx50 does not interact with flottilin-1 when the latter is associated with lipid rafts. Importantly, these results also suggest a strong possibility that Cx50 is incorporated into lipid rafts under specific cellular conditions that have yet to be observed. Furthermore, the results from this study support our previous observations indicating that Cx46 and Cx50 are not associated with the plasma membrane of TtT/GF folliculo-stellate cells under basal conditions.

## 4.4. The presence of Cx46 isoforms within the nuclei of TtT/GF folliculo-stellate cells

Immunofluorescent microscopy studies of Cx46 in the TtT/GF folliculo-stellate cell line revealed strong puncta in the perinuclear area and in some cells there were also puncta within the nucleus; we decided to further investigate the presence of Cx46 labelling in the nucleus as this is an unusual location for gap junction proteins, although it has already been reported for Cx43 (Dang, Doble et al. 2003). The nuclear localization of Cx46 was addressed by a cellular fractionation technique that separates the nucleus from the remainder of the cell (post-nuclear fraction), and by double labelling confocal microscopy of Cx46 and markers of sub-nuclear structures and domains.

The fractionation method allows for the isolation of the nuclei of TtT/GF folliculo-stellate cells such that they can be studied exclusively. The purity of the fractions was shown by the increase in the relative protein quantities of the nuclear markers NOPP-140, PML and coilin/p80 in the nuclear fraction. Furthermore, the absence of the nuclear markers NOPP-140 and PML in the post-nuclear fraction attests to the recovery of most nuclei in the "nuclear fraction". It also indicates that the isolated nuclei were intact, as had they been ruptured, their contents including the nuclear markers, would have contaminated the post-nuclear fraction. The 100 kDa immunoreactive band seen throughout all three fractions in the membrane probed with anti-NOPP-140 represents a non-phosphorylated form of NOPP-140 that is present in the cytoplasm and that requires extensive phosphorylation (the 140 kDa band) to gain access to the nucleus (Li, Meier et al. 1997). Our results show that both phosphorylated and non-phosphorylated versions of the protein are present in the nucleus with enrichment in the phosphorylated form. Also,

Western blots probing for coilin/p80 indicated that the protein was present in the post-nuclear fraction although to a lesser degree than in the nuclear fraction. This observation can be explained by the constant shuttling of coilin/p80 between the nucleus and cytoplasm that is suspected to be related to small nuclear ribonucleic particle (snRNP) transport (Bellini and Gall 1999), which also explains why coilin/p80 showed cytoplasmic labelling (in addition to a nuclear localization) in confocal microscopy.

Some markers for proteins located within the cytoplasmic organelles, cytosol and plasma membrane (GM-130 and GAPDH) (i.e. post-nuclear fraction) were found to be slightly enriched in the post-nuclear fraction as compared to the whole cell lysate. Probing for the ER marker, calnexin, revealed a relatively minor quantity in the nuclear fraction, as compared to the post-nuclear fraction and whole cell lysate. This result can be explained by the physical continuity of the outer nuclear membrane with the membrane of the ER (Lodish 2000). Relatively large quantities of flotillin-1 and caveolin-1 were recovered in the nuclear fractions. Interestingly, both flotillin-1 and caveolin-1 have previously been detected in the nuclei of various cell lines (Santamaria, Castellanos et al. 2005, Sanna, Miotti et al. 2007). The isolation method used employs a detergent that, in a series of steps, solubilises the plasma membrane and membrane bound organelles, leaving the nuclei intact. The presence of flotillin-1 and caveolin-1 in the nuclear fraction of our isolation experiment may have also been due to a contamination phenomena, whereby nuclear fractions are contaminated with plasma membrane lipid rafts (Say and Hooper 2007) . Despite the ambiguity of the results obtained with flotillin-1 and caveolin-1, the absence of the cytoplasmic markers GM-130 and GAPDH in the nuclear fraction suggested

that the nuclear fraction was relatively free of cytoplasmic contaminants (apart from small portions of the ER).

After having ensured the purity of the fractionation experiment, preparations were then probed for Cx46. This uncovered some interesting observations, especially with regard to the separation of the Cx46 isoforms between the post-nuclear and nuclear fractions. The separation of the 48 – 49 kDa doublet between the post-nuclear (48 kDa) and nuclear fraction (49 kDa) raises the question of how such a subtle difference in molecular weight can entail a total change in cellular location. Theoretically, the 49 kDa Cx46 could enter the nucleus via the nuclear pores by passive diffusion, as these pores allow the unaided entry of globular proteins up to 60 kDa (Lodish 2000). Alternatively, the 49 kDa Cx46 may also be actively transported into the nucleus through the nuclear importin system or may directly interact with another protein itself being actively transported into the nucleus, thereby entering indirectly. The phosphorylated version of Cx46 located at 68 kDa was clearly restricted to the post-nuclear fraction, suggesting that phosphorylation occurs by means of a cytoplasmic kinase. Furthermore, the phosphorylation of Cx46 may also obstruct its entry into the nucleus as a 68 kDa band was not noted in the nuclear fraction.

An important aspect of connexins that must be considered when discussing nuclear translocation is that connexins are transmembrane proteins that travel throughout the cytoplasm embedded within vesicle membranes. The concept of a connexin-containing vesicle entering the nucleus via a nuclear pore seems unlikely as this structure would be too large to be granted entry. While our results clearly indicate the presence of the 49 kDa Cx46 isoform in the nucleus, the manner by

which it entered remains to be determined. In general, our western blots of Cx46 focused around the 50 kDa area as this is where we expected to see immunoreactive bands given the predicted molecular weight of the Cx46 protein. A thorough migration of the polyacrylamide gel was necessary to properly separate the doublet present at 48 and 49 kDa. Generally, gels intended for Cx46 were migrated to the extent that the 37 kDa dye indicator would be located at the bottom of the gel, thereby losing any proteins below this molecular mass to the electrophoresis buffer. A less thorough migration of the nuclear isolation preparation revealed immunoreactive bands that were previously not seen, the most notable being a 14 kDa band that was greatly enriched in the nuclear fraction. Published work reported that Cx43 undergoes a cleavage event to produce a 20 kDa C-terminal fragment that then migrates to the nucleus where it affects gene expression (Dang, Doble et al. 2003). Based on our own results, previous research by others, and the similarities between Cx46 and Cx43 (both belong to α-connexin family), it is possible that Cx46 undergoes a similar cleavage and translocation event in the TtT/GF folliculo-stellate cells. Our results also indicate that the cleaved portion of Cx46 is produced from the C-terminal of the protein (calculated molecular weight of 20 kDa (Stothard 2000, Banerjee, Das et al. 2011)), as it is this portion that contains the epitope recognized by the antibody. Furthermore, in support of this conclusion in the fact that our investigation involved three Cx46 antibodies, two of which were generated against the C-terminal and one that targeted the intracellular loop. The antibody generated against the internal region of Cx46 (U.S. Biologicals) was unable to detect the 14 kDa fragment (result not shown). We also investigated the possibility of a nuclear localization signal (NLS) being present within the Cx46 amino acid sequence, although a literature search did not reveal previous work with regard to connexins and NLS. However one study did indicate the absence of a conventional NLS within the Cx43 amino acid sequence (Sin, Crespin et al. 2012).

After having confirmed the presence of several Cx46 immunoreactive forms within the nucleus, we further investigated this finding by double labelling TtT/GF folliculo-stellate cells with Cx46 and markers of sub-nuclear structures and studying their potential co-localization by confocal microscopy. While nuclear Cx46 was not found to co-localize with coilin/p80 or PML, it did co-localize with NOPP-140 in the nuclei of TtT/GF folliculo-stellate cells. In the nucleus, NOPP-140 functions as a chaperone that shuttles small nucleolar ribonucleoprotein complexes (snoRNPs) from coiled bodies to the nucleolus where it plays a role in ribosome biogenesis (He and DiMario 2011). Given the co-localization of nuclear Cx46 with NOPP-140, we suggest that one of the nuclear-localized Cx46 isoforms is implicated in the process of ribosome biogenesis. Furthermore, the fact that nuclear Cx46 did not co-localize with coilin/p80 goes on to suggest that it is likely that this implication occurs at the nucleolus and not within coiled bodies. Taking into consideration previous studies that have found a 20 kDa C-terminal portion of Cx43 localized to the nucleus to inhibit cell growth (Dang, Doble et al. 2003), we suggest that the 14 kDa nuclear Cx46 isoform could play a similar role. The aforementioned study did not identify the mechanism employed by the C-terminal of Cx43 to inhibit cell growth. Given the similarities between Cx43 and Cx46 combined with our results with regard to the nuclear-localized Cx46, it is possible that the mechanism of growth inhibition occurs through the regulation of ribosome biogenesis. Cell growth is highly dependent on protein synthesis and thus, the availability of ribosomes to carry out this function. Through this logic, we suggest that nuclear Cx46 isoforms may influence cell growth by regulating ribosome biogenesis within the nucleolus.

## 4.5. Studies on the response of Cx46 and Cx50 to bFGF treatment of TtT/GF folliculo-stellate cells

As previously explained, we chose bFGF because the TtT/GF folliculo-stellate cells are both a source and target of this growth factor (Vlotides, Chen et al. 2009). Connexins have previously been shown to respond to growth factor treatment (Doble and Kardami 1995). Therefore, we investigated whether Cx46 and Cx50 would respond to bFGF treatment in TtT/GF folliculo-stellate cells. In this investigation, we treated cultured TtT/GF folliculo-stellate cells with bFGF for increasing periods of time then observed the effect of this treatment on the relative quantities of Cx46 and Cx50 through western blot.

The results from the investigation of the response of Cx46 to bFGF allowed us to draw conclusions that could serve to provide direction for more extensive experimentation. Our results show that treatment of TtT/GF folliculo-stellate cells with bFGF over a period of 8 hours causes an overall decrease in the levels of the Cx46 protein despite the different time courses. Further experimentation could be carried out to investigate the other effects of bFGF on Cx46. For example, immunofluorescent labelling will reveal whether there are changes in the intracellular distribution of Cx46 due to bFGF treatment. In addition, investigating changes in the relative levels of the cleaved C-terminal portion of Cx46 may indicate an effect of bFGF on specific proteases or protease signaling cascades. A previous study has demonstrated an inhibitory effect on the activation of caspase-3 by bFGF (Miho, Kouroku et al. 1999). Interestingly, caspase-3 has also been shown to mediate cleavage and truncation events of connexin proteins in the ocular lens (Wang and Schey 2009). Hence, the investigation of Cx46 cleavage in response to bFGF treatment of TtT/GF folliculo-stellate cells may prove a promising direction for future studies. In

addition, the fact that bFGF, a potent mitogen for TtT/GF folliculo-stellate cells, decreases Cx46 expression is in accordance with a potential role of Cx46 in inhibiting ribosome production.

Our studies on the effect of bFGF on Cx50 expression in the TtT/GF folliculo-stellate cells show a transient increase in the levels of the protein. Importantly, bFGF treatment did not generate any additional bands nor did it change the electrophoretic mobility of the Cx50 band, which remained at 52 kDa. This result may suggest that the signaling cascades activated by bFGF do not ultimately result in the phosphorylation of Cx50. However, it must be kept in mind that post-translational modifications do not always result in an alteration of the electrophoretic mobility of proteins and hence, this postulation must be confirmed. bFGF may modulate Cx50 expression by either increasing synthesis or by reducing degradation of the protein, or both. Promoting protein synthesis of Cx50 can occur through the phosphorylation of transcription factors by MAP kinases, which are activated as a result of bFGF binding its receptor followed by subsequent signal transduction cascades (Dailey, Ambrosetti et al. 2005). It is known that bFGF exerts a potent mitogenic effect on the TtT/GF folliculo-stellate cells (Vlotides, Chen et al. 2009); an increase in mitotic activity may represent a physiological event that must be accompanied by an increase in Cx50 expression. Interestingly, a study investigating post-natal lens development demonstrated that Cx50 acts to stimulate mitosis in the developing lens epithelial cells and that its absence results in a decrease in the mitotic index of lens cells (Sellitto, Li et al. 2004). While our preliminary results indicate that bFGF exerts an effect on the expression of Cx50 by the TtT/GF folliculo-stellate cells, further experimentation is required to pursue its role during periods of increased mitosis and to determine the other effects this growth factor may have on Cx50. For example, it would be interesting to investigate whether Cx50 expression is also

increased in response to other TtT/GF folliculo-stellate cell mitogens, such as PACAP (Matsumoto, Koyama et al. 1993). Such an experiment would reveal whether the increase in Cx50 expression is specific to bFGF-induced mitosis, or if it is also responsive to mitosis provoked by other active peptides. Additionally, immunofluorescence microscopy can be used to uncover any changes in cellular distribution of Cx50 in response to bFGF.

From a comparative viewpoint, our results indicate that bFGF exerts an opposite effect on Cx46 and Cx50. This observation adds to our previous suggestion that Cx46 and Cx50 play largely different roles in the TtT/GF folliculo-stellate cells; the differences in these two connexins in this cell line appear to also manifest in their response to growth factors.

## 4.6. Studies on variations in Cx46 and Cx50 during the annual mink reproductive cycle

We investigated the expression profiles of Cx46 and Cx50 in the anterior pituitary gland of mink throughout the annual reproductive cycle using western blot analyses.

Variations of Cx46 and Cx50 levels in female mink anterior pituitary glands have strikingly similar expression profiles. Our results uncovered a substantial increase in expression of both Cx46 and Cx50 in lactating animals when compared to non-lactating animals, suggesting a role of these connexins in the lactation process at the level of the anterior pituitary gland. Taking into consideration previous studies that have demonstrated Cx43 gap junctions between FS cells and lactotrophs (Morand, Fonlupt et al. 1996), it is possible that Cx46 and Cx50 also join these anterior pituitary cells, perhaps forming heteromeric or heterotypic junctions. Earlier studies also performed in lactating and non-lactating mink have shown that, like Cx46 and Cx50, expression of Cx43 is increased in lactating animals and decreased during the autumn months (Vitale, Cardin et al. 2001). This evidence further supports our premise that in the female mink anterior pituitary gland, Cx46 and Cx50 contribute to the lactation process and may play a role similar to that of Cx43. The reason for this increase in expression may be due to the physiological and anatomical changes that occur in the anterior pituitary gland during lactation. Firstly, there is a proliferation of lactotrophs that occurs during pregnancy in preparation for lactation (Strauss, Barbieri et al. 2009). In addition, the lactation status of the animal changes the morphological aspect of the FS cells (Cardin, Carbajal et al. 2000). Taking into account that lactotrophs and FS cells are joined by gap junctions, a greater number of lactotrophs would require an increase in the expression of gap junction proteins. In addition, the synthesis and secretion of PRL may

require a greater metabolic commitment from lactotrophs, increasing the need for the acquisition of nutrients and the disposal of waste. Considering that the FS cells may play a supportive role in the anterior putitary gland (Inoue, Mogi et al. 2002), it is likely that an increase in the number of gap junctional channels between lactotrophs and FS cells are needed to meet this increase in metabolic activity. Another possibility in that Cx46 and Cx50 are only expressed by the FS cells and the increased expression of these proteins is related to the increased activity of these cells during the lactation period (Cardin, Carbajal et al. 2000, Vitale, Cardin et al. 2001)

Conversely to what was observed in the female mink anterior pituitary gland, Cx46 and Cx50 displayed drastically different expression profiles in the male anterior pituitary. While we did not have samples from all months of the year, the variety of samples that we studies did provide us with a general idea regarding the expressional behaviour of Cx46 and Cx50 in the anterior pituitary gland. The expression profile of Cx46 showed a peak in the month of May. Male mink undergo a gradual increase in plasma PRL levels that appears to follow an increasing period of daylight (Kabbaj, Yoon et al. 2003). Given the similarities between our results and the plasma PRL levels of male mink (Kabbaj, Yoon et al. 2003), we suggest that Cx46 is involved in the PRL synthesis/secretion process in the male mink anterior pituitary gland. Studies previously performed in our laboratory demonstrated a similar trend with Cx43, whereby expression was decreased in male mink during November (Vitale, Cardin et al. 2001). Similar to the hypotheses given for female mink, this increase in Cx46 may be as a result of a proliferation of lactotrophs, or an increase in the metabolic demands of lactotrophs, processes that would require an increase in the number of gap junctions with supportive FS cells. This study can be further pursued by

obtaining samples from all months in order to obtain a complete idea of the cyclic changes in expression. In addition, immunolabelling studies can be performed to localize Cx46.

The expression profile of Cx50 in the male mink anterior pituitary gland indicates abrupt changes in the protein levels. Our results suggest the expression of Cx50 for very brief and specific durations of the male mink reproductive cycle. This observation may reflect the need for gap junctions with specific properties by the FS cells, but only for a precise duration of the reproductive cycle. Given the time of the year and abrupt changes that were noted in the expression of Cx50, it is unlikely that this observation is directly related to the change in photoperiod, as the later undergoes a more gradual change spanning over several months (Sundqvist, Amador et al. 1989). Previous studies from our lab have documented that plasma testosterone levels sharply increase to reach a peak in February then drastically decrease thereafter (Kabbaj, Yoon et al. 2003). Considering that testosterone acts directly on the anterior pituitary gland, inhibiting gonadotroph secretion of LH and FSH via a negative feedback mechanism (Bagatell, Dahl et al. 1994), our results may suggest that Cx50 expression in the anterior pituitary gland occurs in response to increasing testosterone levels. Furthermore, FS cells have previously been shown to form Cx43 gap junctions with gonadotrophs (Yamamoto, Hossain et al. 1993) suggesting that the negative feedback mechanism exerted by testosterone may also implicate FS cells and that gap junctions in the anterior pituitary are modulated by gonadal steroid hormones (Soji, Yashiro et al. 1990). These findings can be further pursued by obtaining anterior pituitary tissue from all months of the reproductive cycle. Furthermore, immunolabelling studies can be performed to localize Cx50 within anterior pituitary gland tissue.

# 5. Conclusion and future studies

In this study, we have identified Cx46 and Cx50 in the TtT/GF folliculo-stellate cells of the anterior pituitary gland at transcript and protein level. Our results revealed the presence of several forms of the Cx46 protein (due to post-translational modifications) and a single form of the Cx50 protein in this cell line.

Following identification, we characterized Cx46 and Cx50 in the TtT/GF folliculo-stellate cells with respect to their intracellular localization and association with membrane domains. Our results indicate that Cx46 and Cx50 occupy different sub-cellular locations, suggestive of individual intra-cellular trafficking routes. Importantly, neither Cx46 nor Cx50 was found in observable levels at the plasma membrane or associated with caveolae or lipid raft membrane domains in non-stimulated cells.

Early during our studies, we observed a nuclear localisation of Cx46 and further pursued this finding. Our results indicate that several forms of Cx46 are exclusively located in the nuclear compartment. Given our results and similar findings in Cx43 (Dang, Doble et al. 2003), we presume that a cleavage event takes place producing a C-terminal fraction of Cx46 that translocates to the nucleus.

We conducted two additional studies, the first exploring the effect of bFGF on the protein levels of Cx46 and Cx50. bFGF was found to cause a decrease in Cx46 levels over time, whereas Cx50 protein levels were shown to transiently increase in response to the growth factor. Our second additional study investigated Cx46 and Cx50 levels in male and female mink during the annual

reproductive cycle. Our results indicate a similar pattern in the protein levels of Cx46 and Cx50 in the anterior pituitary glands of females, with a notable increase in lactating animals. In contrast, the patterns observed for Cx46 and Cx50 protein levels throughout the annual reproductive cycle in males was drastically different.

The present study has laid a sound foundation for the future investigation of Cx46 and Cx50 in the FS cells of the anterior pituitary gland. As indicated throughout our discussion, several questions regarding the cellular physiology of Cx46 and Cx50 remain to be answered and represent areas where future studies can be based. For example, the presence of Cx46 and Cx50 at the plasma membrane of the TtT/GF folliculo-stellate cells remains a nebulous topic that will require more sensitive methods in order to be confirmed. Observing the intra-cellular transit of Cx46 and Cx50 in live cells (either under quiescent or stimulated conditions) may localize the proteins to cellular compartments that were not observed with immunofluorescent methods. The addition of a recombinant fluorescent tag (GFP, for example) to Cx46 and Cx50 would allow for their real-time observation in live cells and may prove a useful method that could be used to complement our immunofluorescent labelling studies. The nuclear localization of several Cx46 isoforms was a surprising finding that has the potential to open a new field of study with regard to connexin function. While we hypothesized, based on our findings, that Cx46 may be implicated in ribosome biogenesis, many elements of this hypothesis remain to be confirmed through additional experimentation. For example, the co-localization of Cx46 and NOPP-140 observed in confocal microscopy could be confirmed using co-immunoprecipitation, an experiment that would also serve to clarify the exact Cx46 isoforms interacting with NOPP-140. The simple fact of localizing a connexin protein to the nucleus raises many questions as to the

cellular events and physiological consequences of such an event. Pursuing such a finding will undoubtedly add to the ever-growing list of connexin functions.

Tissue specific knockdown of Cx46 and Cx50 may serve to shed some light on the specific functions of these connexins in the anterior pituitary gland (Liao, Day et al. 2001). It would prove interesting to observe the physiological consequences, especially with respect to endocrine physiology, of an absence of either Cx46 or Cx50 in the anterior pituitary glands of mice. Such an experiment may provoke compensatory mechanisms, as had previously been observed in the ocular lens (Xia, Cheung et al. 2006) and may also further distinguish Cx46 and Cx50 in terms of function. Lastly, the identification of Cx46 and Cx50 in a tissue and cell type that was previously shown to express Cx43 may initiate a "search" for the aforementioned connexins in tissues already known to express Cx43.

# References:


Abraham, V., M. L. Chou, K. M. DeBolt and M. Koval (1999). "Phenotypic control of gap junctional communication by cultured alveolar epithelial cells." Am J Physiol **276**(5 Pt 1): L825-834.

Allaerts, W. and H. Vankelecom (2005). "History and perspectives of pituitary folliculo-stellate cell research." Eur J Endocrinol **153**(1): 1-12.

Altschul, S. F., W. Gish, W. Miller, E. W. Myers and D. J. Lipman (1990). "Basic local alignment search tool." J Mol Biol **215**(3): 403-410.

Anderson, C. L., M. A. Zundel and R. Werner (2005). "Variable promoter usage and alternative splicing in five mouse connexin genes." Genomics **85**(2): 238-244.

Andrade, L. E., E. K. Chan, I. Raska, C. L. Peebles, G. Roos and E. M. Tan (1991). "Human autoantibody to a novel protein of the nuclear coiled body: immunological characterization and cDNA cloning of p80-coilin." J Exp Med **173**(6): 1407-1419.

Bagatell, C. J., K. D. Dahl and W. J. Bremner (1994). "The direct pituitary effect of testosterone to inhibit gonadotropin secretion in men is partially mediated by aromatization to estradiol." J Androl **15**(1): 15-21.

Baird, A., P. Mormede, S. Y. Ying, W. B. Wehrenberg, N. Ueno, N. Ling and R. Guillemin (1985). "A nonmitogenic pituitary function of fibroblast growth factor: regulation of thyrotropin and prolactin secretion." Proc Natl Acad Sci U S A **82**(16): 5545-5549.

Banerjee, D., S. Das, S. A. Molina, D. Madgwick, M. R. Katz, S. Jena, L. K. Bossmann, D. Pal and D. J. Takemoto (2011). "Investigation of the reciprocal relationship between the expression of two gap junction connexin proteins, connexin46 and connexin43." J Biol Chem **286**(27): 24519-24533.

Banerjee, D., G. Gakhar, D. Madgwick, A. Hurt, D. Takemoto and T. A. Nguyen (2010). "A novel role of gap junction connexin46 protein to protect breast tumors from hypoxia." Int J Cancer **127**(4): 839-848.

Bellini, M. and J. G. Gall (1999). "Coilin shuttles between the nucleus and cytoplasm in Xenopus oocytes." Mol Biol Cell **10**(10): 3425-3434.

Bender, F., M. Montoya, V. Monardes, L. Leyton and A. F. Quest (2002). "Caveolae and caveolae-like membrane domains in cellular signaling and disease: identification of downstream targets for the tumor suppressor protein caveolin-1." Biol Res **35**(2): 151-167.

Berthoud, V. M., E. C. Beyer, W. E. Kurata, A. F. Lau and P. D. Lampe (1997). "The gap-junction protein connexin 56 is phosphorylated in the intracellular loop and the carboxy-terminal region." Eur J Biochem **244**(1): 89-97.

Borden, K. L. and B. Culjkovic (2009). "Perspectives in PML: a unifying framework for PML function." Front Biosci **14**: 497-509.

Boswell, B. A., J. K. VanSlyke and L. S. Musil (2010). "Regulation of lens gap junctions by Transforming Growth Factor beta." Mol Biol Cell **21**(10): 1686-1697.

Bradford, M. M. (1976). "A rapid and sensitive method for the quantitation of microgram quantities of protein utilizing the principle of protein-dye binding." Anal Biochem **72**: 248-254.

Brokken, L. J. S., M. Leendertse, O. Bakker, W. M. Wiersinga and M. F. Prummel (2004). "Expression of adenohypophyseal-hormone receptors in a murine folliculo-stellate cell line." Hormone and Metabolic Research **36**(8): 538-541.

Brook, C. G. D. and N. J. Marshall (2001). Essential endocrinology. Oxford ; Malden, MA, Blackwell Science: 48-96.

Brown, D. A. and E. London (1998). "Functions of lipid rafts in biological membranes." Annu Rev Cell Dev Biol **14**: 111-136.

Cardin, J., M. E. Carbajal and M. L. Vitale (2000). "Biochemical and morphological diversity among folliculo-stellate cells of the mink (Mustela vison) anterior pituitary." Gen Comp Endocrinol **120**(1): 75-87.

Chaidarun, S. S., M. C. Eggo, M. C. Sheppard and P. M. Stewart (1994). "Expression of epidermal growth factor (EGF), its receptor, and related oncoprotein (erbB-2) in human pituitary tumors and response to EGF in vitro." Endocrinology **135**(5): 2012-2021.

Chaidarun, S. S., M. C. Eggo, P. M. Stewart, P. C. Barber and M. C. Sheppard (1994). "Role of growth factors and estrogen as modulators of growth, differentiation, and expression of gonadotropin subunit genes in primary cultured sheep pituitary cells." Endocrinology **134**(2): 935-944.

Chaidarun, S. S., M. C. Eggo, P. M. Stewart and M. C. Sheppard (1994). "Modulation of epidermal growth factor binding and receptor gene expression by hormones and growth factors in sheep pituitary cells." J Endocrinol **143**(3): 489-496.

Chalhoub, N. and S. J. Baker (2009). "PTEN and the PI3-kinase pathway in cancer." Annu Rev Pathol **4**: 127-150.

Chandross, K. J., J. A. Kessler, R. I. Cohen, E. Simburger, D. C. Spray, P. Bieri and R. Dermietzel (1996). "Altered connexin expression after peripheral nerve injury." Mol Cell Neurosci **7**(6): 501-518.

Chandross, K. J., D. C. Spray, R. I. Cohen, N. M. Kumar, M. Kremer, R. Dermietzel and J. A. Kessler (1996). "TNF alpha inhibits Schwann cell proliferation, connexin46 expression, and gap junctional communication." Mol Cell Neurosci **7**(6): 479-500.

Chaturvedi, K. and D. K. Sarkar (2005). "Mediation of basic fibroblast growth factor-induced lactotropic cell proliferation by Src-Ras-mitogen-activated protein kinase p44/42 signaling." Endocrinology **146**(4): 1948-1955.

Cheng, A., H. Tang, J. Cai, M. Zhu, X. Zhang, M. Rao and M. P. Mattson (2004). "Gap junctional communication is required to maintain mouse cortical neural progenitor cells in a proliferative state." Dev Biol **272**(1): 203-216.

Cotton, L. M., M. K. O'Bryan and B. T. Hinton (2008). "Cellular signaling by fibroblast growth factors (FGFs) and their receptors (FGFRs) in male reproduction." Endocr Rev **29**(2): 193-216.

Culjkovic, B., I. Topisirovic, L. Skrabanek, M. Ruiz-Gutierrez and K. L. Borden (2006). "eIF4E is a central node of an RNA regulon that governs cellular proliferation." J Cell Biol **175**(3): 415-426.

Dailey, L., D. Ambrosetti, A. Mansukhani and C. Basilico (2005). "Mechanisms underlying differential responses to FGF signaling." Cytokine Growth Factor Rev **16**(2): 233-247.

Dale, N. (2008). "Dynamic ATP signalling and neural development." J Physiol **586**(10): 2429-2436.

Dang, X., B. W. Doble and E. Kardami (2003). "The carboxy-tail of connexin-43 localizes to the nucleus and inhibits cell growth." Mol Cell Biochem **242**(1-2): 35-38.

Das, S., H. Wang, S. A. Molina, F. J. Martinez-Wittinghan, S. Jena, L. K. Bossmann, K. A. Miller, R. T. Mathias and D. J. Takemoto (2011). "PKCgamma, role in lens differentiation and gap junction coupling." Curr Eye Res **36**(7): 620-631.

De Vuyst, E., E. Decrock, M. De Bock, H. Yamasaki, C. C. Naus, W. H. Evans and L. Leybaert (2007). "Connexin hemichannels and gap junction channels are differentially influenced by lipopolysaccharide and basic fibroblast growth factor." Mol Biol Cell **18**(1): 34-46.

Decrock, E., M. Vinken, E. De Vuyst, D. V. Krysko, K. D'Herde, T. Vanhaecke, P. Vandenabeele, V. Rogiers and L. Leybaert (2009). "Connexin-related signaling in cell death: to live or let die?" Cell Death and Differentiation **16**(4): 524-536.

Devnath, S. and K. Inoue (2008). "An insight to pituitary folliculo-stellate cells." Journal of Neuroendocrinology **20**(6): 687-691.

DiGregorio, G. B., A. Gonzalez Reyna and B. D. Murphy (1994). "Roles of melatonin and prolactin in testicular crudescence in mink (Mustela vison)." J Reprod Fertil **102**(1): 1-5.

Doble, B. W., Y. Chen, D. G. Bosc, D. W. Litchfield and E. Kardami (1996). "Fibroblast growth factor-2 decreases metabolic coupling and stimulates phosphorylation as well as masking of connexin43 epitopes in cardiac myocytes." Circ Res **79**(4): 647-658.

Doble, B. W. and E. Kardami (1995). "Basic fibroblast growth factor stimulates connexin-43 expression and intercellular communication of cardiac fibroblasts." Mol Cell Biochem **143**(1): 81-87.

Drouin, J. (2011). The pituitary. S. Melmed (ed). Amsterdam, Elsevier/Academic Press: 4-18.

Dunia, I., C. Cibert, X. Gong, C. H. Xia, M. Recouvreur, E. Levy, N. Kumar, H. Bloemendal and E. L. Benedetti (2006). "Structural and immunocytochemical alterations in eye lens fiber cells from Cx46 and Cx50 knockout mice." Eur J Cell Biol **85**(8): 729-752.

Dvorak, P., A. Hampl, L. Jirmanova, J. Pacholikova and M. Kusakabe (1998). "Embryoglycan ectodomains regulate biological activity of FGF-2 to embryonic stem cells." J Cell Sci **111 ( Pt 19)**: 2945-2952.

el-Fouly, M. H., J. E. Trosko and C. C. Chang (1987). "Scrape-loading and dye transfer. A rapid and simple technique to study gap junctional intercellular communication." Exp Cell Res **168**(2): 422-430.

Evans, W. H., E. De Vuyst and L. Leybaert (2006). "The gap junction cellular internet: connexin hemichannels enter the signalling limelight." Biochem J **397**(1): 1-14.

Evans, W. H. and P. E. Martin (2002). "Gap junctions: structure and function (Review)." Mol Membr Biol **19**(2): 121-136.

Fauquier, T., N. C. Guerineau, R. A. McKinney, K. Bauer and P. Mollard (2001). "Folliculostellate cell network: a route for long-distance communication in the anterior pituitary." Proc Natl Acad Sci U S A **98**(15): 8891-8896.

Fauquier, T., A. Lacampagne, P. Travo, K. Bauer and P. Mollard (2002). "Hidden face of the anterior pituitary." Trends Endocrinol Metab **13**(7): 304-309.

Flieger, O., A. Engling, R. Bucala, H. Lue, W. Nickel and J. Bernhagen (2003). "Regulated secretion of macrophage migration inhibitory factor is mediated by a non-classical pathway involving an ABC transporter." FEBS Lett **551**(1-3): 78-86.

Fortin, M. E., R. M. Pelletier, M. A. Meilleur and M. L. Vitale (2006). "Modulation of GJA1 turnover and intercellular communication by proinflammatory cytokines in the anterior pituitary folliculostellate cell line TtT/GF." Biol Reprod **74**(1): 2-12.

Freeman, S. M., C. N. Abboud, K. A. Whartenby, C. H. Packman, D. S. Koeplin, F. L. Moolten and G. N. Abraham (1993). "The Bystander Effect - Tumor-Regression When a Fraction of the Tumor Mass Is Genetically-Modified." Cancer Research **53**(21): 5274-5283.

Fujimoto, E., H. Sato, S. Shirai, Y. Nagashima, K. Fukumoto, H. Hagiwara, E. Negishi, K. Ueno, Y. Omori, H. Yamasaki, K. Hagiwara and T. Yano (2005). "Connexin32 as a tumor suppressor gene in a metastatic renal cell carcinoma cell line." Oncogene **24**(22): 3684-3690.

Gloddek, J., U. Pagotto, M. Paez Pereda, E. Arzt, G. K. Stalla and U. Renner (1999). "Pituitary adenylate cyclase-activating polypeptide, interleukin-6 and glucocorticoids regulate the release of vascular endothelial growth factor in pituitary folliculostellate cells." J Endocrinol **160**(3): 483-490.

Goldberg, G. S., A. P. Moreno and P. D. Lampe (2002). "Gap junctions between cells expressing connexin 43 or 32 show inverse permselectivity to adenosine and ATP." J Biol Chem **277**(39): 36725-36730.

Gong, X., G. J. Baldo, N. M. Kumar, N. B. Gilula and R. T. Mathias (1998). "Gap junctional coupling in lenses lacking alpha3 connexin." Proc Natl Acad Sci U S A **95**(26): 15303-15308.

Gong, X., C. Cheng and C. H. Xia (2007). "Connexins in lens development and cataractogenesis." J Membr Biol **218**(1-3): 9-12.

Gong, X., E. Li, G. Klier, Q. Huang, Y. Wu, H. Lei, N. M. Kumar, J. Horwitz and N. B. Gilula (1997). "Disruption of alpha3 connexin gene leads to proteolysis and cataractogenesis in mice." Cell **91**(6): 833-843.

Goodenough, D. A. and D. L. Paul (2003). "Beyond the gap: functions of unpaired connexon channels." Nat Rev Mol Cell Biol **4**(4): 285-294.

Gospodarowicz, D. (1974). "Localisation of a fibroblast growth factor and its effect alone and with hydrocortisone on 3T3 cell growth." Nature **249**(453): 123-127.

Gospodarowicz, D., N. Ferrara, L. Schweigerer and G. Neufeld (1987). "Structural characterization and biological functions of fibroblast growth factor." Endocr Rev **8**(2): 95-114.

He, F. and P. DiMario (2011). Structure and Function of Nopp140 and Treacle. The Nucleolus. M. O. J. Olson. New York, Springer**:** 253-278.

Heaney, A. P. and S. Melmed (2004). "Molecular targets in pituitary tumours." Nat Rev Cancer **4**(4): 285-295.

Heffner, L. J. and D. J. Schust (2010). The reproductive system at a glance. Chichester, West Sussex, UK ; Hoboken, NJ, Wiley-Blackwell: 35-45.

Henderson, H. L., D. J. Hodson, S. J. Gregory, J. Townsend and D. J. Tortonese (2008). "Gonadotropin-releasing hormone stimulates prolactin release from lactotrophs in photoperiodic species through a gonadotropin-independent mechanism." Biol Reprod **78**(2): 370-377.

Herkenham, M. (2005). "Folliculo-stellate (FS) cells of the anterior pituitary mediate interactions between the endocrine and immune systems." Endocrinology **146**(1): 33-34.

Herr, J. C. (1976). "Reflexive gap junctions. Gap junctions between processing arising from the same ovarian decidual cell." J Cell Biol **69**(2): 495-501.

Hestrin, S. (2011). "Neuroscience. The strength of electrical synapses." Science **334**(6054): 315-316.

Imamura, M., H. Negoro, A. Kanematsu, S. Yamamoto, Y. Kimura, K. Nagane, T. Yamasaki, I. Kanatani, N. Ito, Y. Tabata and O. Ogawa (2009). "Basic fibroblast growth factor causes urinary bladder overactivity through gap junction generation in the smooth muscle." Am J Physiol Renal Physiol **297**(1): F46-54.

Imura, H. (1985). The pituitary gland. New York, Raven Press.

Inoue, K., E. F. Couch, K. Takano and S. Ogawa (1999). "The structure and function of folliculo-stellate cells in the anterior pituitary gland." Arch Histol Cytol **62**(3): 205-218.

Inoue, K., H. Matsumoto, C. Koyama, K. Shibata, Y. Nakazato and A. Ito (1992). "Establishment of a folliculo-stellate-like cell line from a murine thyrotropic pituitary tumor." Endocrinology **131**(6): 3110-3116.

Inoue, K., C. Mogi, S. Ogawa, M. Tomida and S. Miyai (2002). "Are folliculo-stellate cells in the anterior pituitary gland supportive cells or organ-specific stem cells?" Arch Physiol Biochem **110**(1-2): 50-53.

Isaac, C., Y. Yang and U. T. Meier (1998). "Nopp140 functions as a molecular link between the nucleolus and the coiled bodies." J Cell Biol **142**(2): 319-329.

Jiang, J. X. and D. A. Goodenough (1996). "Heteromeric connexons in lens gap junction channels." Proc Natl Acad Sci U S A **93**(3): 1287-1291.

Jiang, J. X. and S. Gu (2005). "Gap junction- and hemichannel-independent actions of connexins." Biochim Biophys Acta **1711**(2): 208-214.

Jiang, J. X., D. L. Paul and D. A. Goodenough (1993). "Posttranslational phosphorylation of lens fiber connexin46: a slow occurrence." Invest Ophthalmol Vis Sci **34**(13): 3558-3565.

Johnstone, S. R., M. Billaud, A. W. Lohman, E. P. Taddeo and B. E. Isakson (2012). "Posttranslational modifications in connexins and pannexins." J Membr Biol **245**(5-6): 319-332.

Jordan, K., R. Chodock, A. R. Hand and D. W. Laird (2001). "The origin of annular junctions: a mechanism of gap junction internalization." Journal of Cell Science **114**(4): 763-773.

Junqueira, L. C. U., J. Carneiro and J. A. Long (1986). Basic histology. Los Altos, Calif. Norwalk, Conn., Lange Medical Publications ;
Appleton-Century-Crofts.

Kabbaj, O., S. R. Yoon, C. Holm, J. Rose, M. L. Vitale and R. M. Pelletier (2003). "Relationship of the hormone-sensitive lipase-mediated modulation of cholesterol metabolism in individual compartments of the testis to serum pituitary hormone and testosterone concentrations in a seasonal breeder, the mink (Mustela vison)." Biol Reprod **68**(3): 722-734.

Kabir, N., K. Chaturvedi, L. S. Liu and D. K. Sarkar (2005). "Transforming growth factor-beta3 increases gap-junctional communication among folliculostellate cells to release basic fibroblast growth factor." Endocrinology **146**(9): 4054-4060.

Kjenseth, A., T. A. Fykerud, S. Sirnes, J. Bruun, Z. Yohannes, M. Kolberg, Y. Omori, E. Rivedal and E. Leithe (2012). "The gap junction channel protein connexin 43 is covalently modified and regulated by SUMOylation." J Biol Chem **287**(19): 15851-15861.

Koval, M. (2006). "Pathways and control of connexin oligomerization." Trends Cell Biol **16**(3): 159-166.

Koval, M., J. E. Harley, E. Hick and T. H. Steinberg (1997). "Connexin46 is retained as monomers in a trans-Golgi compartment of osteoblastic cells." J Cell Biol **137**(4): 847-857.

Krauchunas, A. R., V. L. Horner and M. F. Wolfner (2012). "Protein phosphorylation changes reveal new candidates in the regulation of egg activation and early embryogenesis in D. melanogaster." Dev Biol **370**(1): 125-134.

Krysko, D. V., L. Leybaert, P. Vandenabeele and K. D'Herde (2005). "Gap junctions and the propagation of cell survival and cell death signals." Apoptosis **10**(3): 459-469.

Kumar, N. M. and N. B. Gilula (1996). "The gap junction communication channel." Cell **84**(3): 381-388.

Laing, J. G., P. N. Tadros, E. M. Westphale and E. C. Beyer (1997). "Degradation of connexin43 gap junctions involves both the proteasome and the lysosome." Exp Cell Res **236**(2): 482-492.

Laird, D. W. (2005). "Connexin phosphorylation as a regulatory event linked to gap junction internalization and degradation." Biochim Biophys Acta **1711**(2): 172-182.

Laird, D. W. (2006). "Life cycle of connexins in health and disease." Biochem J **394**(Pt 3): 527-543.

Langlois, S., K. N. Cowan, Q. Shao, B. J. Cowan and D. W. Laird (2008). "Caveolin-1 and -2 interact with connexin43 and regulate gap junctional intercellular communication in keratinocytes." Mol Biol Cell **19**(3): 912-928.

Langlois, S., K. N. Cowan, Q. Shao, B. J. Cowan and D. W. Laird (2010). "The tumor-suppressive function of Connexin43 in keratinocytes is mediated in part via interaction with caveolin-1." Cancer Res **70**(10): 4222-4232.

Larsen, W. J. (2003). Embryologie humaine. Bruxelles, De Boeck: 290-300.

Leithe, E. and E. Rivedal (2007). "Ubiquitination of gap junction proteins." J Membr Biol **217**(1-3): 43-51.

Lewis, B. M., A. Pexa, K. Francis, V. Verma, A. M. McNicol, M. Scanlon, A. Deussen, W. H. Evans, D. A. Rees and J. Ham (2006). "Adenosine stimulates connexin 43 expression and gap junctional communication in pituitary folliculostellate cells." FASEB J **20**(14): 2585-2587.

Li, D., U. T. Meier, G. Dobrowolska and E. G. Krebs (1997). "Specific interaction between casein kinase 2 and the nucleolar protein Nopp140." J Biol Chem **272**(6): 3773-3779.

Li, W. E., K. Waldo, K. L. Linask, T. Chen, A. Wessels, M. S. Parmacek, M. L. Kirby and C. W. Lo (2002). "An essential role for connexin43 gap junctions in mouse coronary artery development." Development **129**(8): 2031-2042.

Liao, Y., K. H. Day, D. N. Damon and B. R. Duling (2001). "Endothelial cell-specific knockout of connexin 43 causes hypotension and bradycardia in mice." Proc Natl Acad Sci U S A **98**(17): 9989-9994.

Lichtenstein, A., P. J. Minogue, E. C. Beyer and V. M. Berthoud (2011). "Autophagy: a pathway that contributes to connexin degradation." J Cell Sci **124**(Pt 6): 910-920.

Lin, D., S. Lobell, A. Jewell and D. J. Takemoto (2004). "Differential phosphorylation of connexin46 and connexin50 by H2O2 activation of protein kinase Cgamma." Mol Vis **10**: 688-695.

Lin, J. S., S. Fitzgerald, Y. Dong, C. Knight, P. Donaldson and J. Kistler (1997). "Processing of the gap junction protein connexin50 in the ocular lens is accomplished by calpain." Eur J Cell Biol **73**(2): 141-149.

Liu, J., J. F. Ek Vitorin, S. T. Weintraub, S. Gu, Q. Shi, J. M. Burt and J. X. Jiang (2011). "Phosphorylation of connexin 50 by protein kinase A enhances gap junction and hemichannel function." J Biol Chem **286**(19): 16914-16928.

Lodish, H. F; A. Berk; S. L. Zipursky; P. Matsudaira; D. Baltimore; J.E. Darnell (2000). Molecular cell biology. New York, W.H. Freeman: 870-890.

Mallo, F., E. Wilson, C. B. Whorwood, S. Singh and M. C. Sheppard (1995). "Basic and acidic fibroblast growth factor increase prolactin mRNA in a dose-dependent and specific manner in GH3 cells." Mol Cell Endocrinol **114**(1-2): 117-125.

Matsumoto, H., C. Koyama, T. Sawada, K. Koike, K. Hirota, A. Miyake, A. Arimura and K. Inoue (1993). "Pituitary folliculo-stellate-like cell line (TtT/GF) responds to novel hypophysiotropic peptide (pituitary adenylate cyclase-activating peptide), showing increased adenosine 3',5'-monophosphate and interleukin-6 secretion and cell proliferation." Endocrinology **133**(5): 2150-2155.

McKinley, M. P. and V. D. O'Loughlin (2012). Human anatomy. New York, McGraw-Hill: 609-620.

Medina, J. M. and A. Tabernero (2005). "Lactate utilization by brain cells and its role in CNS development." J Neurosci Res **79**(1-2): 2-10.

Meilleur, M. A., C. D. Akpovi, R. M. Pelletier and M. L. Vitale (2007). "Tumor necrosis factor-alpha-induced anterior pituitary folliculostellate TtT/GF cell uncoupling is mediated by connexin 43 dephosphorylation." Endocrinology **148**(12): 5913-5924.

Mennecier, G., M. Derangeon, V. Coronas, J. C. Herve and M. Mesnil (2008). "Aberrant expression and localization of connexin43 and connexin30 in a rat glioma cell line." Molecular Carcinogenesis **47**(5): 391-401.

Mese, G., G. Richard and T. W. White (2007). "Gap junctions: basic structure and function." J Invest Dermatol **127**(11): 2516-2524.

Miho, Y., Y. Kouroku, E. Fujita, T. Mukasa, K. Urase, T. Kasahara, A. Isoai, M. Y. Momoi and T. Momoi (1999). "bFGF inhibits the activation of caspase-3 and apoptosis of P19 embryonal carcinoma cells during neuronal differentiation." Cell Death Differ **6**(5): 463-470.

Miro-Casas, E., M. Ruiz-Meana, E. Agullo, S. Stahlhofen, A. Rodriguez-Sinovas, A. Cabestrero, I. Jorge, I. Torre, J. Vazquez, K. Boengler, R. Schulz, G. Heusch and D. Garcia-Dorado (2009). "Connexin43 in cardiomyocyte mitochondria contributes to mitochondrial potassium uptake." Cardiovasc Res **83**(4): 747-756.

Mizeres, N. J. (1981). Human anatomy : a synoptic approach. New York, Elsevier: 250-265.

Molloy, S. S., L. Thomas, J. K. VanSlyke, P. E. Stenberg and G. Thomas (1994). "Intracellular trafficking and activation of the furin proprotein convertase: localization to the TGN and recycling from the cell surface." EMBO J **13**(1): 18-33.

Morand, I., P. Fonlupt, A. Guerrier, J. Trouillas, A. Calle, C. Remy, B. Rousset and Y. Munari-Silem (1996). "Cell-to-cell communication in the anterior pituitary: evidence for gap junction-mediated exchanges between endocrine cells and folliculostellate cells." Endocrinology **137**(8): 3356-3367.

Morrow, I. C., S. Rea, S. Martin, I. A. Prior, R. Prohaska, J. F. Hancock, D. E. James and R. G. Parton (2002). "Flotillin-1/reggie-2 traffics to surface raft domains via a novel golgi-independent pathway. Identification of a novel membrane targeting domain and a role for palmitoylation." J Biol Chem **277**(50): 48834-48841.

Nadarajah, B., H. Makarenkova, D. L. Becker, W. H. Evans and J. G. Parnavelas (1998). "Basic FGF increases communication between cells of the developing neocortex." J Neurosci **18**(19): 7881-7890.

Nakajima, T., H. Yamaguchi and K. Takahashi (1980). "S100 protein in folliculostellate cells of the rat pituitary anterior lobe." Brain Res **191**(2): 523-531.

Nielsen, P. A., A. Baruch, V. I. Shestopalov, B. N. Giepmans, I. Dunia, E. L. Benedetti and N. M. Kumar (2003). "Lens connexins alpha3Cx46 and alpha8Cx50 interact with zonula occludens protein-1 (ZO-1)." Mol Biol Cell **14**(6): 2470-2481.

Niger, C., C. Hebert and J. P. Stains (2010). "Interaction of connexin43 and protein kinase C-delta during FGF2 signaling." BMC Biochem **11**: 14.

Ornitz, D. M. and N. Itoh (2001). "Fibroblast growth factors." Genome Biol **2**(3): REVIEWS3005.

Pearson, R. A., N. Dale, E. Llaudet and P. Mobbs (2005). "ATP released via gap junction hemichannels from the pigment epithelium regulates neural retinal progenitor proliferation." Neuron **46**(5): 731-744.

Pelletier, R. M. (1986). "Cyclic formation and decay of the blood-testis barrier in the mink (Mustela-vision), a seasonal breeder." American Journal of Anatomy **175**(1): 91-117.

Pelletier, R. M. (1988). "Cyclic modulation of sertoli-cell junctional complexes in a seasonal breeder - the mink (Mustela-vision)." American Journal of Anatomy **183**(1): 68-102.

Pelletier, R. M. (1995). "Freeze-fracture study of cell junctions in the epididymis and vas deferens of a seasonal breeder: the mink (Mustela vison)." Microsc Res Tech **30**(1): 37-53.

Pelletier, R. M., C. D. Akpovi, L. Chen, R. Day and M. L. Vitale (2011). "CX43 expression, phosphorylation, and distribution in the normal and autoimmune orchitic testis with a look at gap junctions joining germ cell to germ cell." Am J Physiol Regul Integr Comp Physiol **300**(1): R121-139.

Pelletier, R. M., S. R. Yoon, C. D. Akpovi, E. Silvas and M. A. L. Vitale (2009). "Defects in the regulatory clearance mechanisms favor the breakdown of self-tolerance during spontaneous autoimmune orchitis." American Journal of Physiology-Regulatory Integrative and Comparative Physiology **296**(3): R743-R762.

Peytevin, J., M. MassonPevet and L. Martinet (1997). "Ontogenesis of the retinohypothalamic tract, vasoactive intestinal polypeptide- and peptide histidine isoleucine-containing neurons and melatonin binding in the hypothalamus of the mink." Cell and Tissue Research **289**(3): 427-437.

Philippova, M. P., V. N. Bochkov, D. V. Stambolsky, V. A. Tkachuk and T. J. Resink (1998). "T-cadherin and signal-transducing molecules co-localize in caveolin-rich membrane domains of vascular smooth muscle cells." FEBS Lett **429**(2): 207-210.

Pruitt, K. D., T. Tatusova and D. R. Maglott (2005). "NCBI Reference Sequence (RefSeq): a curated non-redundant sequence database of genomes, transcripts and proteins." Nucleic Acids Res **33**(Database issue): D501-504.

Renner, U., P. Lohrer, L. Schaaf, M. Feirer, K. Schmitt, C. Onofri, E. Arzt and G. K. Stalla (2002). "Transforming growth factor-beta stimulates vascular endothelial growth factor production by folliculostellate pituitary cells." Endocrinology **143**(10): 3759-3765.

Rhee, D. Y., X. Q. Zhao, R. J. Francis, G. Y. Huang, J. D. Mably and C. W. Lo (2009). "Connexin 43 regulates epicardial cell polarity and migration in coronary vascular development." Development **136**(18): 3185-3193.

Rhoades, R. and D. R. Bell (2009). Medical physiology : principles for clinical medicine. Philadelphia, Wolters KLUwer|Lippincott Williams & Wilkins: 608-620.

Rinehart, J. F. and M. G. Farquhar (1953). "Electron microscopic studies of the anterior pituitary gland." J Histochem Cytochem **1**(2): 93-113.

Rizzoti, K. and R. Lovell-Badge (2005). "Early development of the pituitary gland: induction and shaping of Rathke's pouch." Rev Endocr Metab Disord **6**(3): 161-172.

Rudolph, C. D., A. Rudolph, G. Lister, L. First, A. Gershon (2011). Rudolph's pediatrics. New York, McGraw Hill Medical: 260-275.

Saleh, S. M., L. J. Takemoto, D. Zoukhri and D. J. Takemoto (2001). "PKC-gamma phosphorylation of connexin 46 in the lens cortex." Mol Vis **7**: 240-246.

Sambrook, J., E. F. Fritsch and T. Maniatis (1989). Molecular cloning : a laboratory manual. Cold Spring Harbor, N.Y., Cold Spring Harbor Laboratory.

Sanches, D. S., C. G. Pires, H. Fukumasu, B. Cogliati, P. Matsuzaki, L. M. Chaible, L. N. Torres, C. R. Ferrigno and M. L. Dagli (2009). "Expression of connexins in normal and neoplastic canine bone tissue." Vet Pathol **46**(5): 846-859.

Sanna, E., S. Miotti, M. Mazzi, G. De Santis, S. Canevari and A. Tomassetti (2007). "Binding of nuclear caveolin-1 to promoter elements of growth-associated genes in ovarian carcinoma cells." Exp Cell Res **313**(7): 1307-1317.

Santamaria, A., E. Castellanos, V. Gomez, P. Benedit, J. Renau-Piqueras, J. Morote, J. Reventos, T. M. Thomson and R. Paciucci (2005). "PTOV1 enables the nuclear translocation and mitogenic activity of flotillin-1, a major protein of lipid rafts." Mol Cell Biol **25**(5): 1900-1911.

Say, Y. H. and N. M. Hooper (2007). "Contamination of nuclear fractions with plasma membrane lipid rafts." Proteomics **7**(7): 1059-1064.

Schubert, A. L., W. Schubert, D. C. Spray and M. P. Lisanti (2002). "Connexin family members target to lipid raft domains and interact with caveolin-1." Biochemistry **41**(18): 5754-5764.

Schwartz, J. (2000). "Intercellular communication in the anterior pituitary." Endocrine Reviews **21**(5): 488-513.

Sellitto, C., L. Li and T. W. White (2003). "Connexin50 and lens cell proliferation." Investigative Ophthalmology & Visual Science **44**: U535-U535.

Sellitto, C., L. Li and T. W. White (2004). "Connexin50 is essential for normal postnatal lens cell proliferation." Invest Ophthalmol Vis Sci **45**(9): 3196-3202.

Shakespeare, T. I., C. Sellitto, L. Li, C. Rubinos, X. Gong, M. Srinivas and T. W. White (2009). "Interaction between Connexin50 and mitogen-activated protein kinase signaling in lens homeostasis." Mol Biol Cell **20**(10): 2582-2592.

Simon, A. M. and D. A. Goodenough (1998). "Diverse functions of vertebrate gap junctions." Trends Cell Biol **8**(12): 477-483.

Sin, W. C., S. Crespin and M. Mesnil (2012). "Opposing roles of connexin43 in glioma progression." Biochim Biophys Acta **1818**(8): 2058-2067.

Sohl, G. and K. Willecke (2004). "Gap junctions and the connexin protein family." Cardiovasc Res **62**(2): 228-232.

Soji, T., T. Yashiro and D. C. Herbert (1990). "Intercellular communication within the rat anterior pituitary gland. I. Postnatal development and changes after injection of luteinizing hormone-releasing hormone (LH-RH) or testosterone." Anat Rec **226**(3): 337-341.

Spivak-Kroizman, T., M. A. Lemmon, I. Dikic, J. E. Ladbury, D. Pinchasi, J. Huang, M. Jaye, G. Crumley, J. Schlessinger and I. Lax (1994). "Heparin-induced oligomerization of FGF molecules is responsible for FGF receptor dimerization, activation, and cell proliferation." Cell **79**(6): 1015-1024.

Spuch, C., Y. Diz-Chaves, D. Perez-Tilve and F. Mallo (2006). "Fibroblast growth factor-2 and epidermal growth factor modulate prolactin responses to TRH and dopamine in primary cultures." Endocrine **29**(2): 317-324.

Stilling, G. A., J. M. Bayliss, L. Jin, H. Zhang and R. V. Lloyd (2005). "Chromogranin A transcription and gene expression in Folliculostellate (TtT/GF) cells inhibit cell growth." Endocr Pathol **16**(3): 173-186.

Stothard, P. (2000). "The sequence manipulation suite: JavaScript programs for analyzing and formatting protein and DNA sequences." Biotechniques **28**(6): 1102, 1104.

Straub, A. C., M. Billaud, S. R. Johnstone, A. K. Best, S. Yemen, S. T. Dwyer, R. Looft-Wilson, J. J. Lysiak, B. Gaston, L. Palmer and B. E. Isakson (2011). "Compartmentalized connexin 43 s-nitrosylation/denitrosylation regulates heterocellular communication in the vessel wall." Arterioscler Thromb Vasc Biol **31**(2): 399-407.

Strauss, J. F., R. L. Barbieri and S. S. C. Yen (2009). Yen and Jaffe's reproductive endocrinology : physiology, pathophysiology, and clinical management. F. Jerome (ed), Philadelphia, PA, Saunders/Elsevier: 4-30.

Sundqvist, C., A. G. Amador and A. Bartke (1989). "Reproduction and Fertility in the Mink (Mustela-Vison)." Journal of Reproduction and Fertility **85**(2): 413-441.

Sundqvist, C., L. C. Ellis and A. Bartke (1988). "Reproductive endocrinology of the mink (Mustela vison)." Endocr Rev **9**(2): 247-266.

Tagawa, A., A. Mezzacasa, A. Hayer, A. Longatti, L. Pelkmans and A. Helenius (2005). "Assembly and trafficking of caveolar domains in the cell: caveolae as stable, cargo-triggered, vesicular transporters." J Cell Biol **170**(5): 769-779.

Tremblay, J. J., A. Marcil, Y. Gauthier and J. Drouin (1999). "Ptx1 regulates SF-1 activity by an interaction that mimics the role of the ligand-binding domain." Embo Journal **18**(12): 3431-3441.

Valiunas, V., Y. Y. Polosina, H. Miller, I. A. Potapova, L. Valiuniene, S. Doronin, R. T. Mathias, R. B. Robinson, M. R. Rosen, I. S. Cohen and P. R. Brink (2005). "Connexin-specific cell-to-cell transfer of short interfering RNA by gap junctions." J Physiol **568**(Pt 2): 459-468.

van Deurs, B., K. Roepstorff, A. M. Hommelgaard and K. Sandvig (2003). "Caveolae: anchored, multifunctional platforms in the lipid ocean." Trends Cell Biol **13**(2): 92-100.

Vila-Porcile, E. (1972). "[The network of the folliculo-stellate cells and the follicles of the adenohypophysis in the rat (pars distalis)]." Z Zellforsch Mikrosk Anat **129**(3): 328-369.

Vitale, M. L., C. D. Akpovi and R. M. Pelletier (2009). "Cortactin/tyrosine-phosphorylated cortactin interaction with connexin 43 in mouse seminiferous tubules." Microsc Res Tech **72**(11): 856-867.

Vitale, M. L., J. Cardin, N. B. Gilula, M. E. Carbajal and R. M. Pelletier (2001). "Dynamics of connexin 43 levels and distribution in the mink (Mustela vison) anterior pituitary are associated with seasonal changes in anterior pituitary prolactin content." Biol Reprod **64**(2): 625-633.

Vlotides, G., Y. H. Chen, T. Eigler, S. G. Ren and S. Melmed (2009). "Fibroblast growth factor-2 autofeedback regulation in pituitary folliculostellate TtT/GF cells." Endocrinology **150**(7): 3252-3258.

Vlotides, G., M. Cruz-Soto, T. Rubinek, T. Eigler, C. J. Auernhammer and S. Melmed (2006). "Mechanisms for growth factor-induced pituitary tumor transforming gene-1 expression in pituitary folliculostellate TtT/GF cells." Mol Endocrinol **20**(12): 3321-3335.

Vlotides, G., K. Zitzmann, S. Hengge, D. Engelhardt, G. K. Stalla and C. J. Auernhammer (2004). "Expression of novel neurotrophin-1/B-cell stimulating factor-3 (NNT-1/BSF-3) in murine pituitary folliculostellate TtT/GF cells: pituitary adenylate cyclase-activating polypeptide and vasoactive intestinal peptide-induced stimulation of NNT-1/BSF-3 is mediated by protein kinase A, protein kinase C, and extracellular-signal-regulated kinase1/2 pathways." Endocrinology **145**(2): 716-727.

Wang, Z. and K. L. Schey (2009). "Phosphorylation and truncation sites of bovine lens connexin 46 and connexin 50." Exp Eye Res **89**(6): 898-904.

White, T. W., R. Bruzzone, S. Wolfram, D. L. Paul and D. A. Goodenough (1994). "Selective interactions among the multiple connexin proteins expressed in the vertebrate lens: the second extracellular domain is a determinant of compatibility between connexins." J Cell Biol **125**(4): 879-892.

White, T. W., D. A. Goodenough and D. L. Paul (1998). "Targeted ablation of connexin50 in mice results in microphthalmia and zonular pulverulent cataracts." J Cell Biol **143**(3): 815-825.

Xia, C. H., D. Cheung, A. M. DeRosa, B. Chang, W. K. Lo, T. W. White and X. Gong (2006). "Knock-in of alpha3 connexin prevents severe cataracts caused by an alpha8 point mutation." J Cell Sci **119**(Pt 10): 2138-2144.

Yamamoto, T., M. Z. Hossain, E. L. Hertzberg, H. Uemura, L. J. Murphy and J. I. Nagy (1993). "Connexin43 in rat pituitary: localization at pituicyte and stellate cell gap junctions and within gonadotrophs." Histochemistry **100**(1): 53-64.

Yu, W. H., M. Kimura, A. Walczewska, J. C. Porter and S. M. McCann (1998). "Adenosine acts by A(1) receptors to stimulate release of prolactin from anterior-pituitaries in vitro." Proceedings of the National Academy of Sciences of the United States of America **95**(13): 7795-7798.

Zampighi, G. A., A. M. Planells, D. Lin and D. Takemoto (2005). "Regulation of lens cell-to-cell communication by activation of PKCgamma and disassembly of Cx50 channels." Invest Ophthalmol Vis Sci **46**(9): 3247-3255.

Zhang, X., O. A. Ibrahimi, S. K. Olsen, H. Umemori, M. Mohammadi and D. M. Ornitz (2006). "Receptor specificity of the fibroblast growth factor family. The complete mammalian FGF family." J Biol Chem **281**(23): 15694-15700.

Zhao, W., H. B. Han and Z. Q. Zhang (2011). "Suppression of lung cancer cell invasion and metastasis by connexin43 involves the secretion of follistatin-like 1 mediated via histone acetylation." Int J Biochem Cell Biol **43**(10): 1459-1468.

Zhu, X., J. Wang, B. G. Ju and M. G. Rosenfeld (2007). "Signaling and epigenetic regulation of pituitary development." Curr Opin Cell Biol **19**(6): 605-611.